국가수리과학연구소
National Institute for Mathematical Sciences
UNIST
ULSAN NATIONAL INSTITUTE OF SCIENCE AND TECHNOLOGY
ICRR
Institute for Cosmic Ray Research University of Tokyo
NAOJ
KAGRA

Identifying and Mitigating Transient Noises for Gravitational Wave Detectors

J. J. Oh (NIMS)

Based on works published in
PTEP2022, 073H01 (2022) | PRD 106, 042010 (2022) | PTEP2023, 043F01 (2023)

The 70th Workshop on Gravitational Waves and Numerical Relativity

APCTP Topical Research Program 2023

Contents

- Introduction - GW detection & Noise Mitigation

- CAGMon Tool:
  - Goal & Workflow
  - Code Test

- MIC Parameter Optimization

- Application to GW Data
  - Magnetic Field Transients from Lightning Strokes
  - Periodic Noises from Air Compressors
  - Glimpse of Gravity Gradient Noise from Winds

- Low-frequency Noise Mitigation using Bandgap Engineering

- Conclusions

Gravitational-wave Detection and Noise Mitigation

- GWs detected from BBHs, BNS, NSBH sources by LIGO, Virgo, and KAGRA collaborations
- It opens new era of observational astronomy, together with EM, so called 'multi-messenger astronomy'
- GW detectors on Earth have enormous noises sources that affect to the detection of GWs - environmental and instrumental origins
- Thus understanding and mitigating them are of great importance for successful GW signals – *'Detector's characterization'*

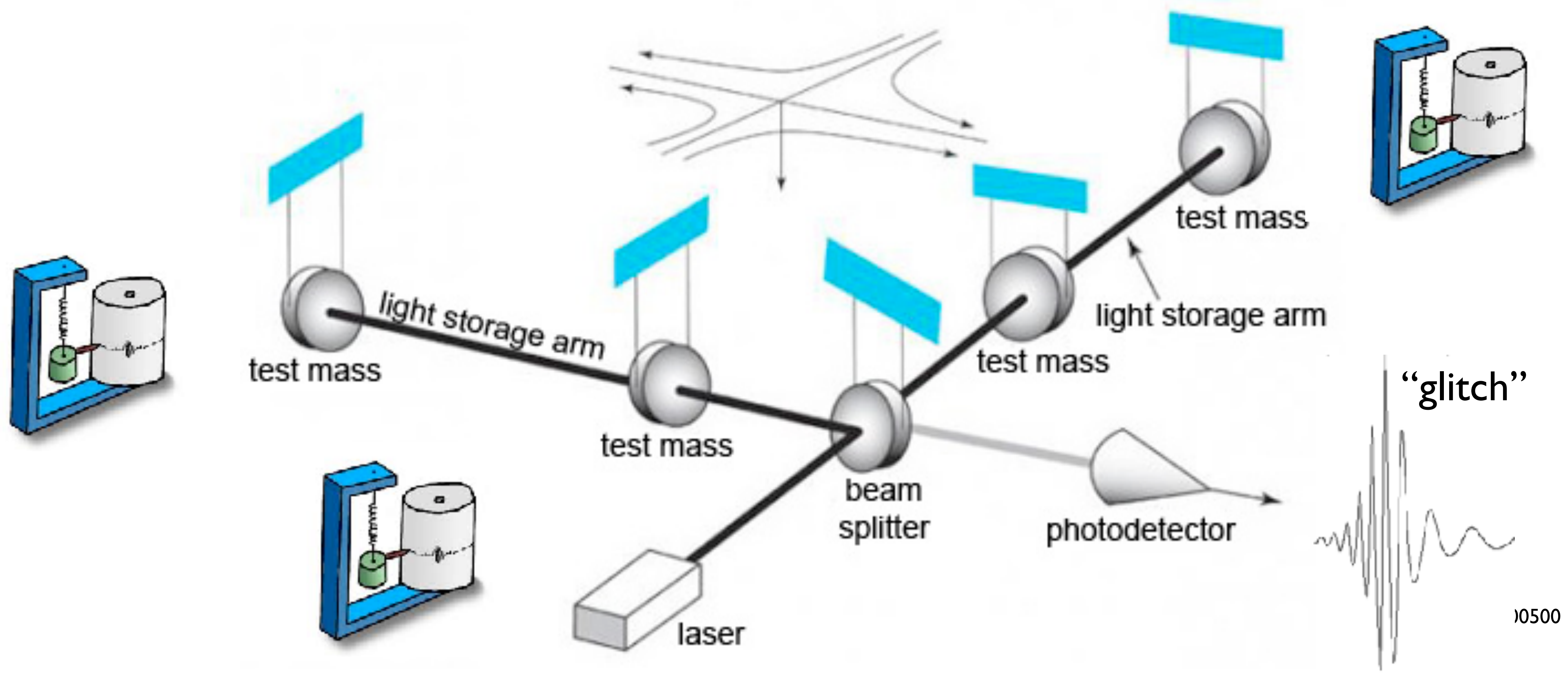

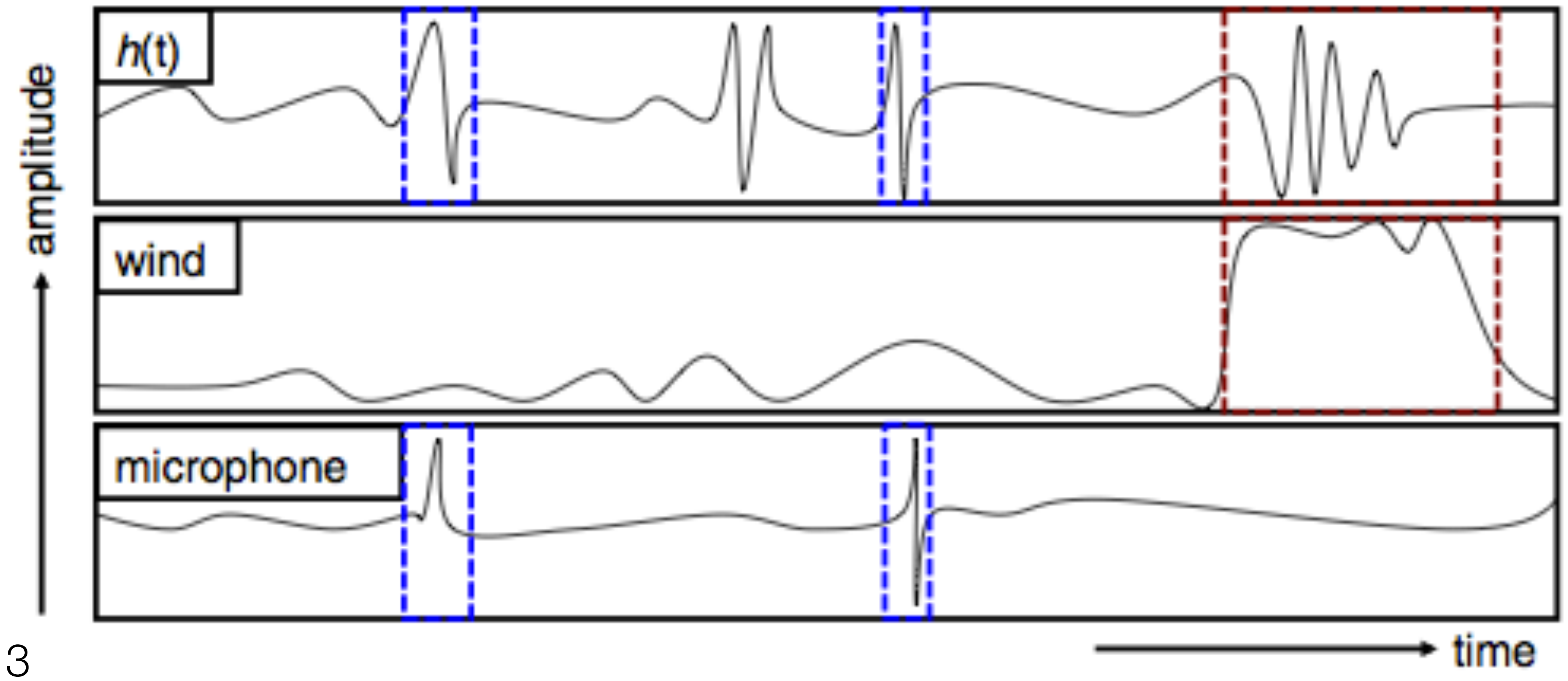

Why Glitch Studies in Gravitational Wave Detection?

- **Glitch** - transient noisy triggers that have nothing to do with gravitational wave signals caused by instrumental faults or environmental changes.
- These are very harmful to detecting gravitational wave signals if they are around the event time - lowering the signal-to-noise ratio (SNR).
- They are also harmful to compute a false-alarm probability (FAP) since glitches with high SNR can generate significant background triggers with high SNR. Eventually, they increase the FAP for a certain event candidate.
- Some glitches have similar shape and behavior to the chirp-like signals - raising FAP and lowering significance. (ex. blip transient)
- For this reason, glitches in the gravitational wave data should be well-understood, mitigated, or removed if possible.
- Detector's characterization - understanding glitches and their origins in the viewpoint of the detector and its environment.

Identifying noise sources

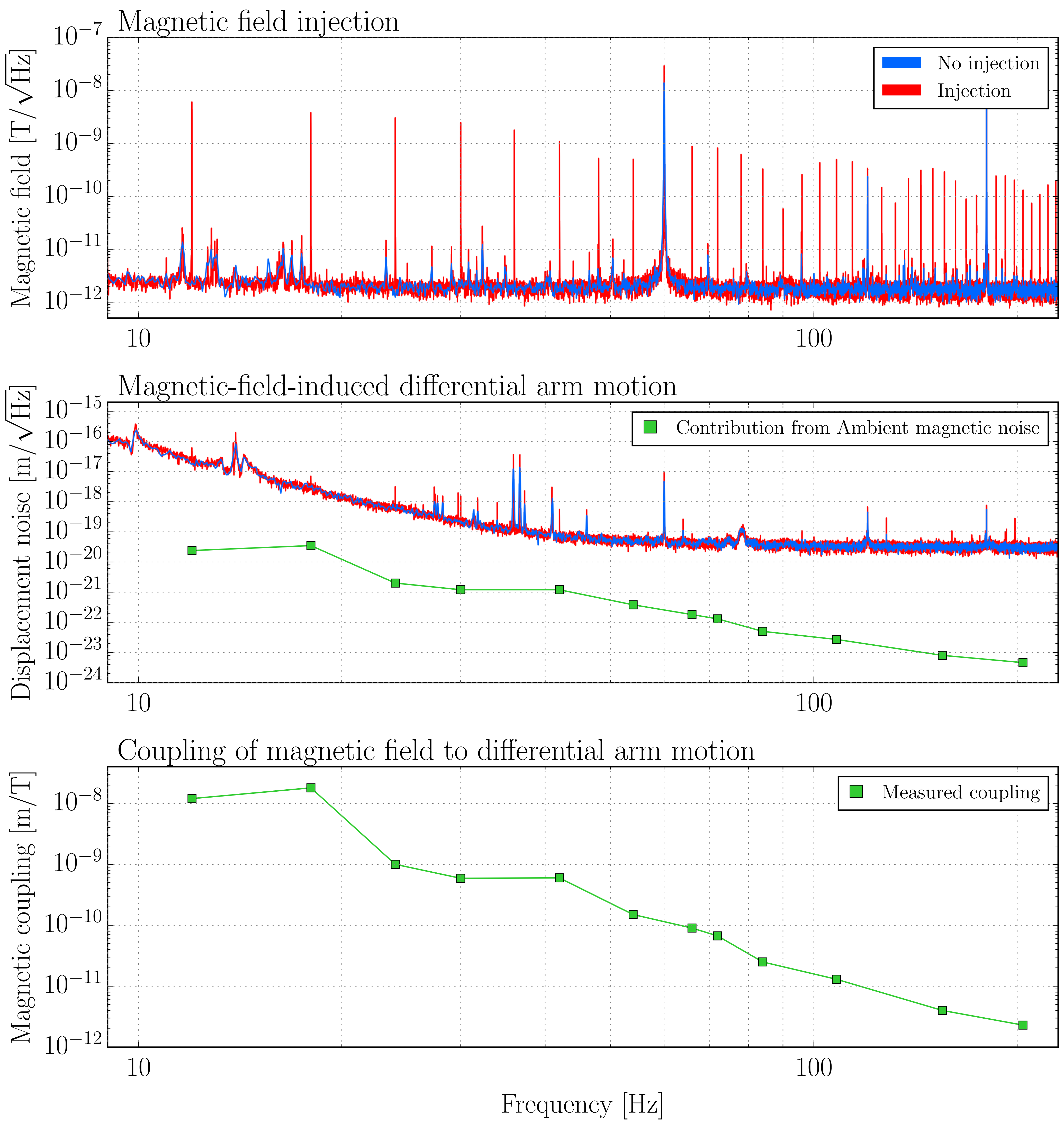

This kind of injection test should be performed in other locations throughout the detector site for radio, acoustic, and mechanical vibration sources

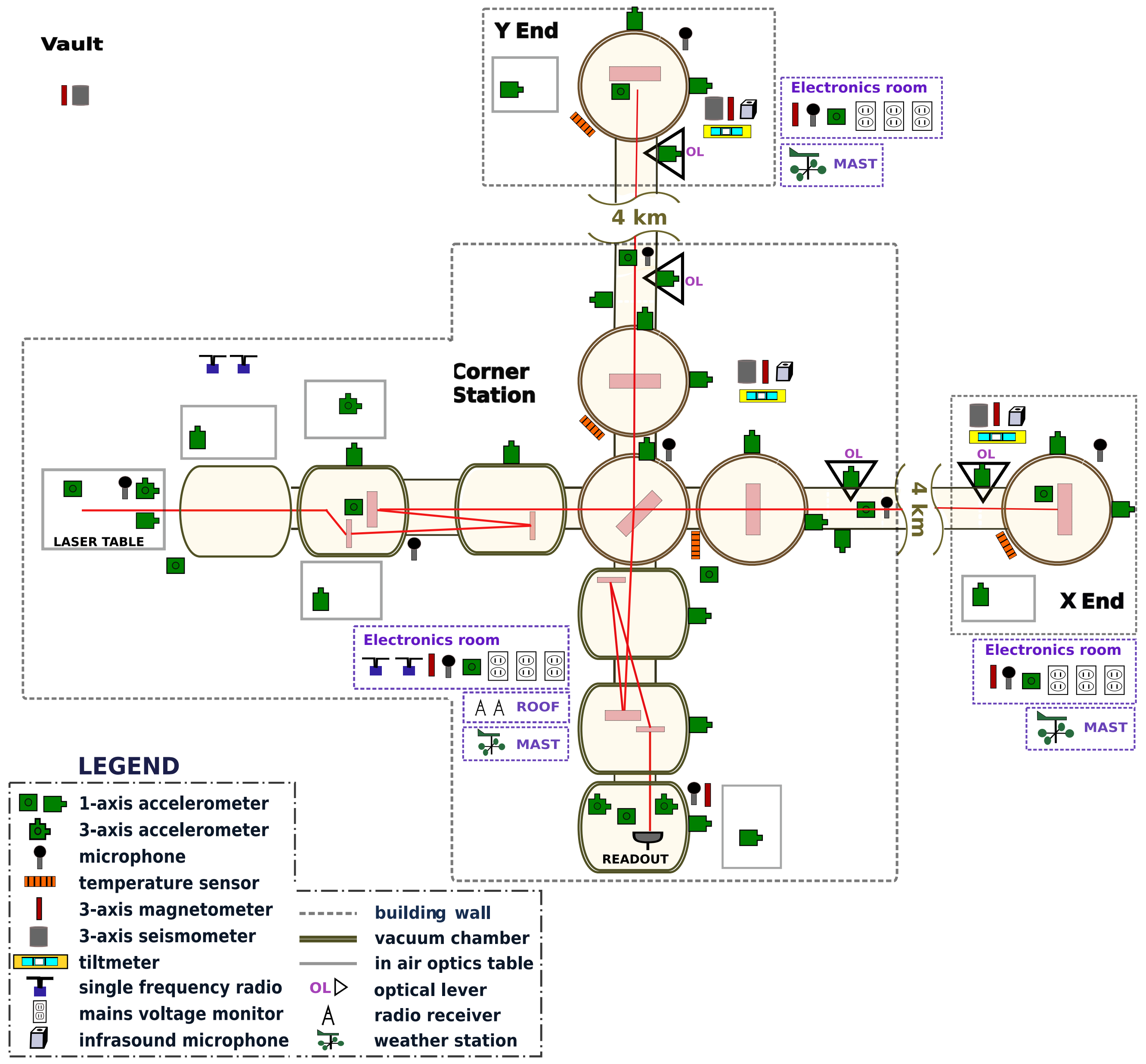

- **GW channel**, h(t)
- **200,000 auxiliary channels** - monitor 1) instrument behavior 2) environmental conditions

a) witness a broad spectrum of potential coupling mechanism

b) useful for diagnosing instrument faults and identifying noise correlation

- **PEM (physical environment monitor)** : monitor the local surroundings for potential disturbance that may affect GW channel - ground motion, optical table motion, magnetic field variation, acoustic disturbance, cosmic ray showers

* *injection studies* - in order to know the relationship between PEM and GW channels (by intentional stimulus)

Potential noise sources

Uncorrelated noise: this contribution is well-estimated using time shifts

Anthropogenic noise - human activity in rooms / chambers, infrequent ground motion, noises from nearby locations **not entering the room during taking data**

monitored by arrays of accelerometers, seismometers, and microphones

Earthquakes - 0.03~0.1Hz (higher if epicenter nearby)

* Majorly R-wave most likely impact the DQ - up-converted to high-f. : monitored by a network of seismometer at the site.

Radio Frequency (RF) modulation - faults in the 45MHz electro-optic modulator driver can cause the 10-2000Hz CBC band noises : Data vetoed not analyzed

Blip transients - short transient noise btw 30-250Hz

- symmetric "teardrop" shape
- Unidentified yet
- contribute to most significant background triggers

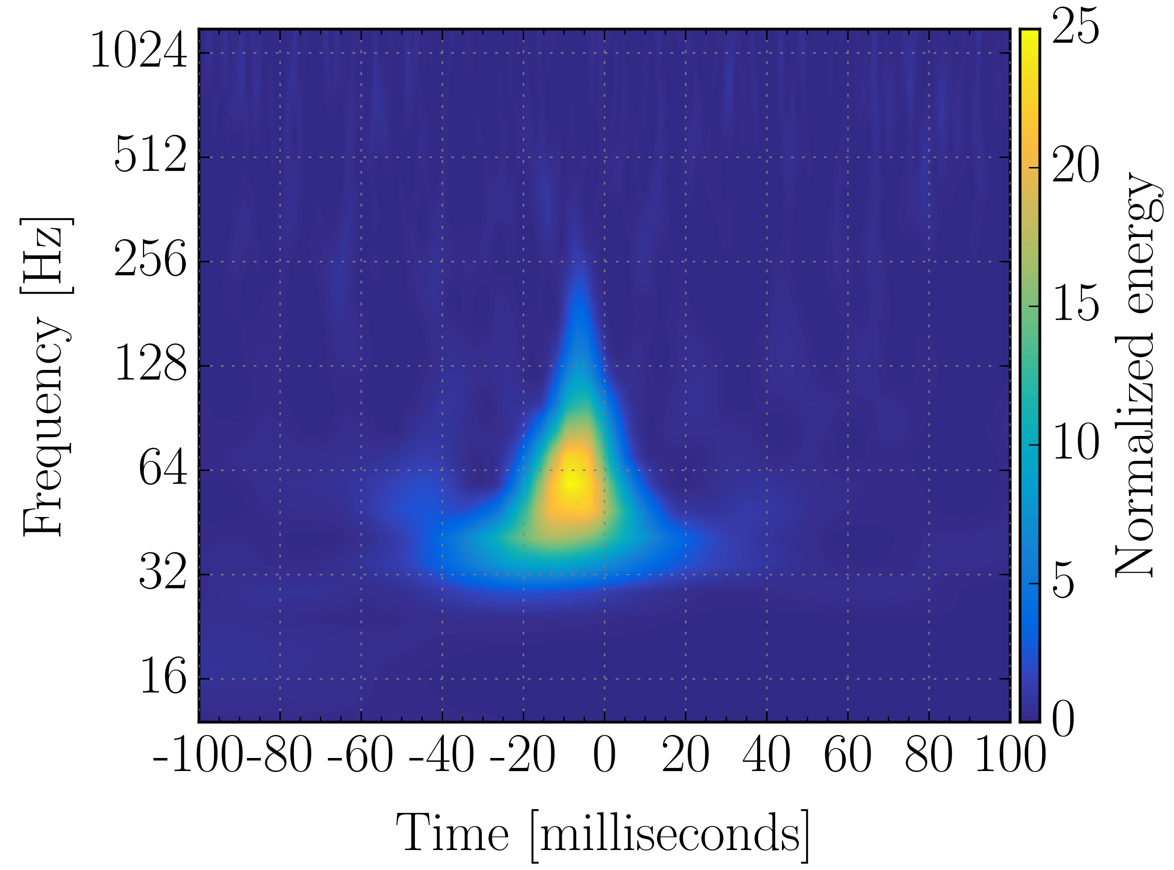

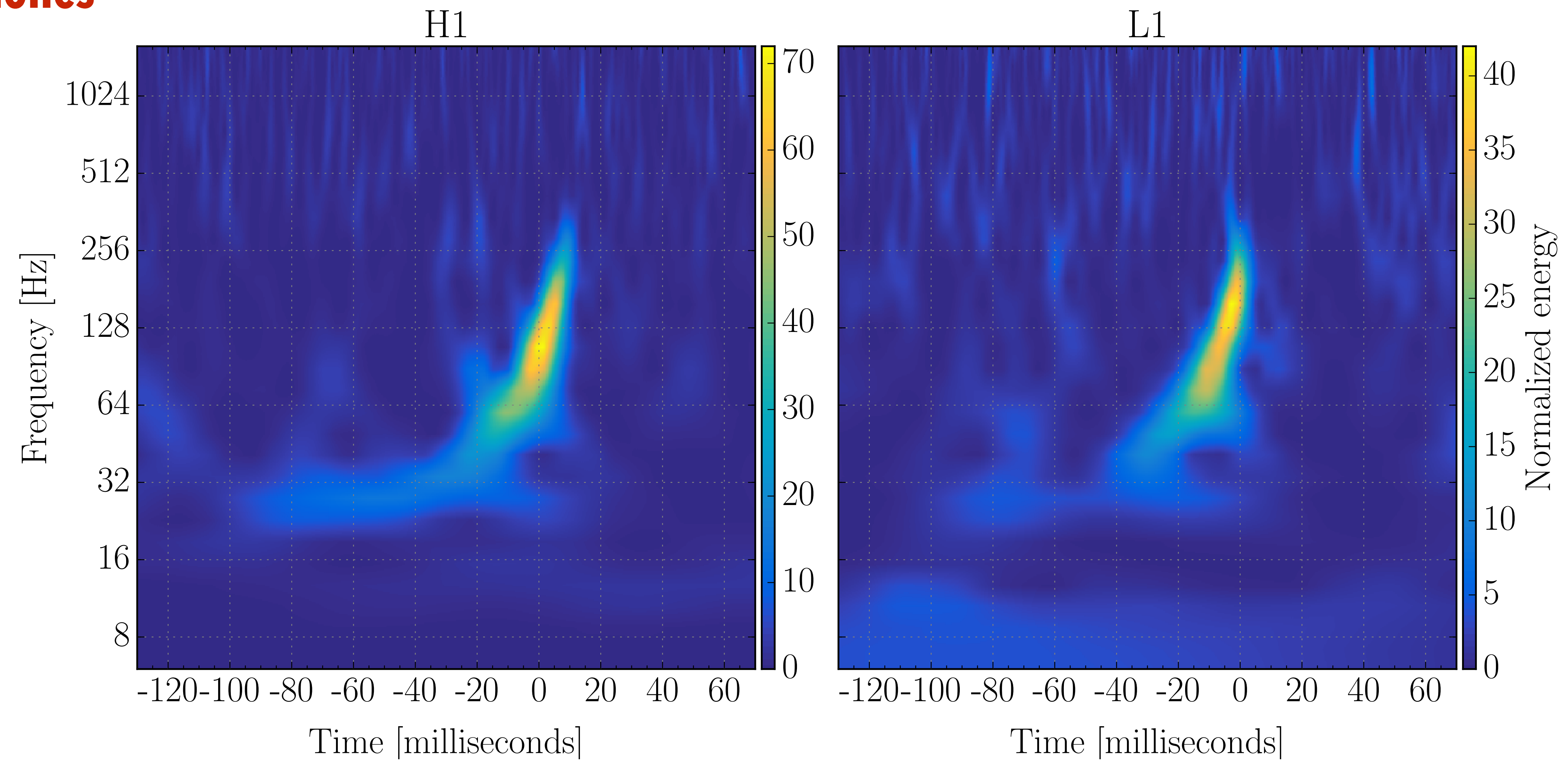

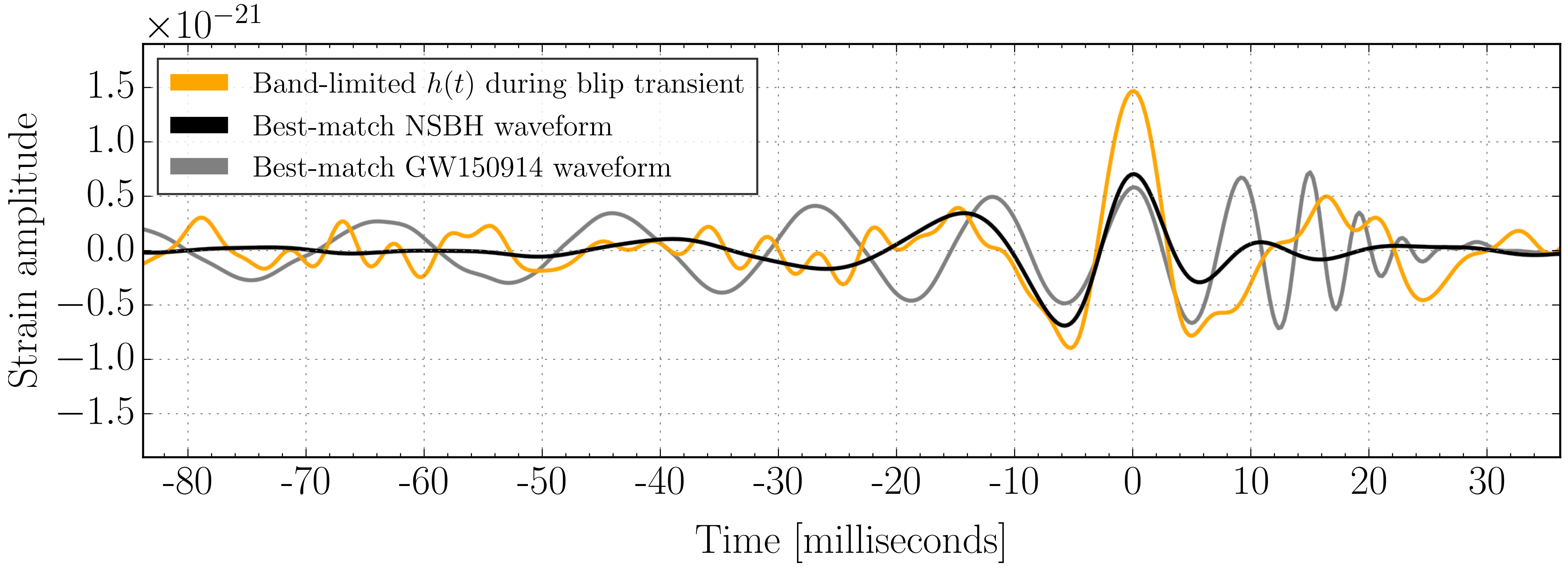

Potential noise sources

Correlated noise: noise sources that may affect both detectors almost simultaneously - potentially imitate a GW event: not captured by time shifts for the background estimation

Potential electromagnetic noise sources

- lightning strikes, solar events, solar-wind driven noise, RF communication
- if it is very significant, witnessed with high-SNR radio receiver and magnetometers

- global strikes cause Schumann resonance but the magnetic amplitude is an order of pico-Tesla (not affected in h(t))

- nearby lightning strikes produce audio-frequency magnetic fields by lightning current (>hundreds of kA); affect h(t), detected by the magnetometers at the detectors

- Electromagnetic fields in audio-frequency band generated by human and solar sources has no effect in h(t) at the detectors.

- Electromagnetic fields outside the audio-frequency band may be concerned because LIGO can be affected by the 9 and 45MHz RF modulations.

Cosmic ray showers - no coupling between showers and h(t)

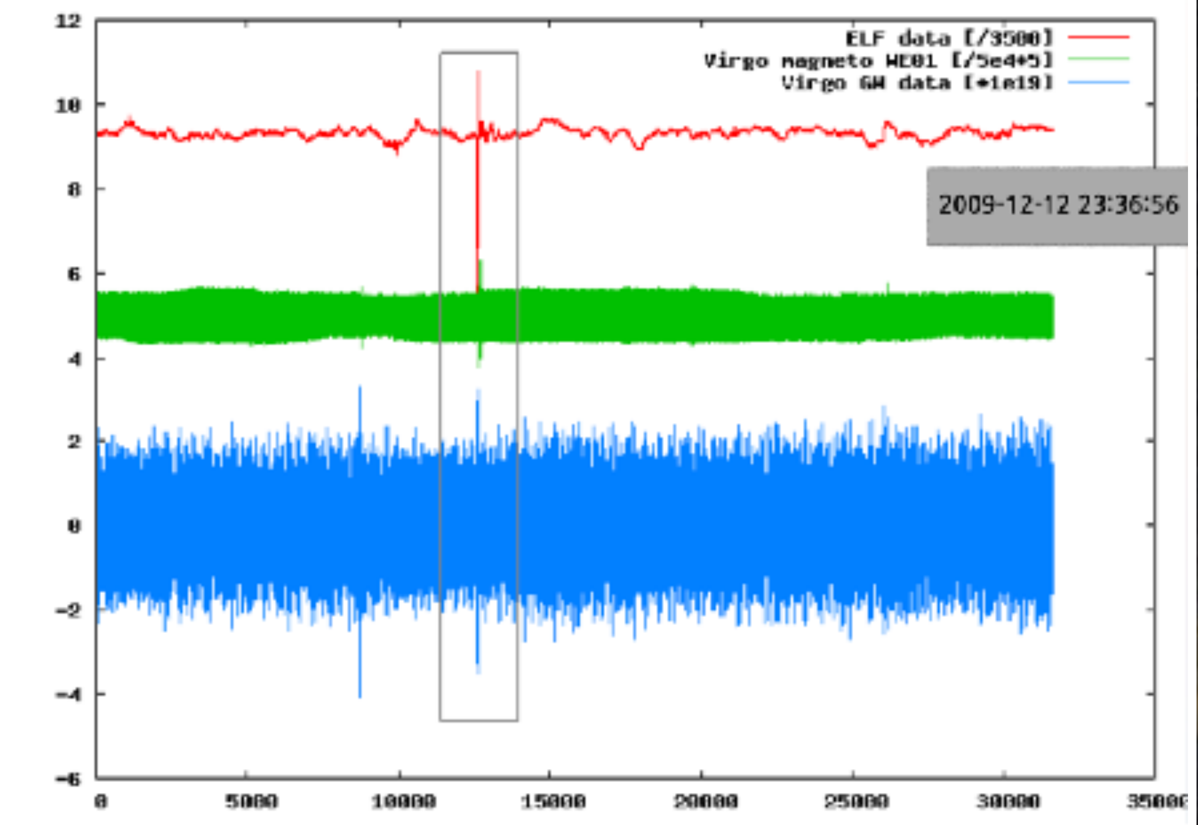

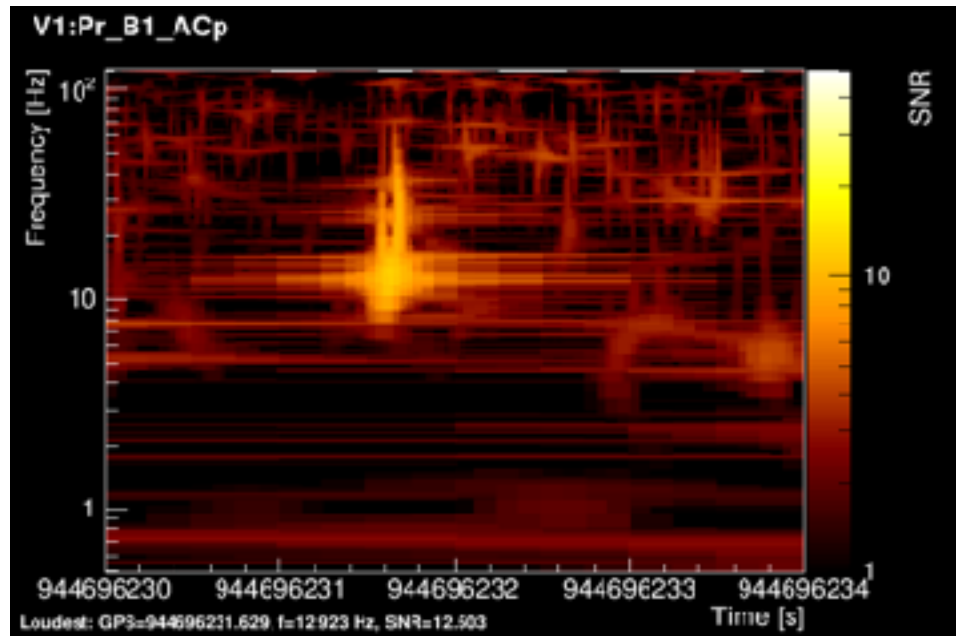

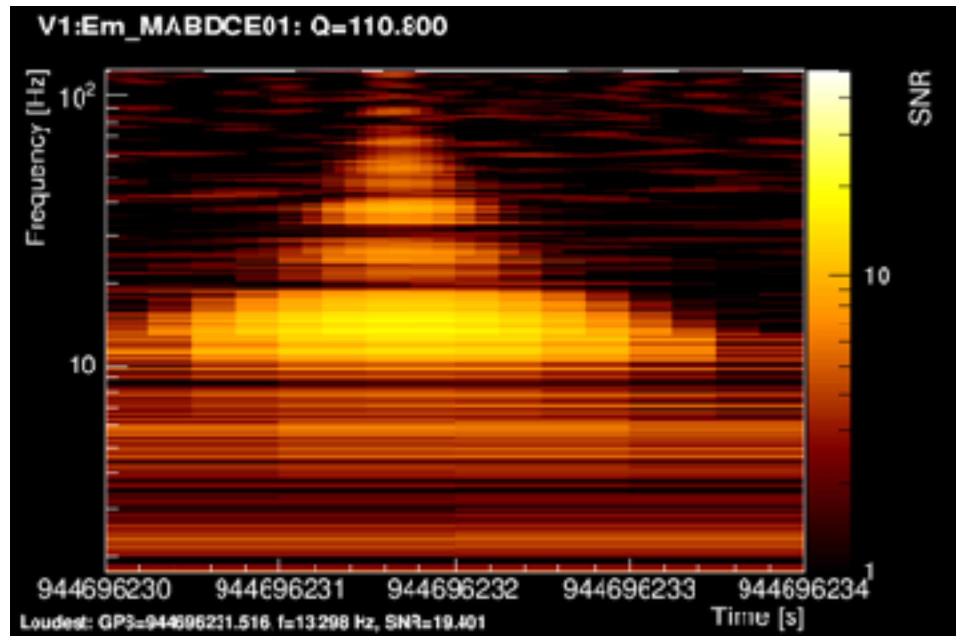

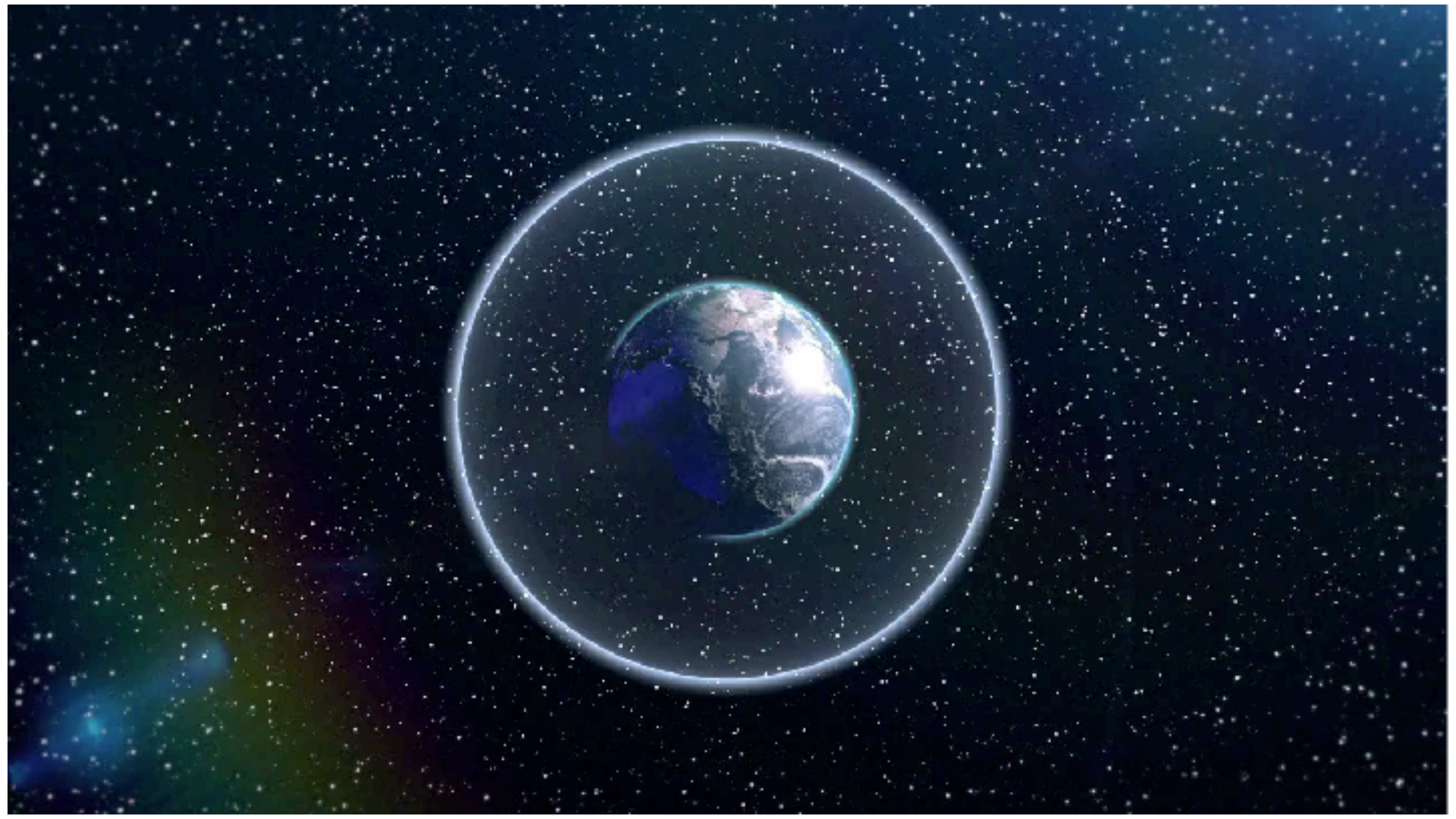

Potential noise sources

Correlated noise: noise sources that may affect both detectors almost simultaneously - potentially imitate a GW event: not captured by time shifts for the background estimation

Potential electromagnetic noise sources

- lightning strikes, solar events, solar-wind driven noise, RF communication
- if it is very significant, witnessed with high-SNR radio receiver and magnetometers

- global strikes cause Schumann resonance but the magnetic amplitude is an order of pico-Tesla (not affected in h(t))

- nearby lightning strikes produce audio-frequency magnetic fields by lightning current (>hundreds of kA); affect h(t), detected by the magnetometers at the detectors

- Electromagnetic fields in audio-frequency band generated by human and solar sources has no effect in h(t) at the detectors.

- Electromagnetic fields outside the audio-frequency band may be concerned because LIGO can be affected by the 9 and 45MHz RF modulations.

Cosmic ray showers - no coupling between showers and h(t)

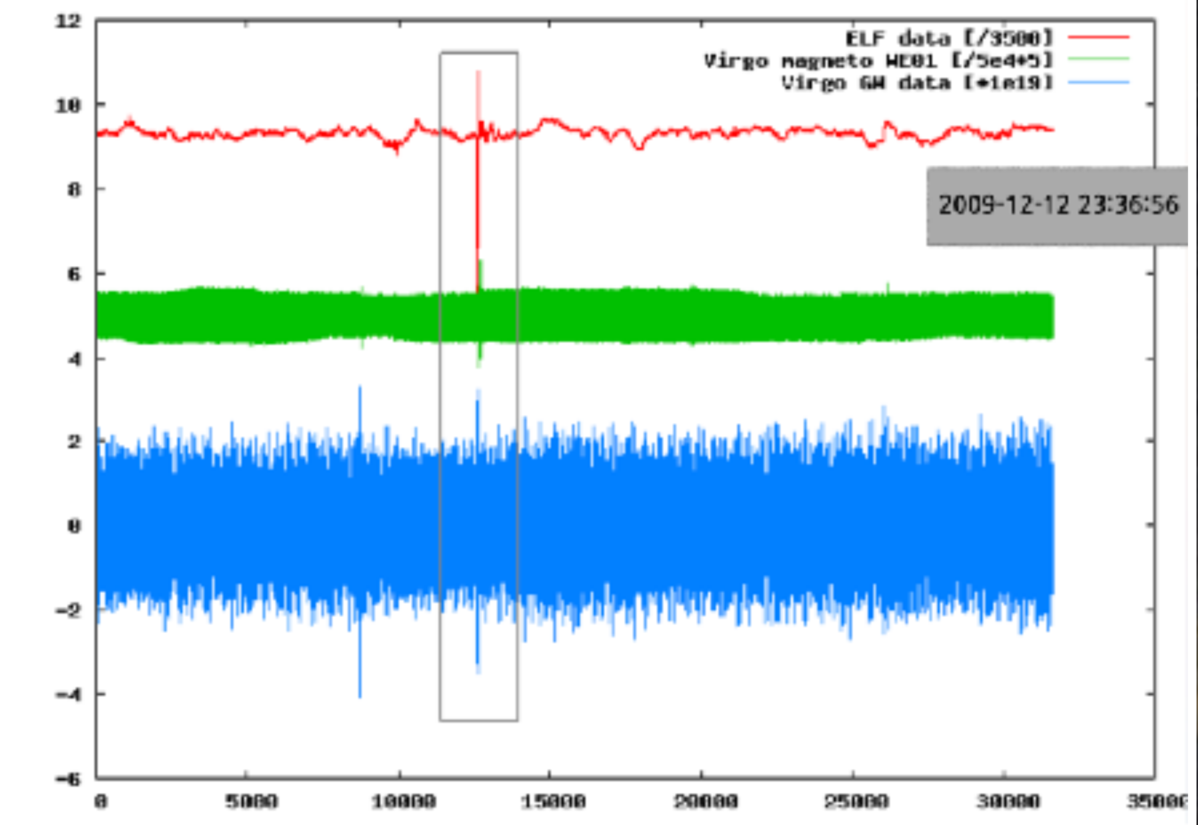

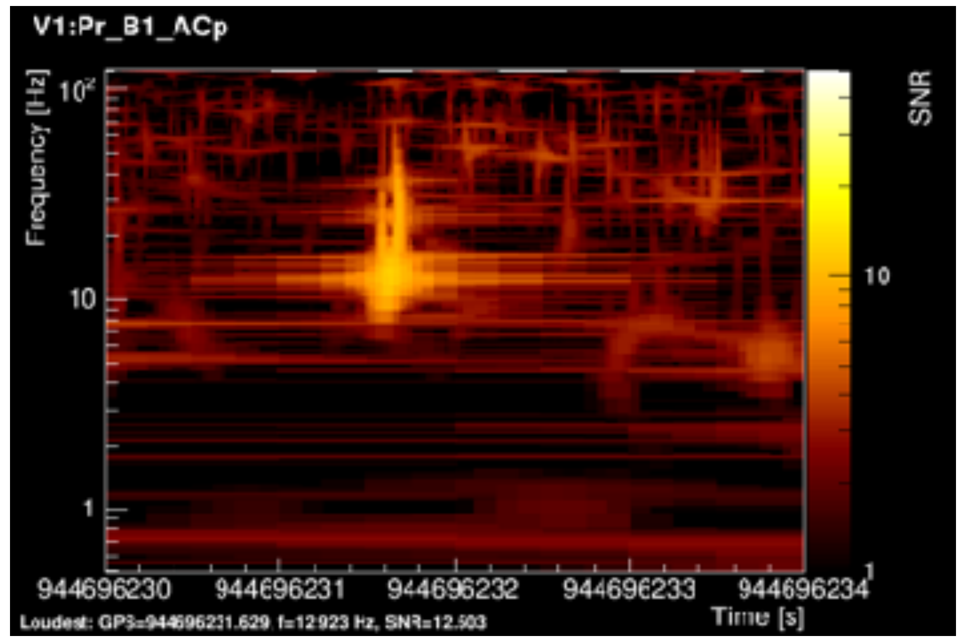

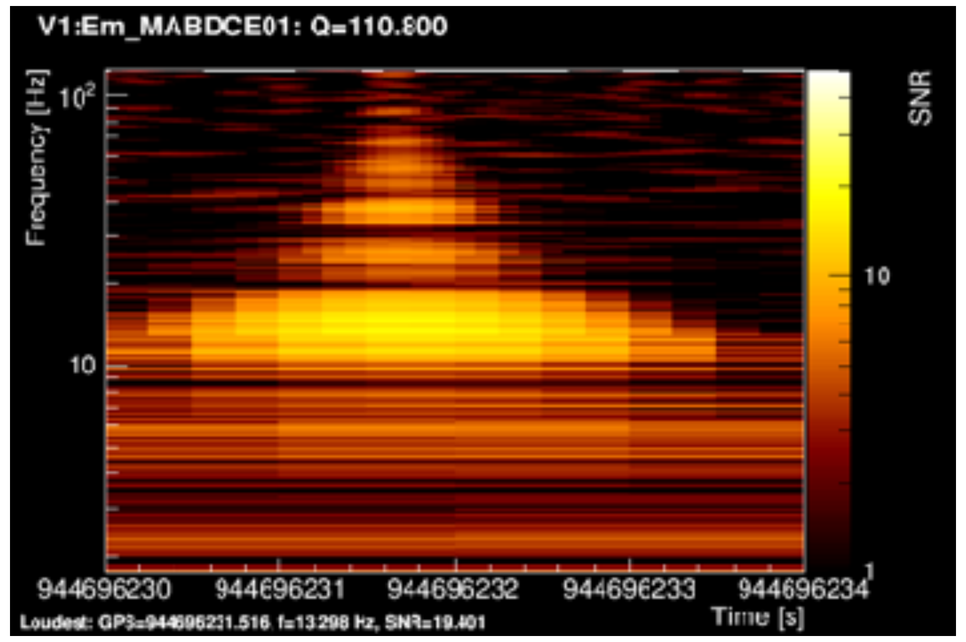

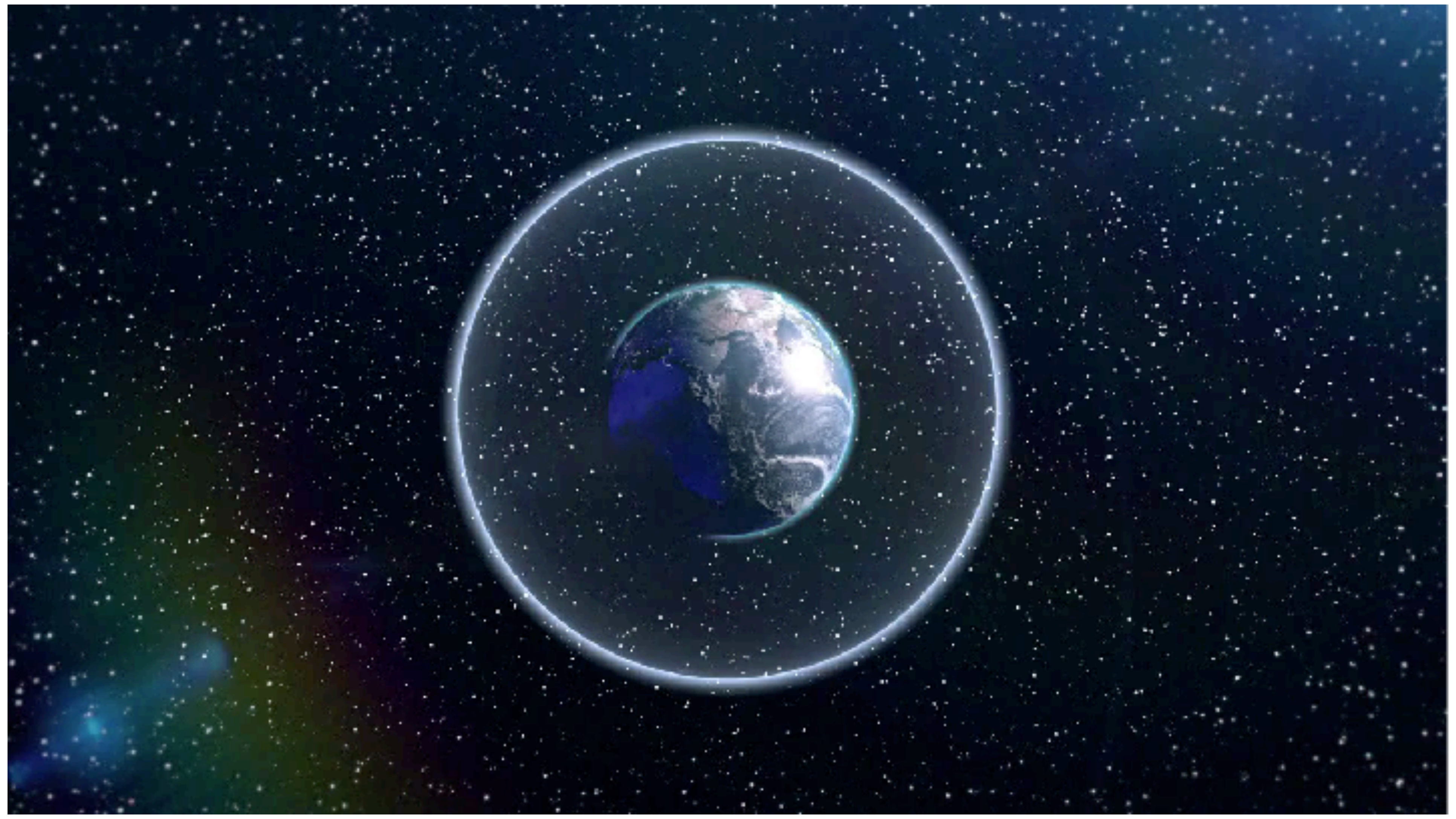

CAGMon

- Correlative Analysis Glitch Monitor

- **CAGMon** is a glitch monitoring tool between channels using correlation scores
- It is trigger-based and compute "Correlation Value" between GW and Aux. channels at a certain Trigger time
- With these values, one finds which aux. channels among many channels proposed by ETGs are statistically involved with the correlation to the glitch in GW channel
- For comparision, basic correlation algorithms are
  - Pearson's R correlation : linear correlation measure
  - Kendall's tau correlation : non-parametric linear measure by ranking
  - Maximal Information Coefficient : nonlinear measure
- Correlation Matrix (TFCMap) at a given trigger time
  - Correlation information between GW and Aux Channels
  - Linear and Nonlinear correlation information

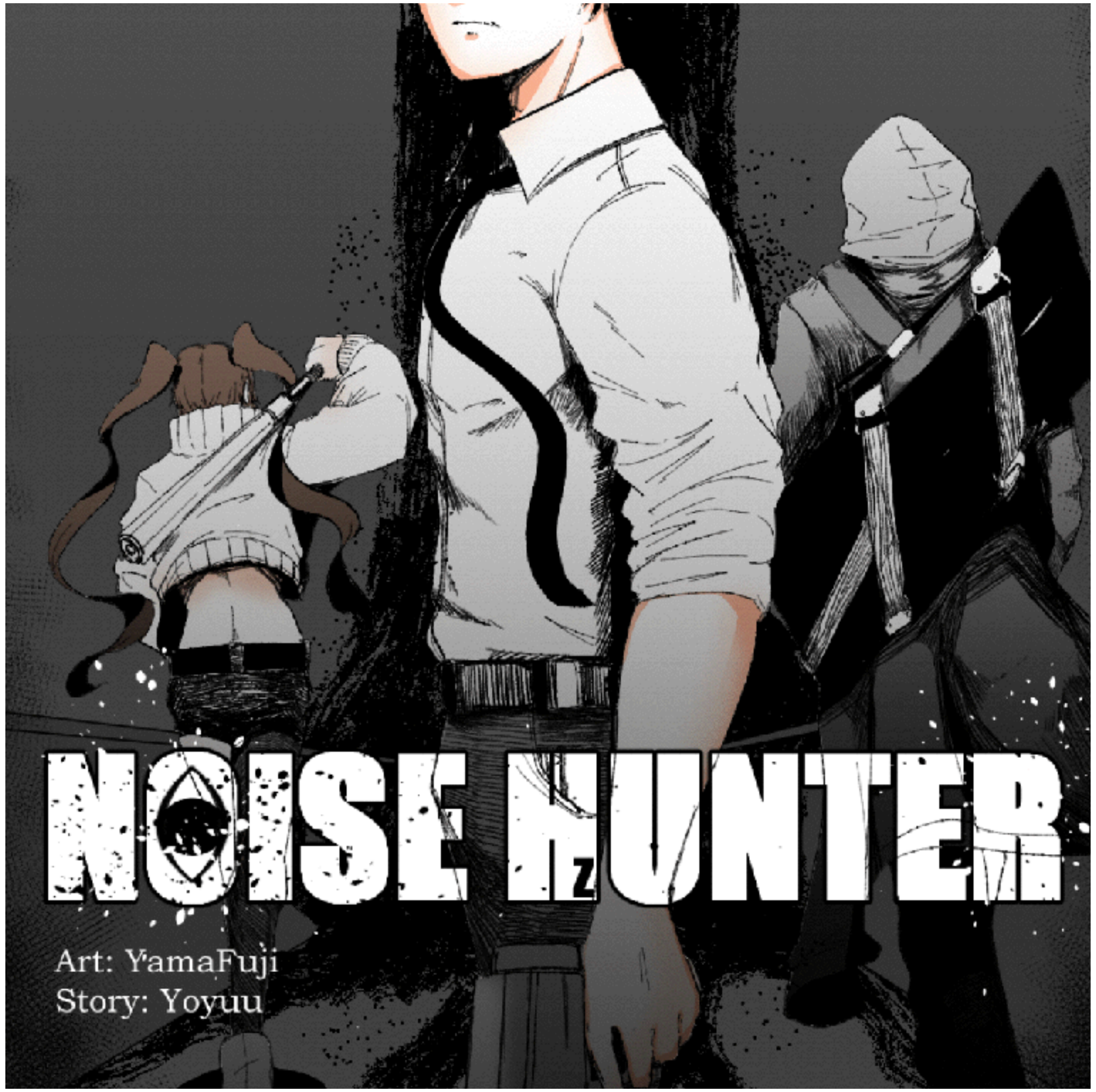

Pearson Product-moment Correlation Coefficient

- **Definition**

$$\rho = \frac{\sum_{i=1}^{n}(x_i - \bar{x})(y_i - \bar{y})}{\sqrt{\sum_{i=1}^{n}(x_i - \bar{x})^2}\sqrt{\sum_{i=1}^{n}(y_i - \bar{y})^2}}$$

cov. of x & y

std. of x & y

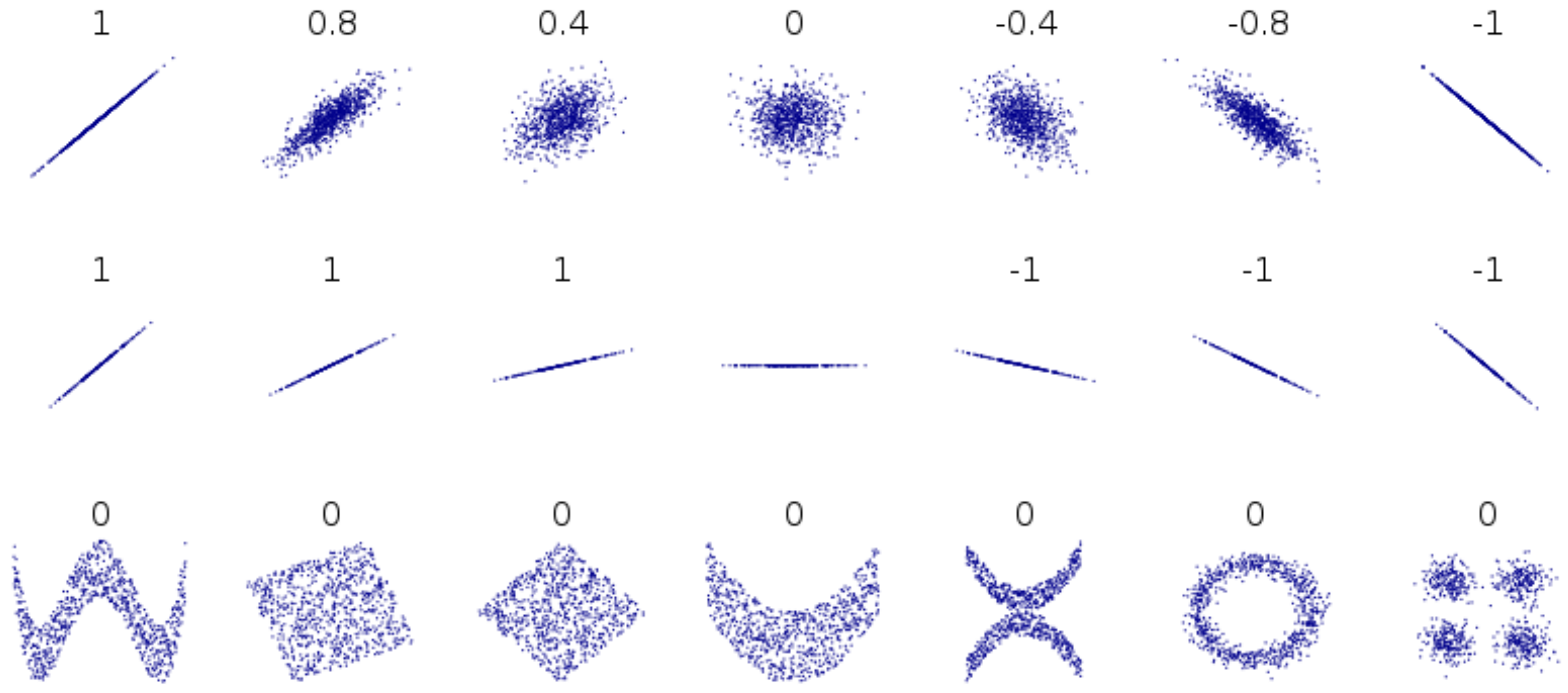

drawback for discriminating non-linearity

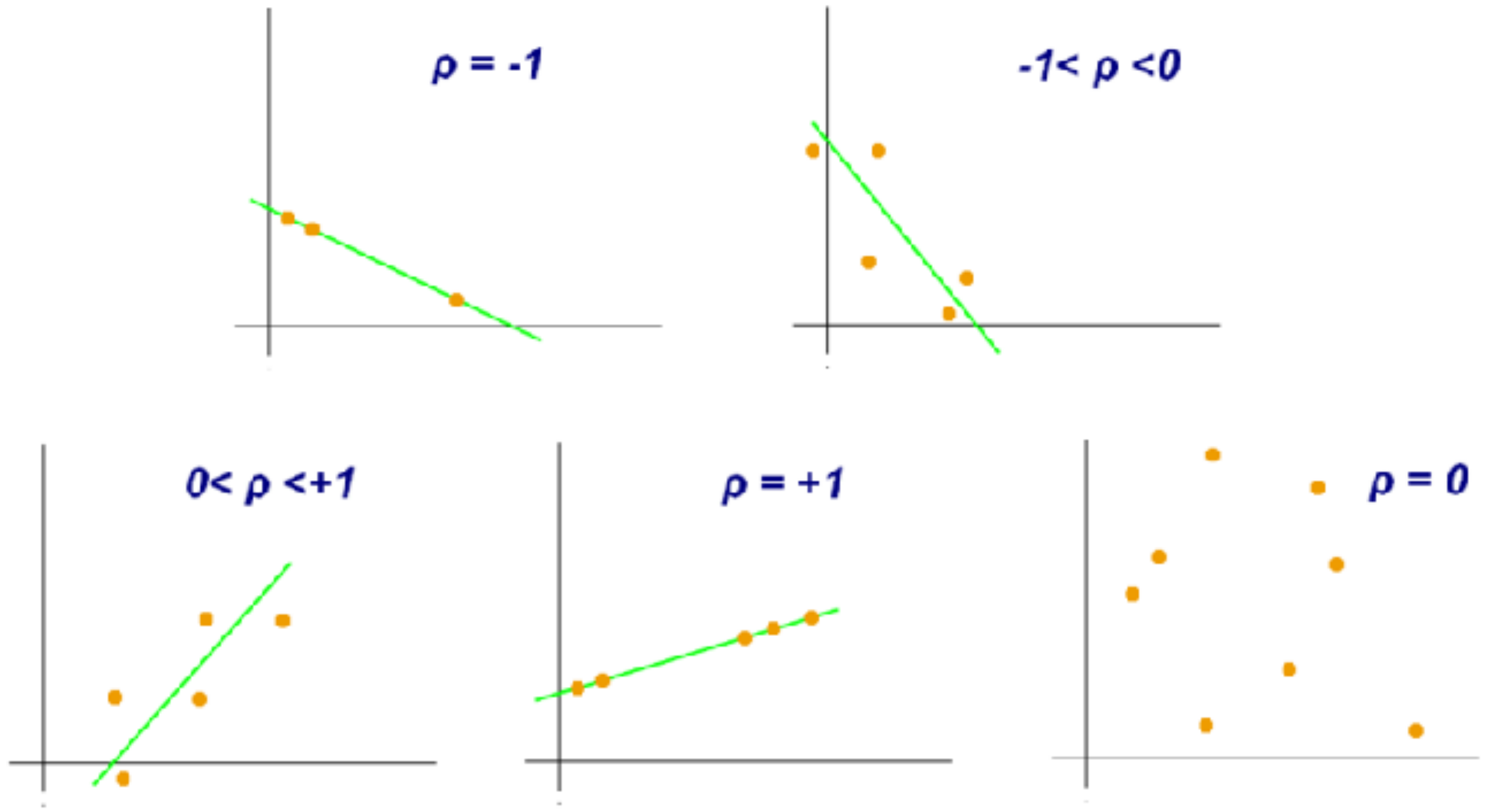

Interpretation of Pearson R Coefficient	
0.70~	Very strong positive correlation
0.40~0.69	Strong positive correlation
0.30~0.39	Moderate positive correlation
0.20~0.29	Weak positive correlation
-0.19~0.19	No or negligible correlation
-0.20~-0.29	Weak negative correlation
-0.30~-0.39	Moderate negative correlation
-0.40~-0.69	Strong negative correlation
-0.70~	Very strong negative correlation

Kendall's tau Correlation Score

- **Definition**

$$\tau = \frac{2(C-D)}{n(n-1)}$$

C: # of concordant pairs
D: # of disconcordant pairs

for two random variables, x and y,
- if xi > xj & yi > yj or xi < xj & yi < yj :concordant
- if xi > xj & yi < yj or xi < xj & yi > yj: disconcordant
tau has the value between -1 and 1.

tau	Interpretation
0.5~1.0 or -1.0~-0.5	Strong positive (negative) correlation
0.0~0.49 or -0.49~0.0	Weak positive (negative) correlation
0	No correlation

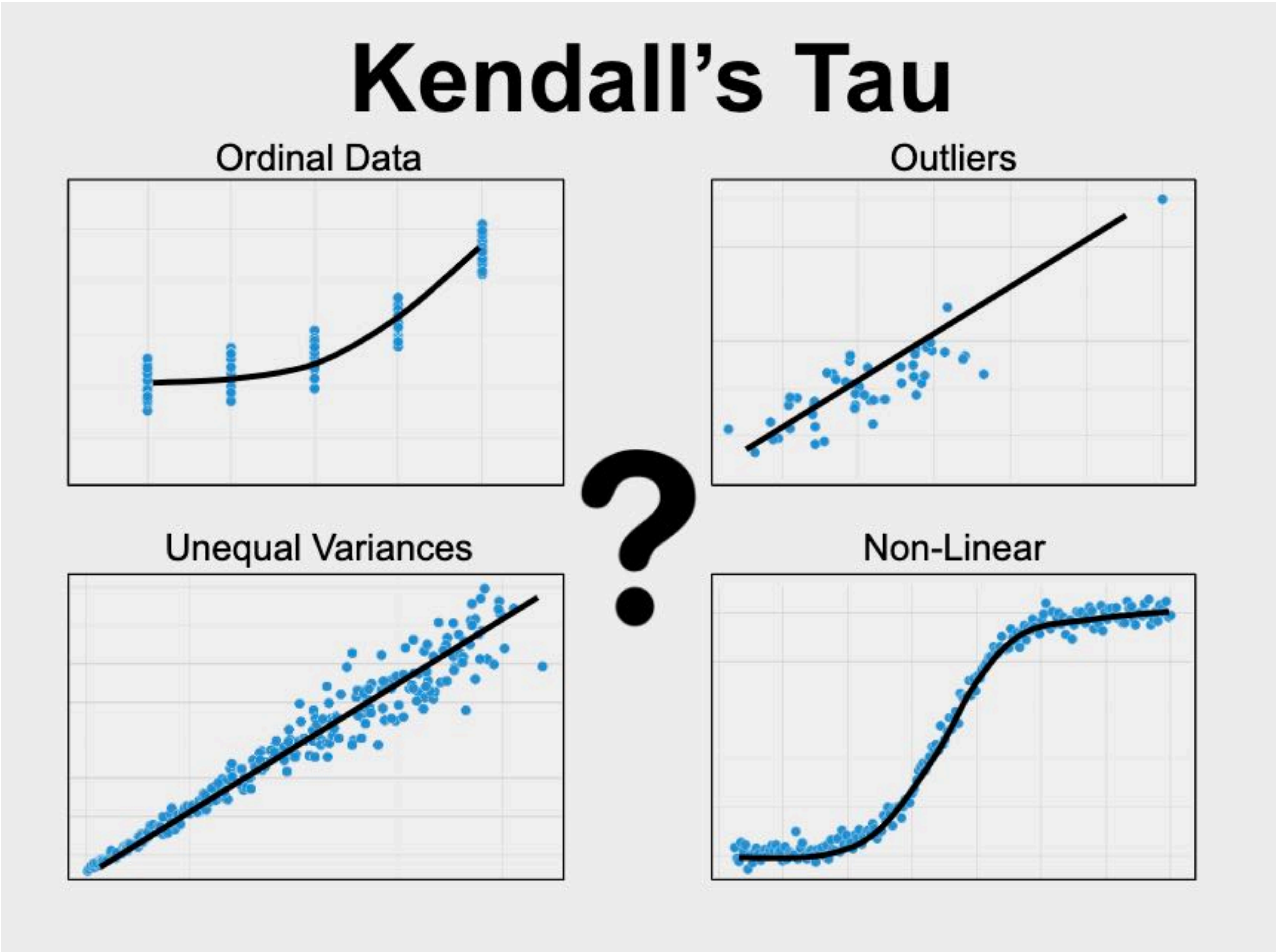

Maximal Information Coefficient

- **Definition** MIC uses the mutual information score defined by

$$I(X;Y) = \int_Y \int_X p(x,y) \log\left(\frac{p(x,y)}{p(x)p(y)}\right) dxdy$$

Maximum of Mutual information over all possible grid

$$I^*(D,x,y) = \max I(D|_G)$$

Characteristic Matrix

$$M(D)_{x,y} = \frac{I^*(D,x,y)}{\log \min\{x,y\}}$$

Maximal Information Coefficient

$$\mathrm{MIC}(D) = \max_{xy<B(n)} \{M(D)_{x,y}\}$$

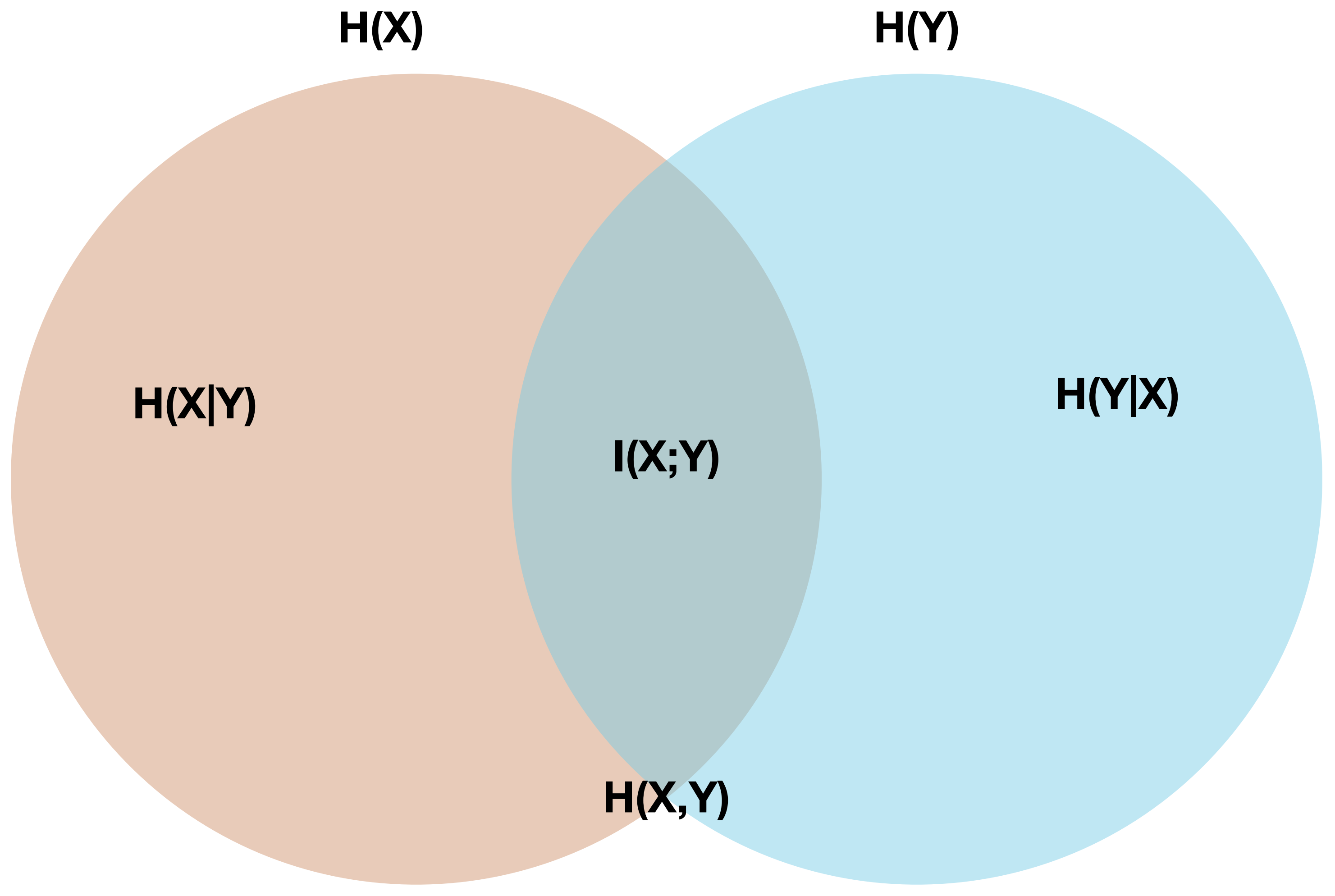

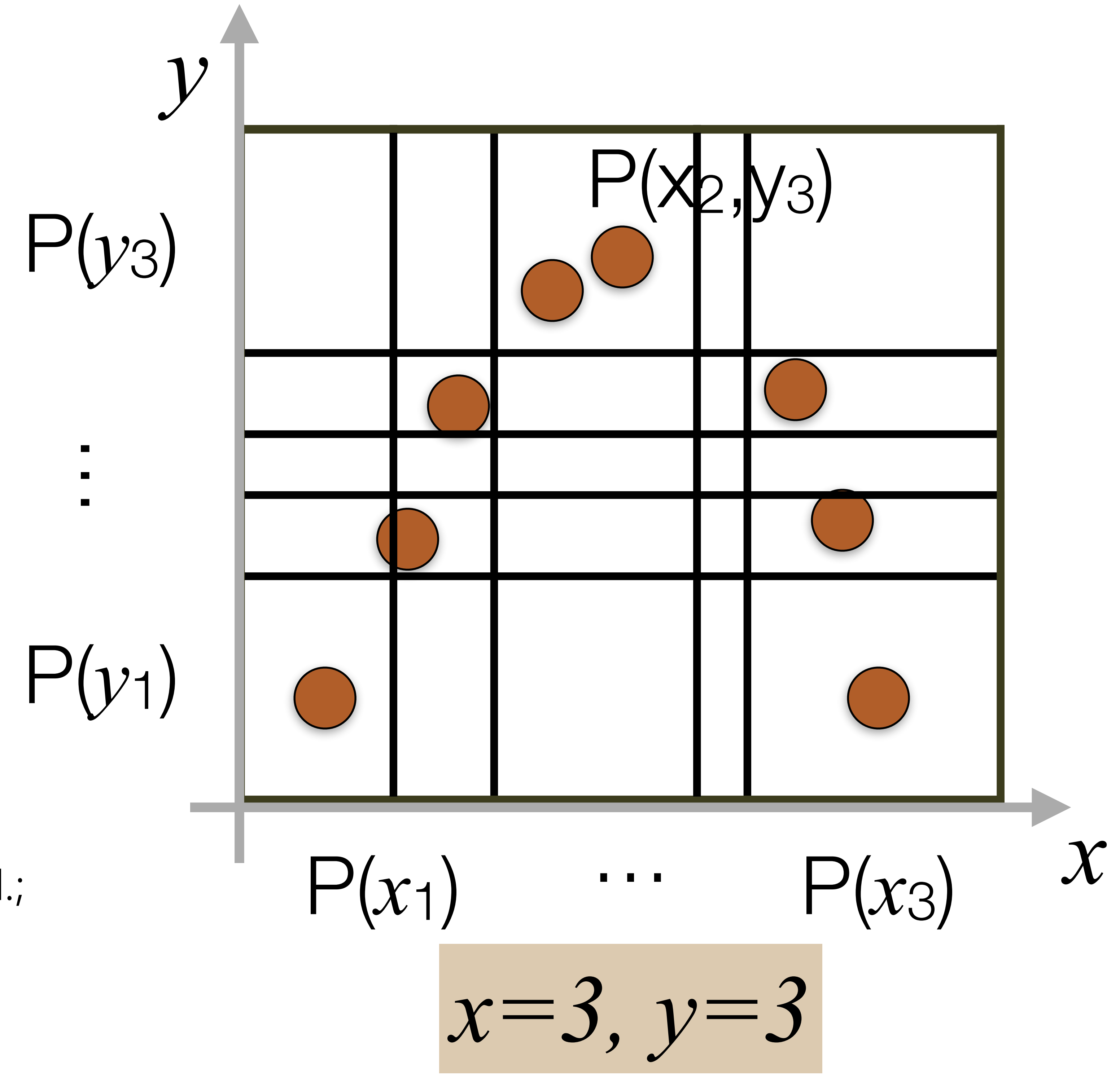

Ref) Reshef, D. N.; Reshef, Y. A.; Finucane, H. K.; Grossman, S. R.; McVean, G.; Turnbaugh, P. J.; Lander, E. S.; Mitzenmacher, M.; Sabeti, P. C. (2011). "Detecting Novel Associations in Large Data Sets". *Science*. **334** (6062): 1518–1524

Computing MIC: Simple Example

Probability of a box = # of data points in that box

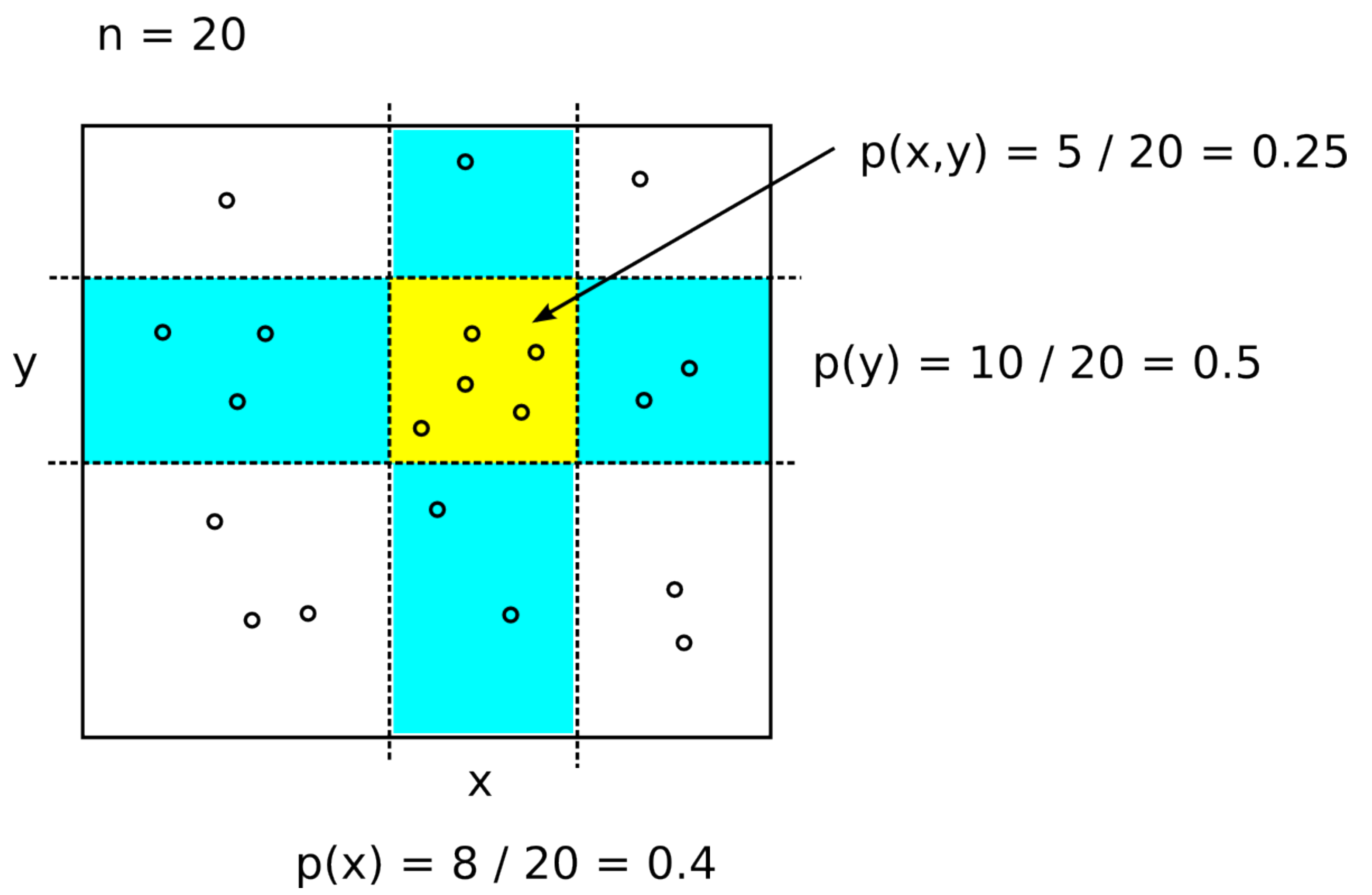

$$p(x,y)\log\left(\frac{p(x,y)}{p(x)\,p(y)}\right) = 0.25\log\left(\frac{0.25}{0.4\times 0.5}\right) \approx 0.056$$

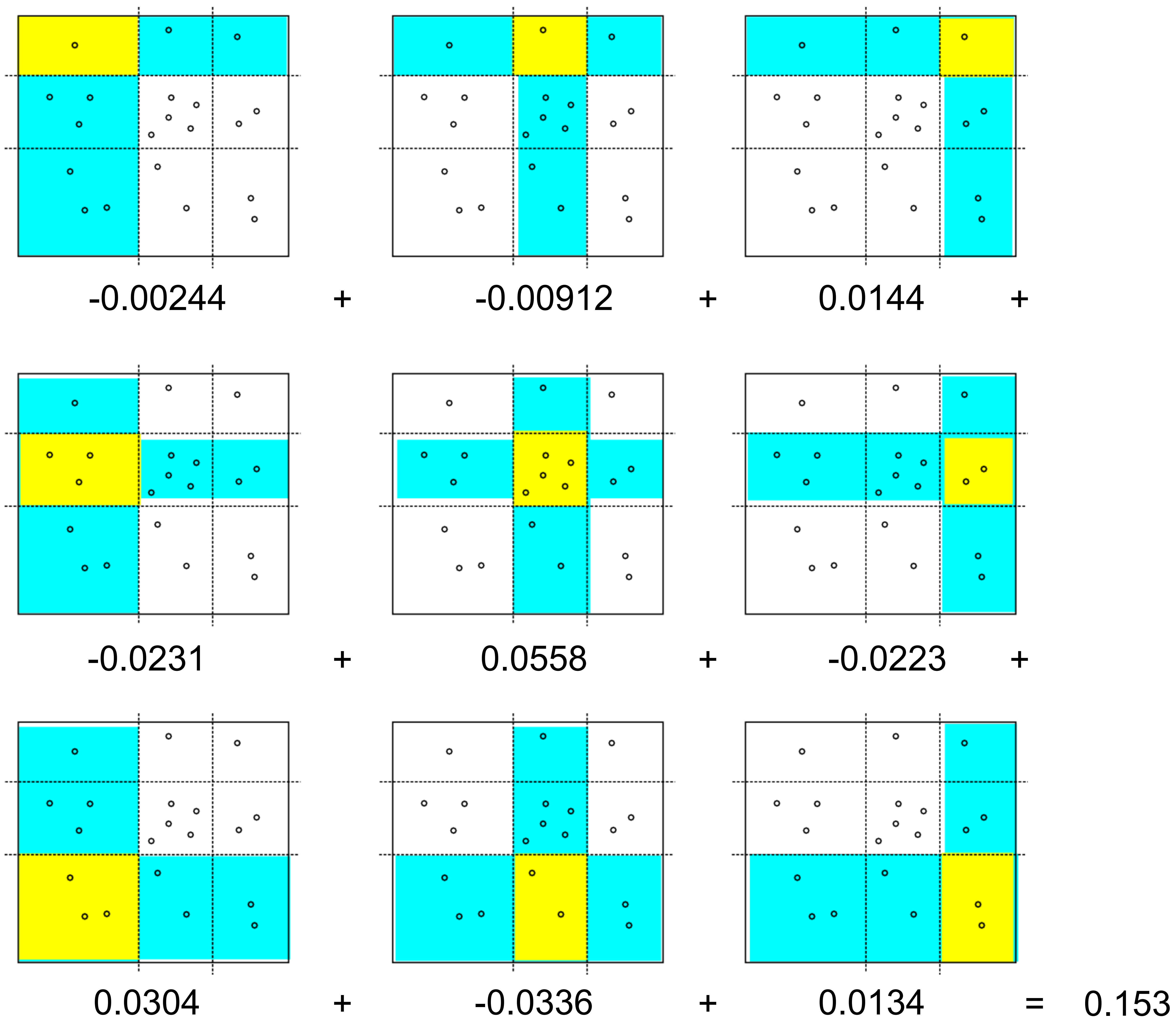

Comparison: Pearson R vs. MIC

For linear relationship,
MIC ~ (Pearson r)^2

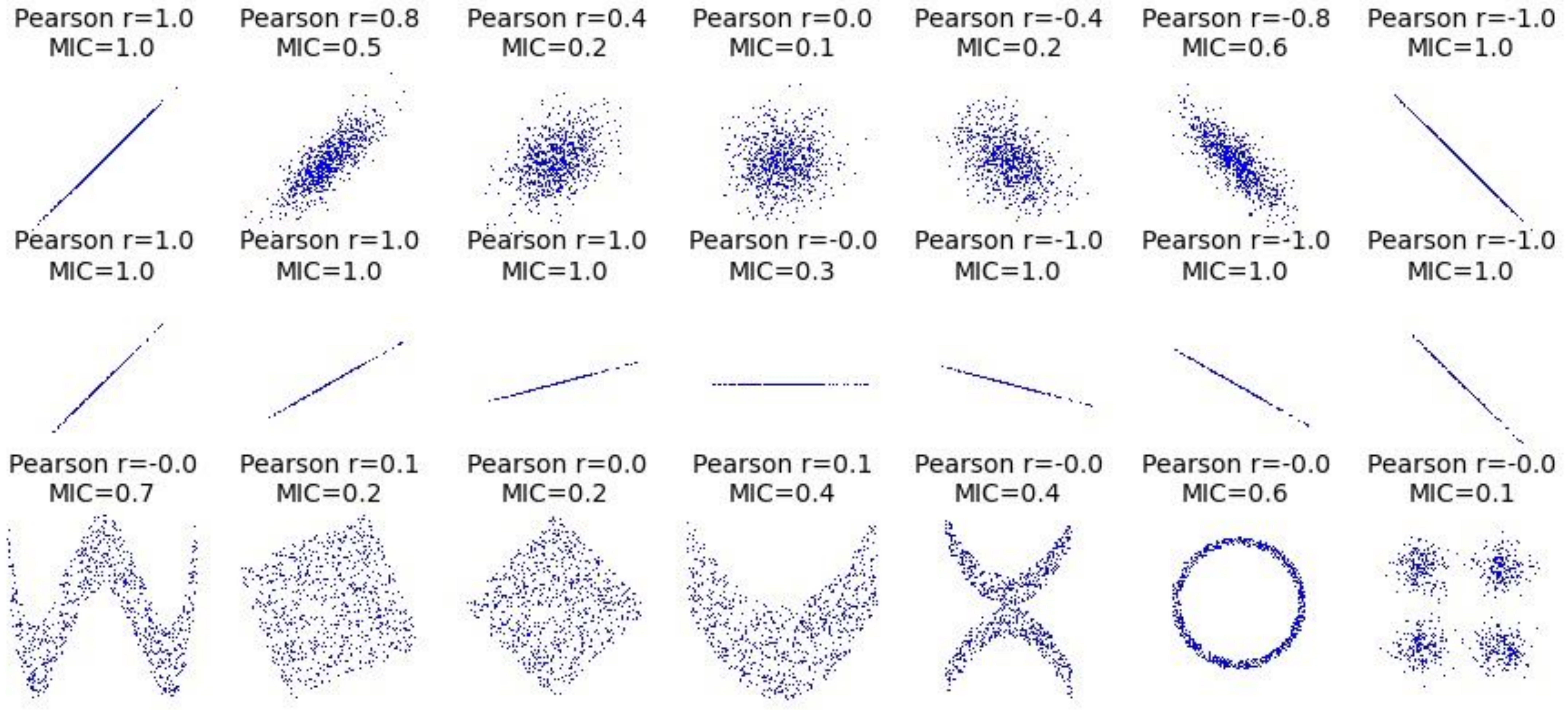

CAGMon: Feasibility Test

Question:

At a given trigger time,
ETG finds that
the trigger in GW channel
has timing-coincidence
with triggers in 11 auxiliary channels

```
GPS(sec+ms) 9xxxxxxx.xxx 516.0 SNR 0.0 signf 11.006
ChName signf dt dur freq npts

AuxCh1 8.775 -0.073 0.003 1352.3 711.0
AuxCh2 9.483 -0.063 1.862 269.8 966.0
AuxCh3 14.982 0.031 0.85 32.7 40.0
AuxCh4 8.222 0.046 0.103 32.6 9.0
AuxCH5 29.763 0.0 1.357 34.0 46.0
AuxCh6 31.797 0.0 1.59 34.0 46.0
AuxCh7 54.079 -0.016 1.482 34.0 46.0
AuxCh8 13.848 -0.016 0.264 34.0 32.0
AuxCh9 53.882 -0.016 1.41 34.0 49.0
AuxCh10 10.752 0.015 0.331 32.0 55.0
AuxCh11 18.932 -0.016 0.746 41.2 102.0
```

Q) How many triggers in those channels are statistically related to the glitch in the GW channel from the viewpoint of data correlation?
Furthermore, can we detect a nonlinearity for computing MIC between channels?

Trigger-based Analysis Scheme

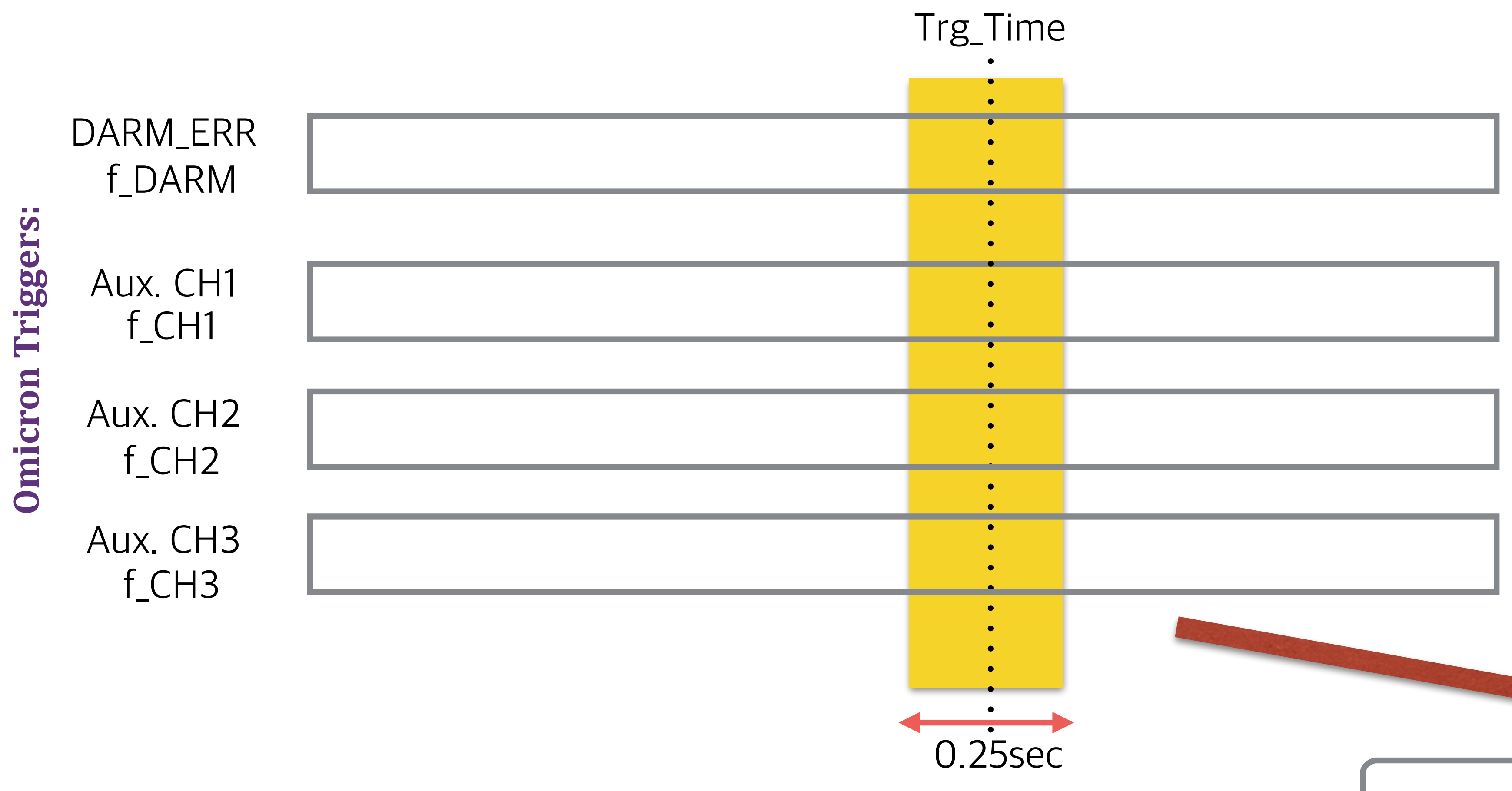

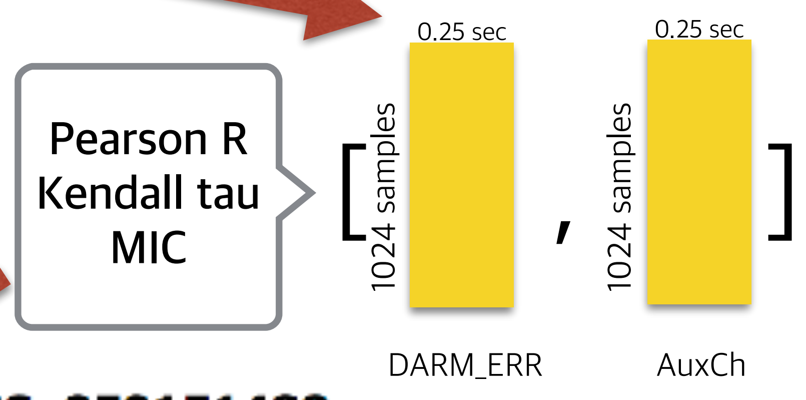


```
GPS(sec+ms) 959167951.0 516.0 SNR 0.0 signf 11.006
ChIndx ChName signf dt dur freq npts
48 L0_PEM-LVEA_MIC 8.775 -0.073 0.003 1352.3 711.0
72 L1_OMC-ASC_POS_X_IN1_DAQ 9.483 -0.063 1.862 269.8 966.0
86 L1_OMC-QPD4_P_OUT_DAQ 14.982 0.031 0.85 32.7 40.0
87 L1_OMC-QPD4_Y_OUT_DAQ 8.222 0.046 0.103 32.6 9.0
153 L1_ASC-ITMX_P 29.763 0.0 1.357 34.0 46.0
155 L1_ASC-ITMY_P 31.797 0.0 1.59 34.0 46.0
168 L1_ASC-WFS3_IP 54.079 -0.016 1.482 34.0 46.0
169 L1_ASC-WFS3_IY 13.848 -0.016 0.264 34.0 32.0
170 L1_ASC-WFS4_IP 53.882 -0.016 1.41 34.0 49.0
183 L1_LSC-PRC_CTRL 10.752 0.015 0.331 32.0 55.0
187 L1_LSC-REFL_Q 18.932 -0.016 0.746 41.2 102.0
```

Omicron generates 11 aux. channel triggers in 32-4096 Hz

Check the instrumental components that is responsible for this suspecting channel by Detector operators

- **GPS: 959151488**
  - Trigger time: 959151544.227, f_DARM = 949.469Hz
  - AuxChannel Triggers : OM_TRGS_959151544.227.txt
  - Channel List by CAGMon

Channel Name	Frequency Range	Pearson R	Ktau	MIC
L1_OMC-QPD1_P_OUT_DAQ_32_2048	512-1024	0.43	0.09	0.13
L1_OMC-QPD1_SUM_OUT_DAQ_32_2048	512-1024	0.39	0.13	0.16
L1_OMC-QPD2_P_OUT_DAQ_32_2048	512-1024	0.59	0.04	0.13
L1_OMC-QPD2_SUM_OUT_DAQ_32_2048	512-1024	0.49	0.05	0.13

  - Correlation Map at Trigger Time by CAGMon

Pearson's R	Kendall's tau	Maximal Information Coefficient
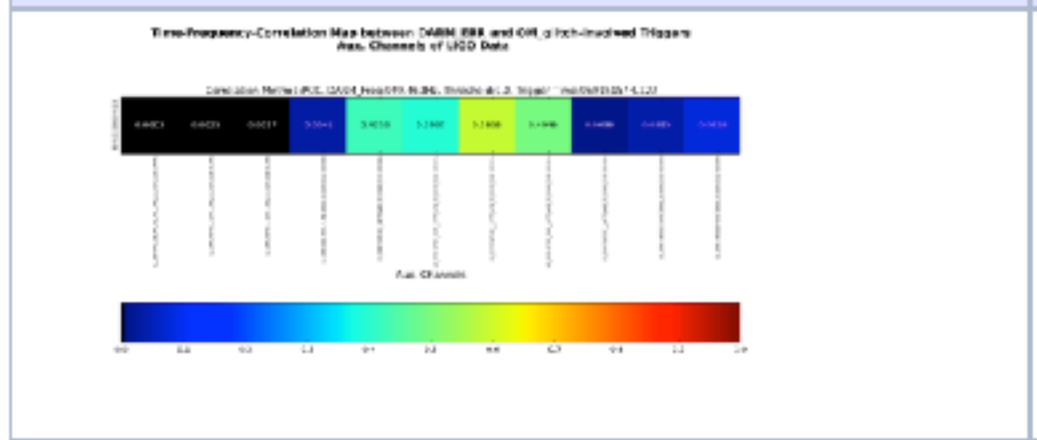	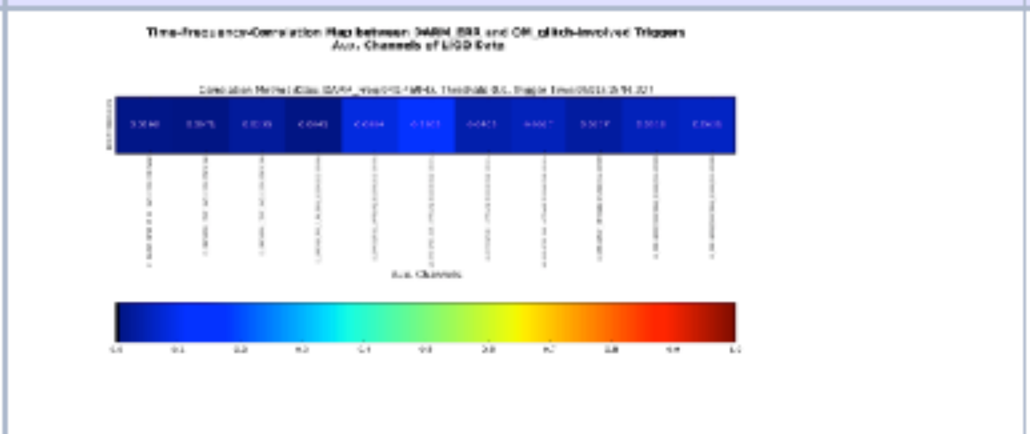	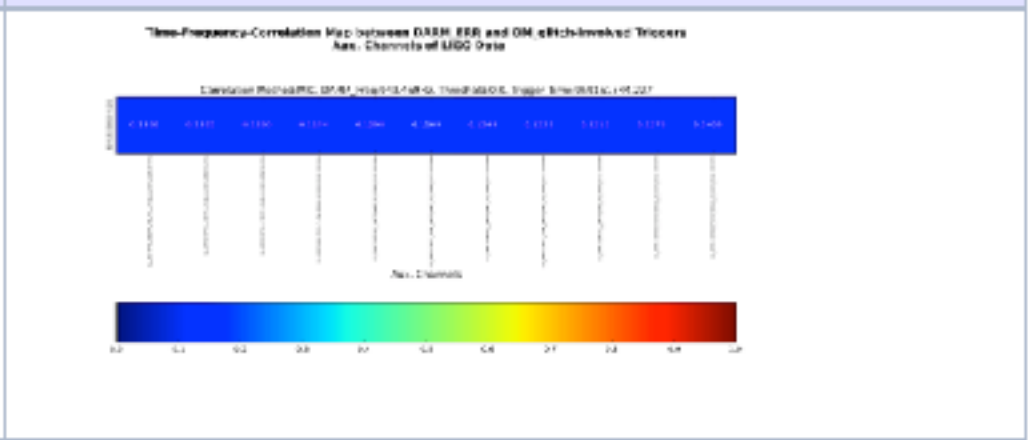

- **select channels with corr. value > 0.25 (> mild correlation)**

Trigger-based Analysis Scheme: Nonlinear Example

```
GPS(sec+ms) 959203889.0 812.0 SNR 0.0 signf 25.918
ChIndx ChName signf dt dur freq npts
58 L1_ISI-OMC_CONT_RY_IN1_DAQ 8.409 0.04 0.011 344.8 228.0
79 L1_OMC-QPD1_SUM_OUT_DAQ 647.327 -0.093 6.28 80.7 1893.0
84 L1_OMC-QPD3_P_OUT_DAQ 607.505 -0.046 2.983 100.2 984.0
85 L1_OMC-QPD3_Y_OUT_DAQ 673.485 -0.099 2.14 151.7 984.0
86 L1_OMC-QPD4_P_OUT_DAQ 754.049 -0.042 2.328 195.9 982.0
145 L1_TCS-ITMX_PD_ISS_OUT_AC 8.822 -0.007 0.02 70.4 49.0
```

Omicron generates 6 aux. channel triggers in 32-4096 Hz

- **GPS: 959203840**
  - Trigger time: 959203889.812, f_DARM = 34.3594Hz
  - AuxChannel Triggers : OM_TRGS_959203889.812.txt
  - Channel List by CAGMon

Channel Name	Frequency Range	Pearson R	Ktau	MIC
L1_OMC-QPD3_P_OUT_DAQ_8_1024	64-128	0.02	0.04	0.43
L1_TSC-ITMX_PD_ISS_OUT_AC_8_1024	64-128	0.02	0.01	0.31

  - Correlation Map at Trigger Time by CAGMon

Pearson's R

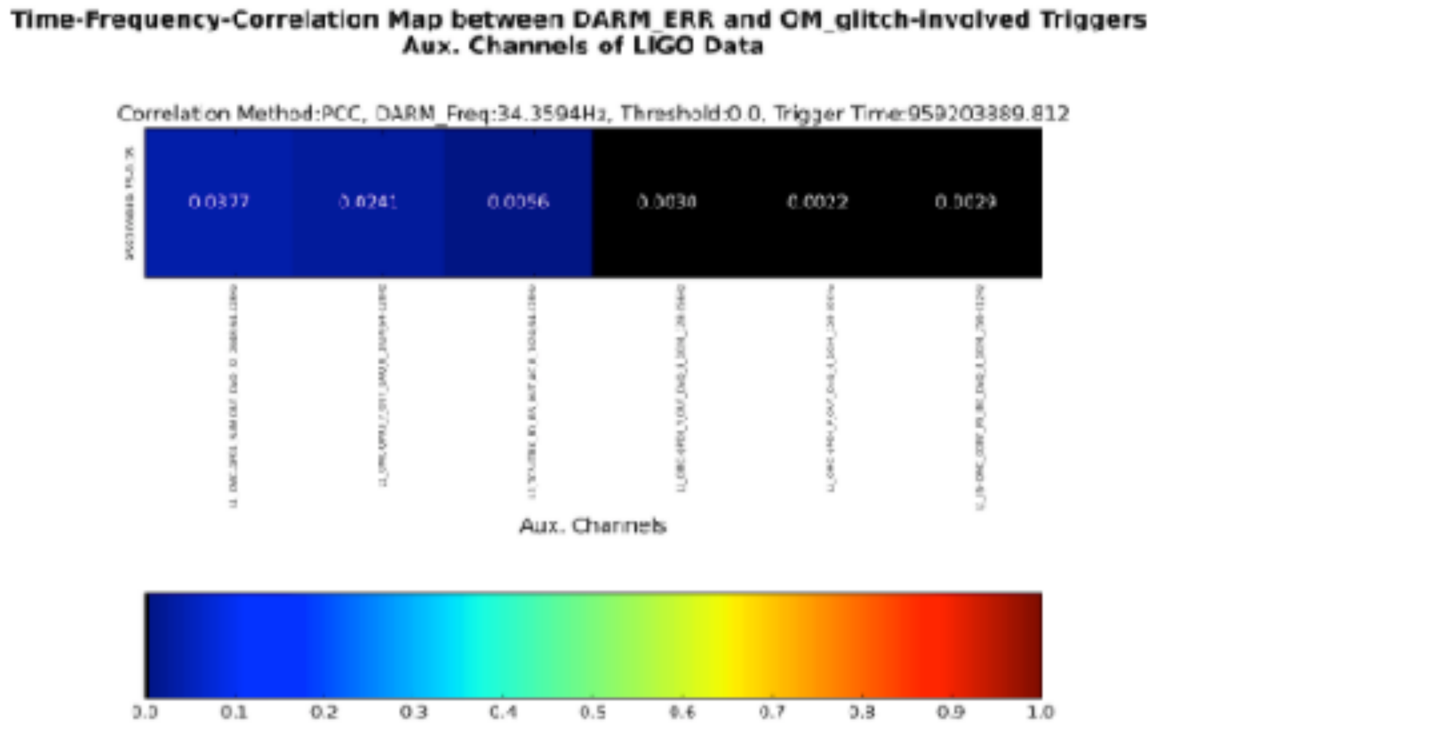

Kendall's tau

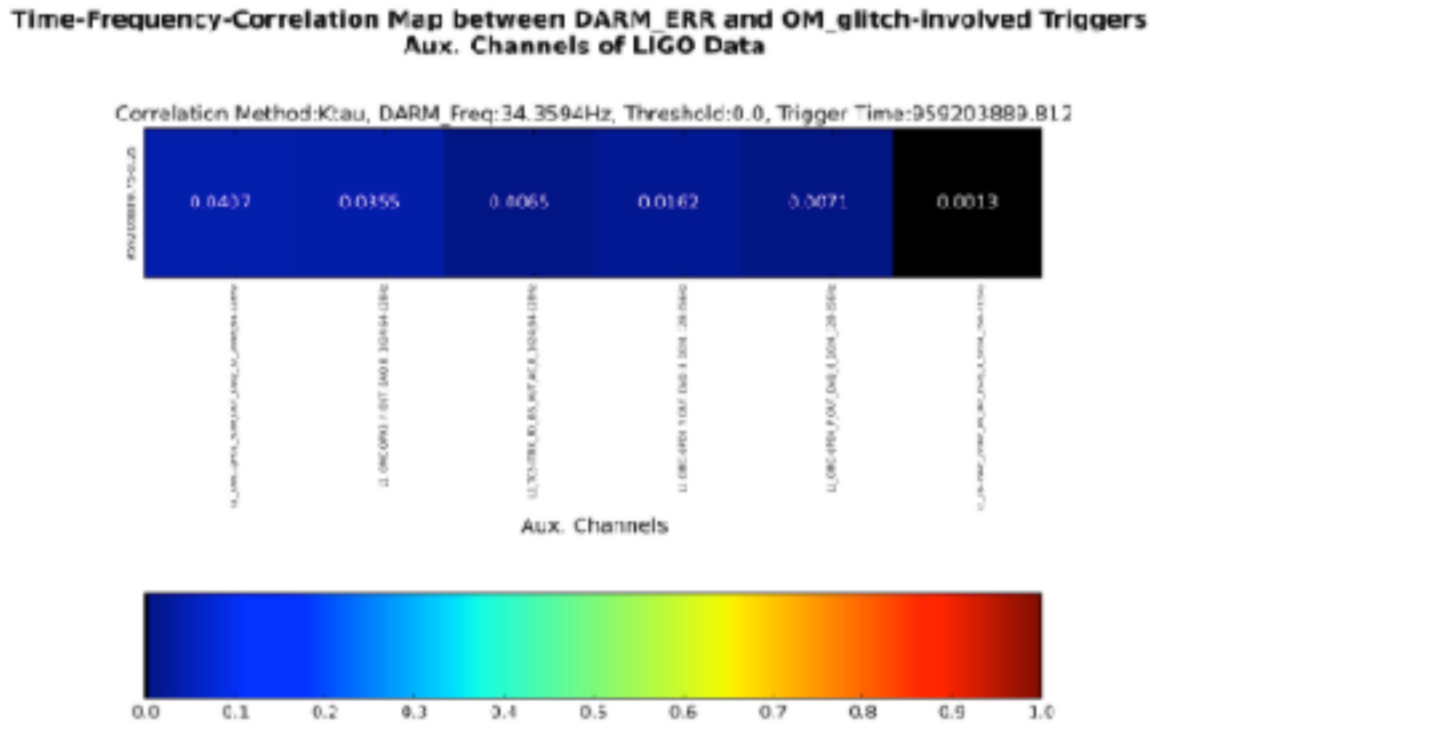

Maximal Information Coefficient

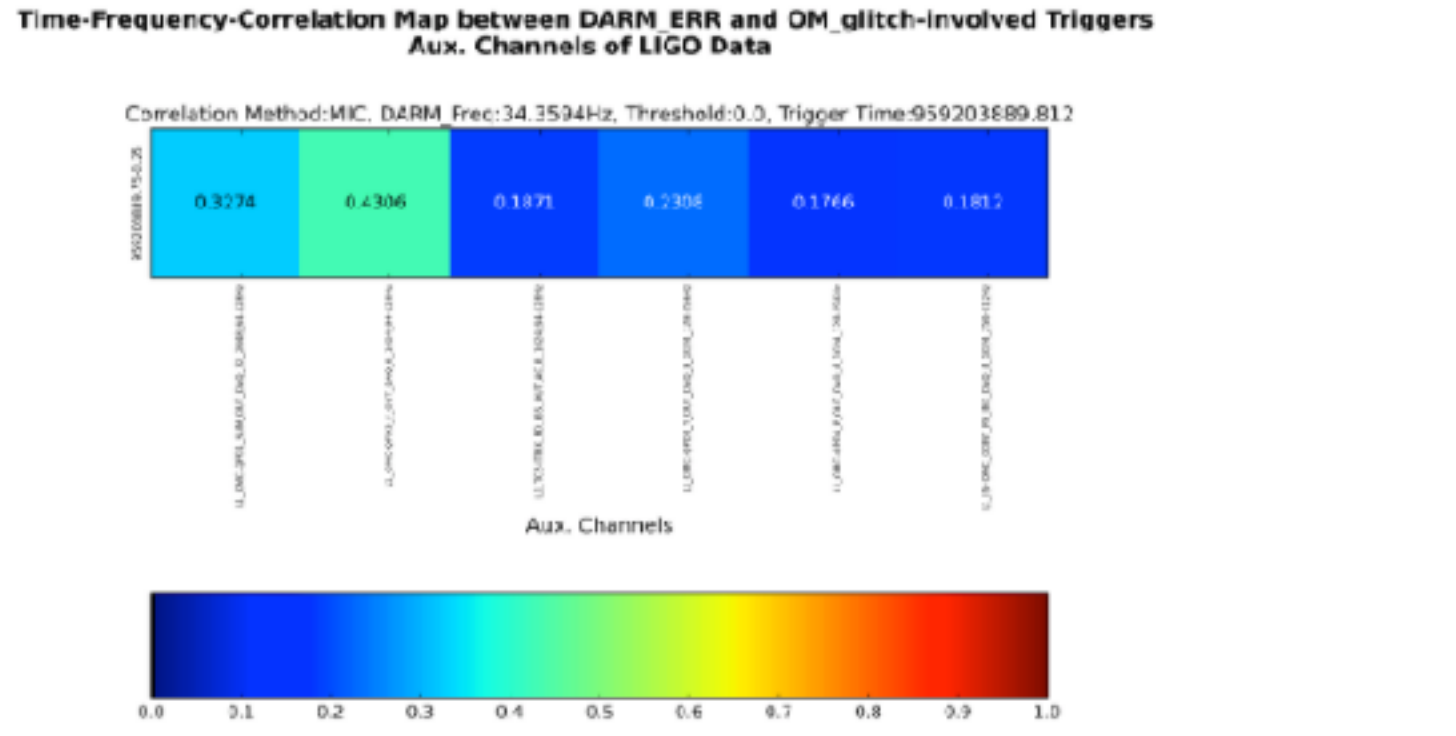

- **select channels with corr. value > 0.25 (> mild correlation)**

Time-Series Analysis Scheme

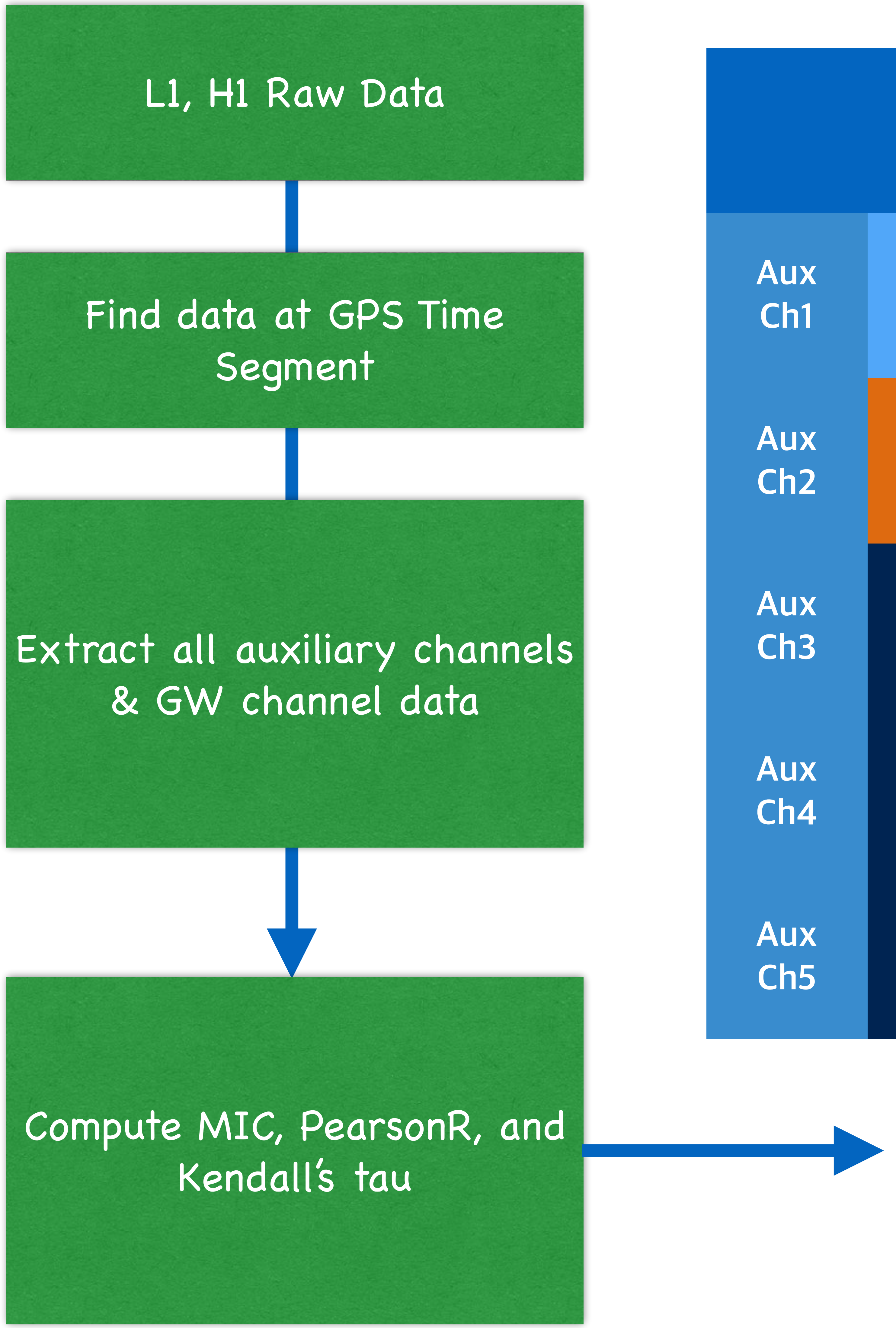

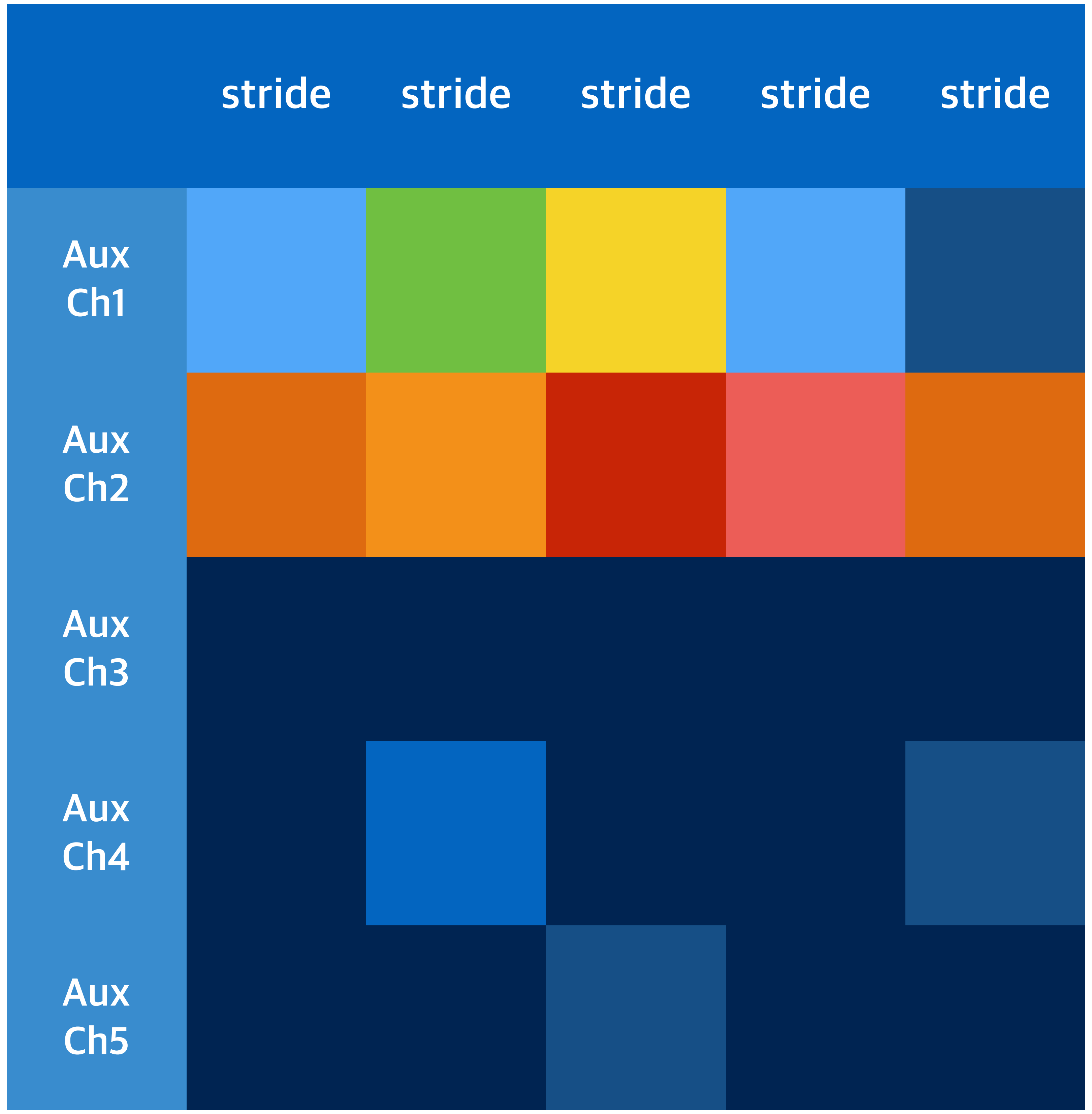

Correlation Matrix

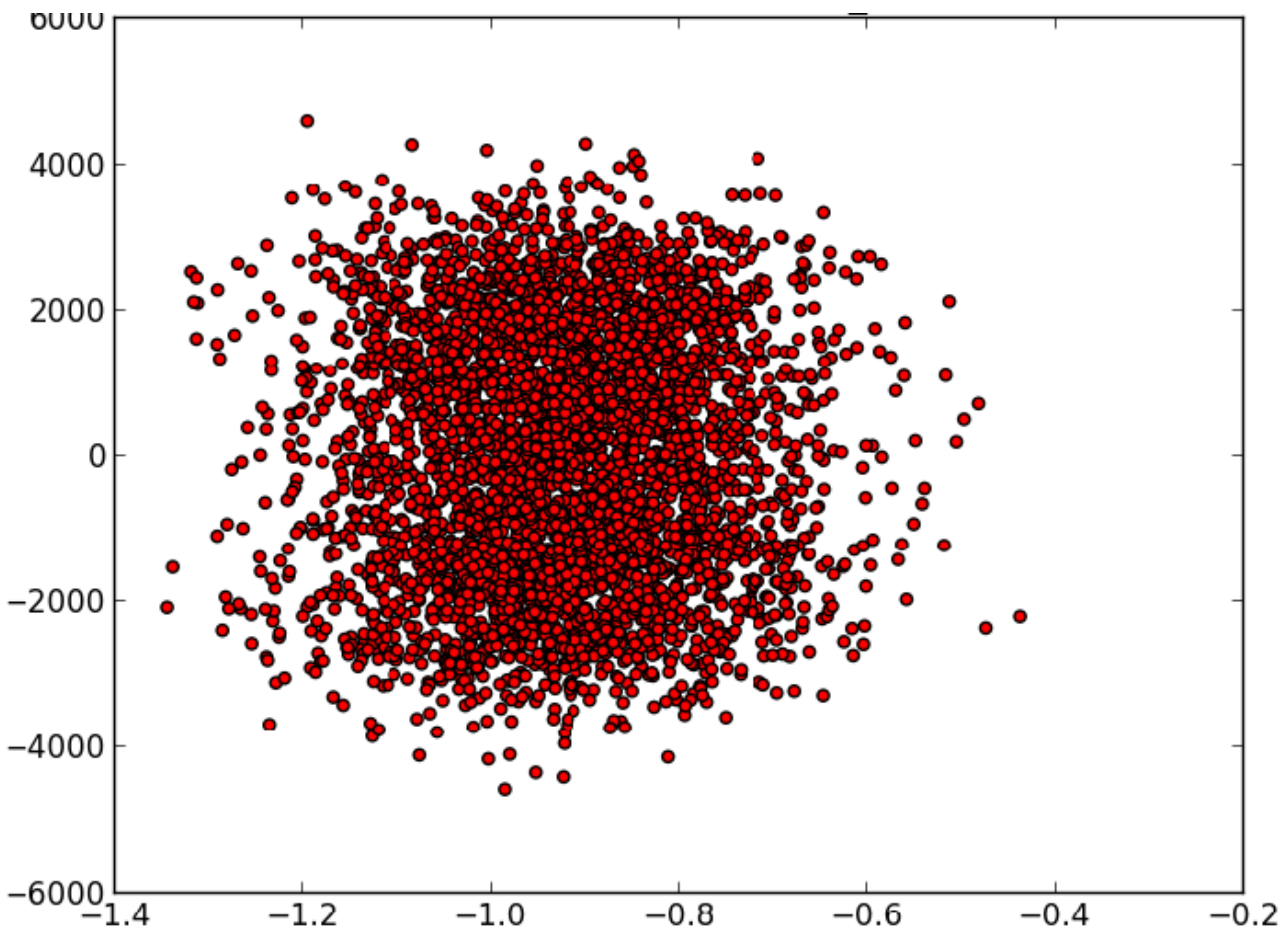

Scattered Plot

Time Series Monitoring

ASC (Alignment Sensing Control) Channels - nonlinearity

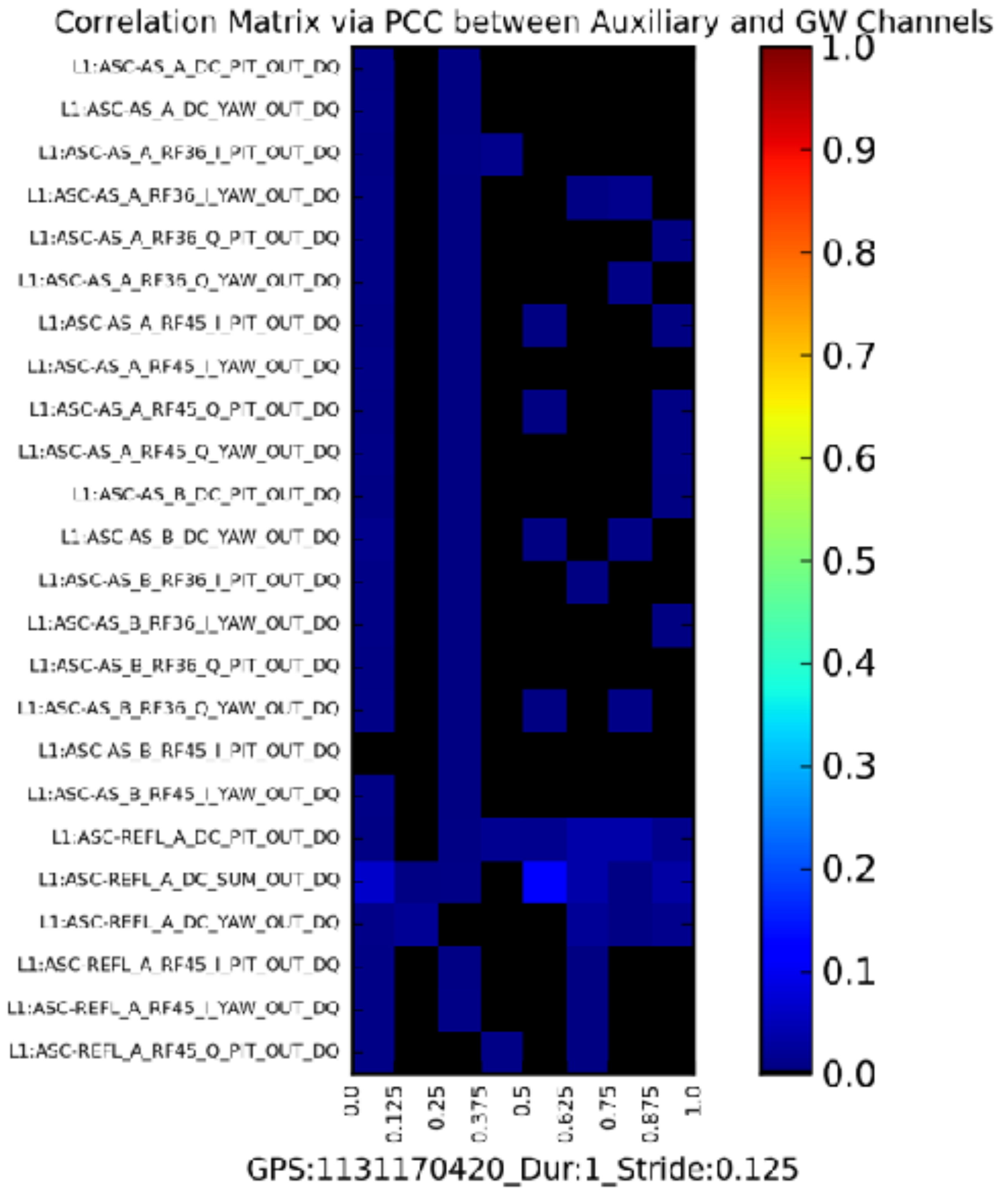

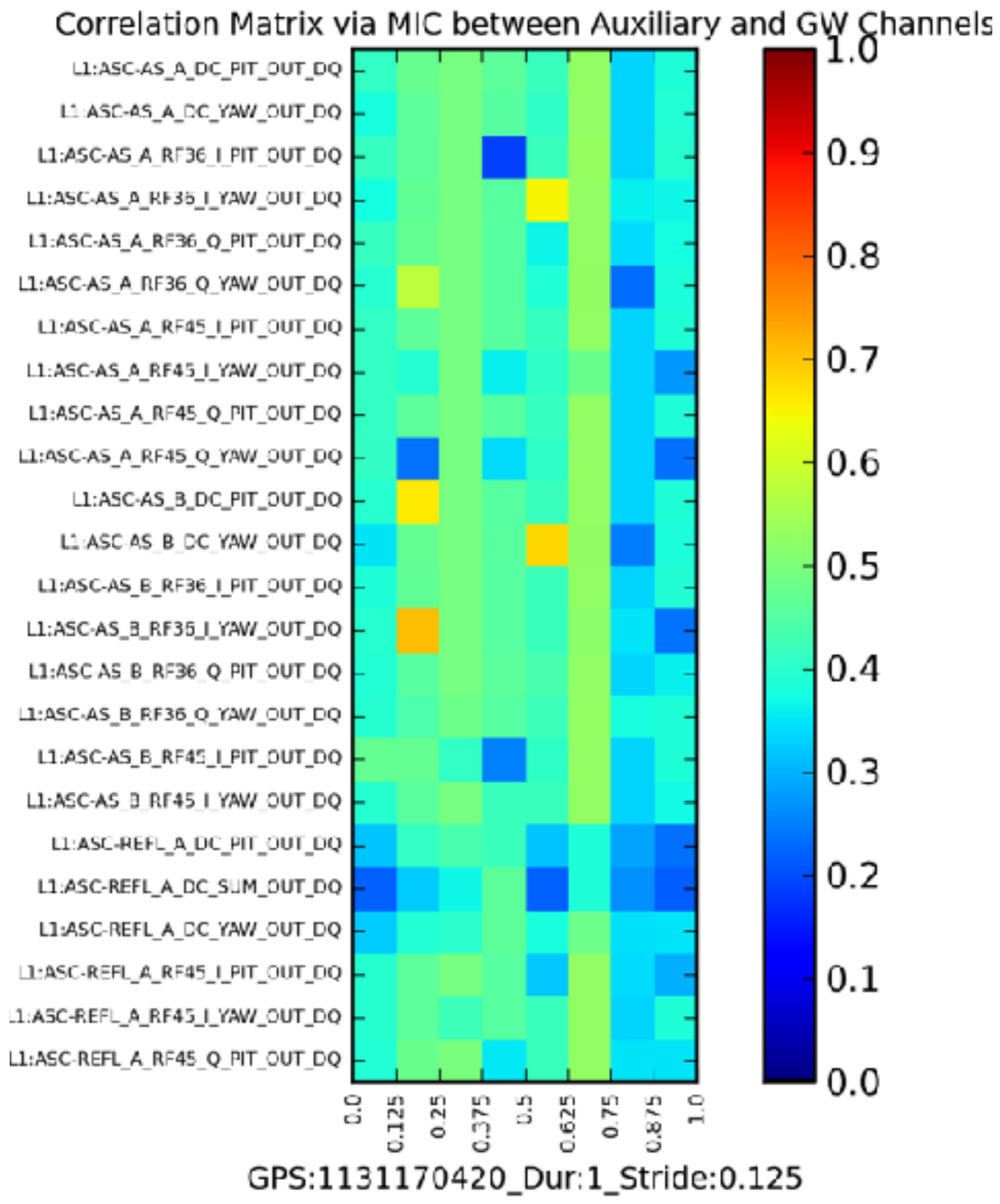

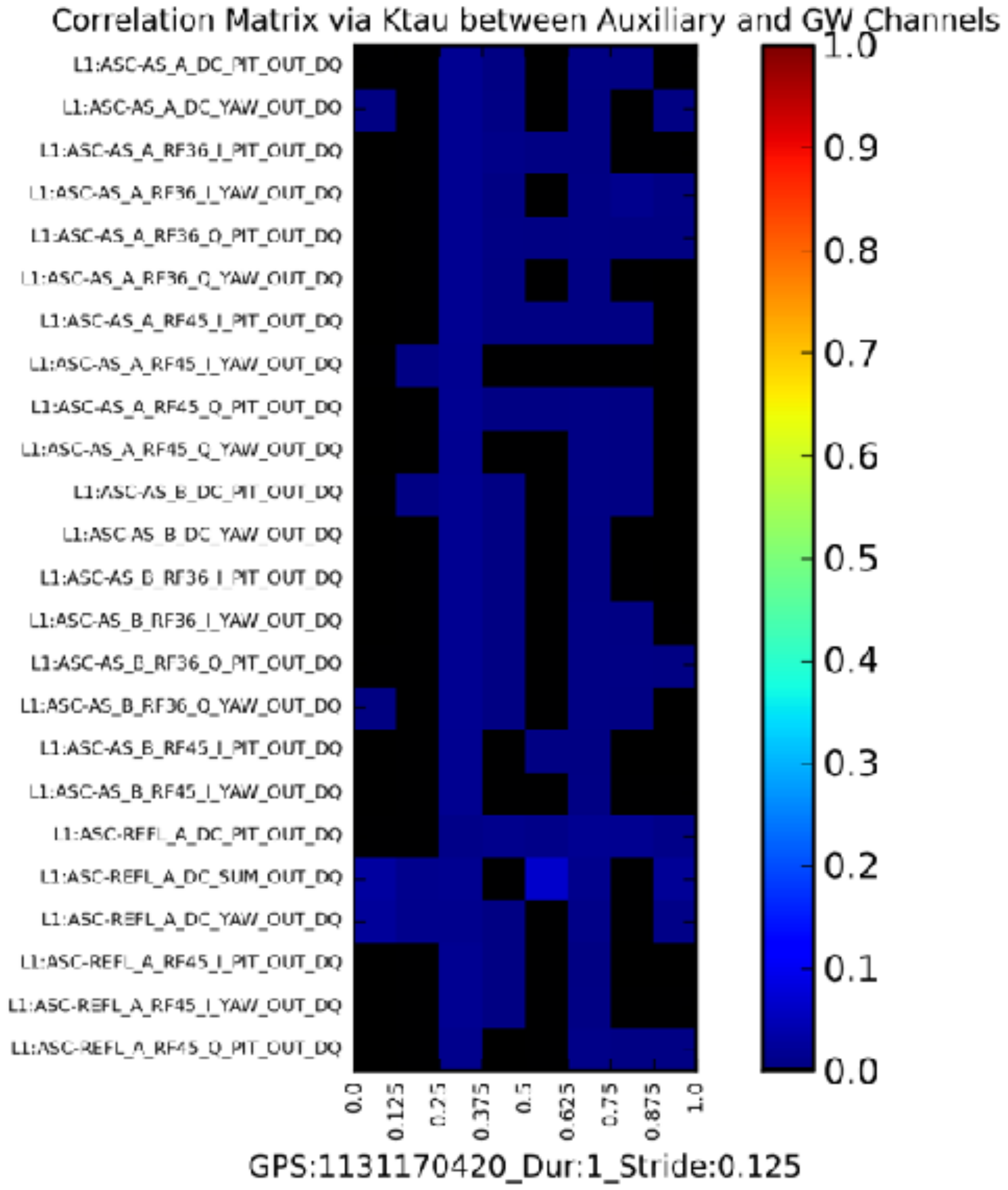

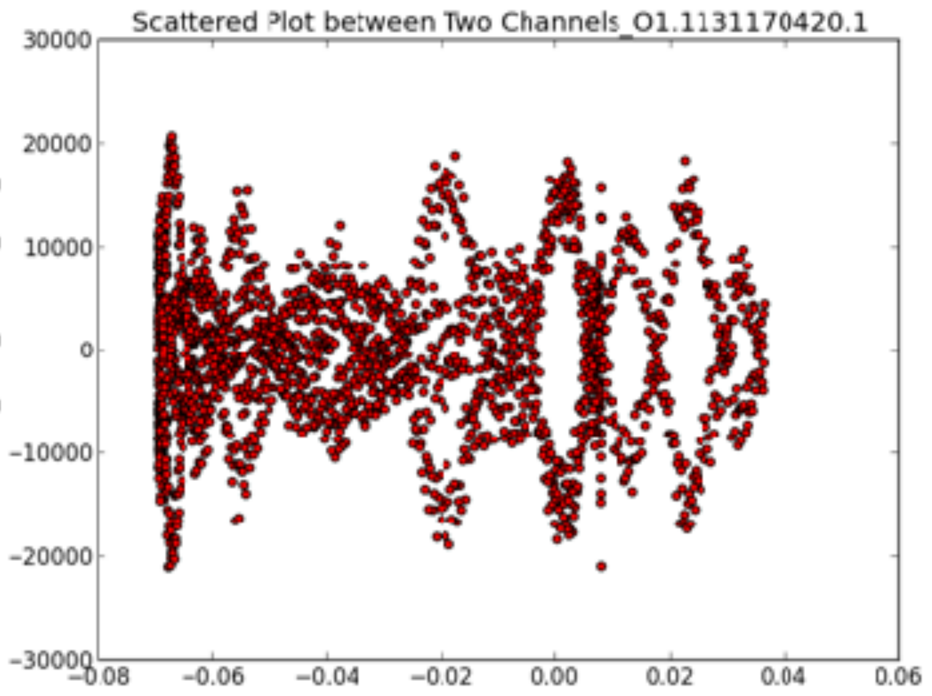

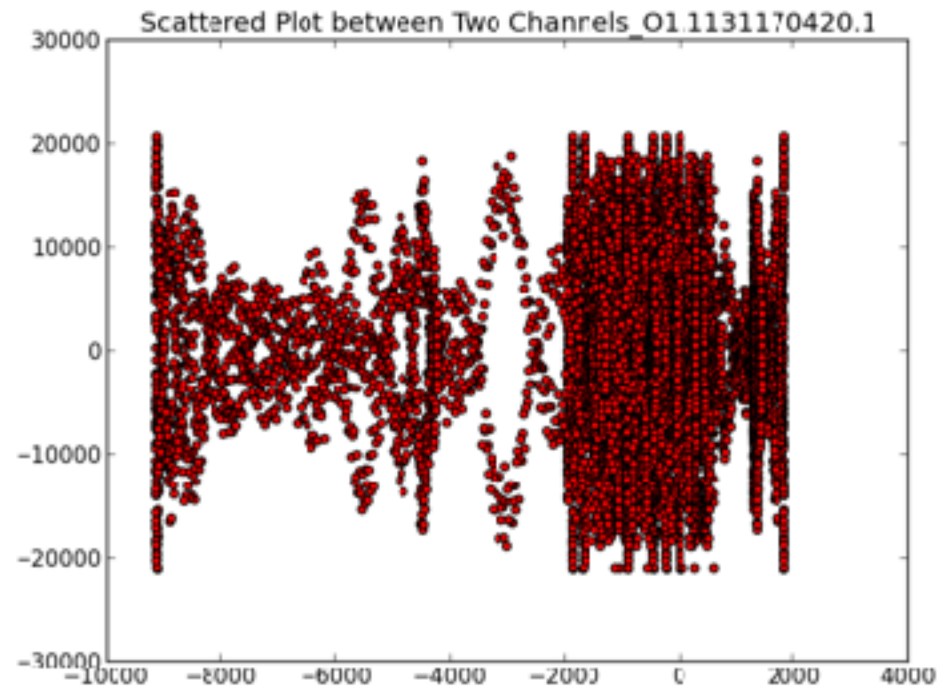

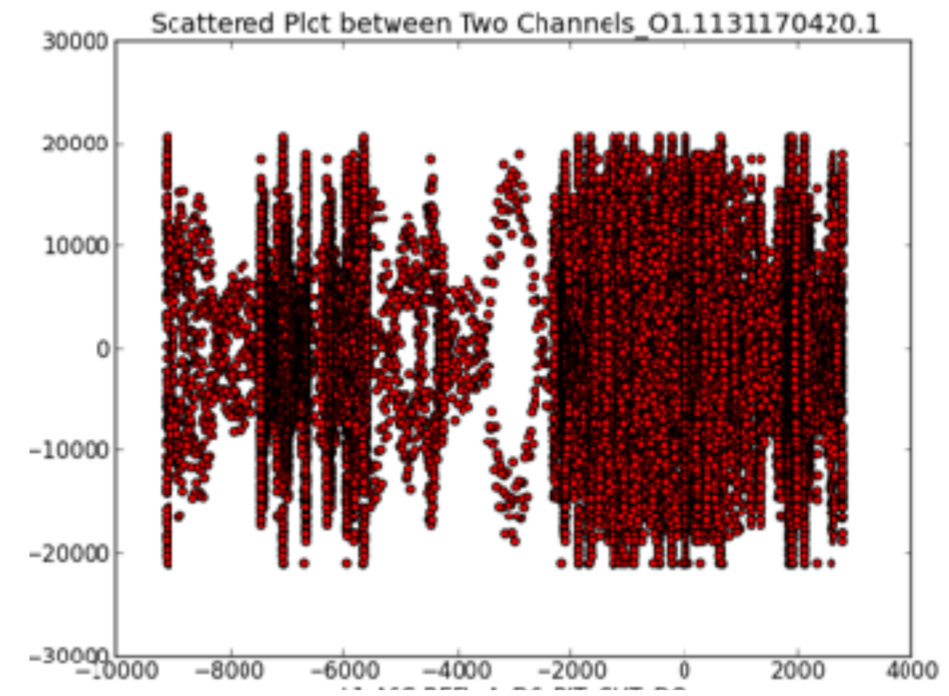

LIGO's Noise Hunting

L1:CAL-PCALY_RX_PD_OUT_DQ

L1:CAL-PCALY_TX_PD_OUT_DQ

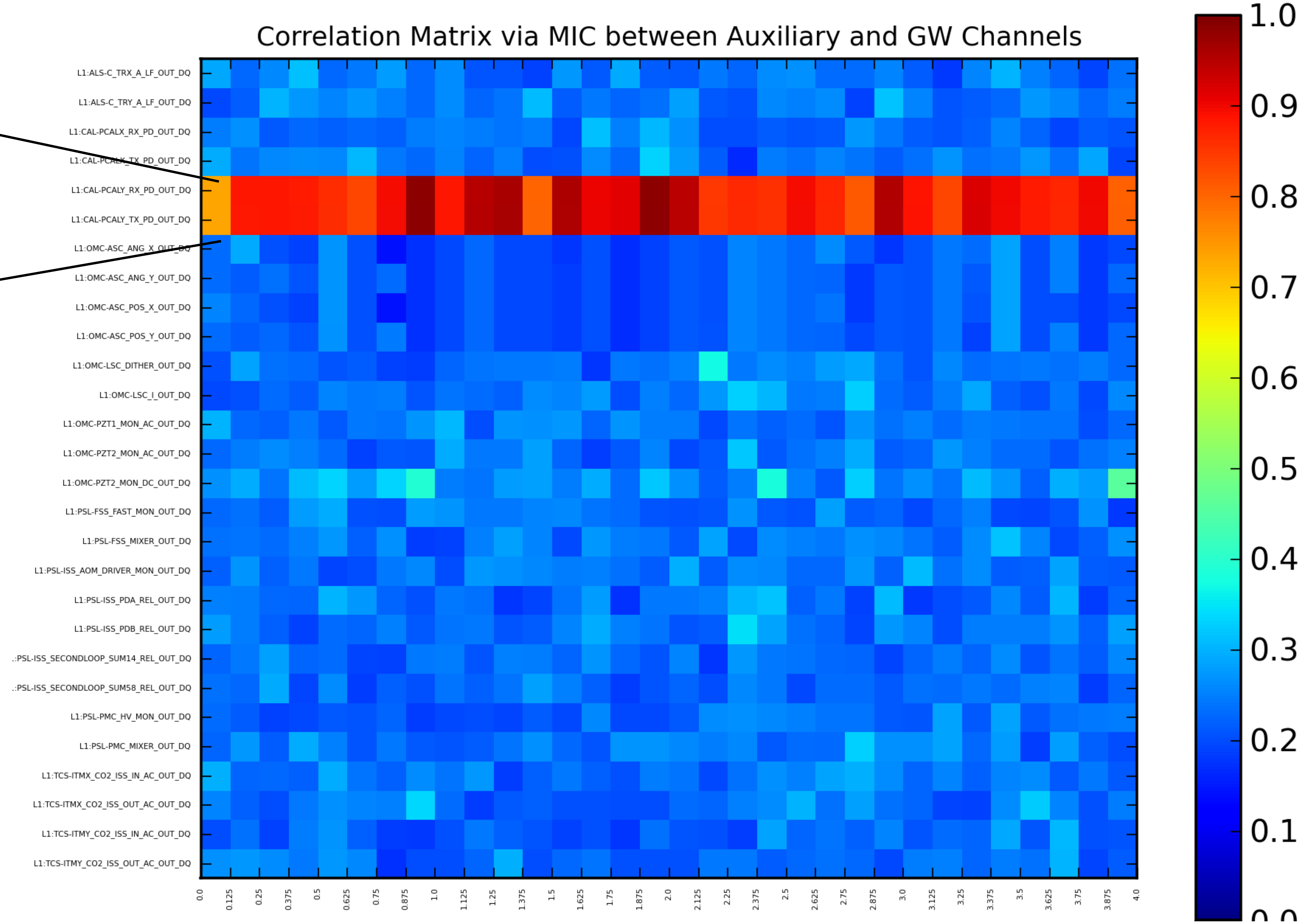

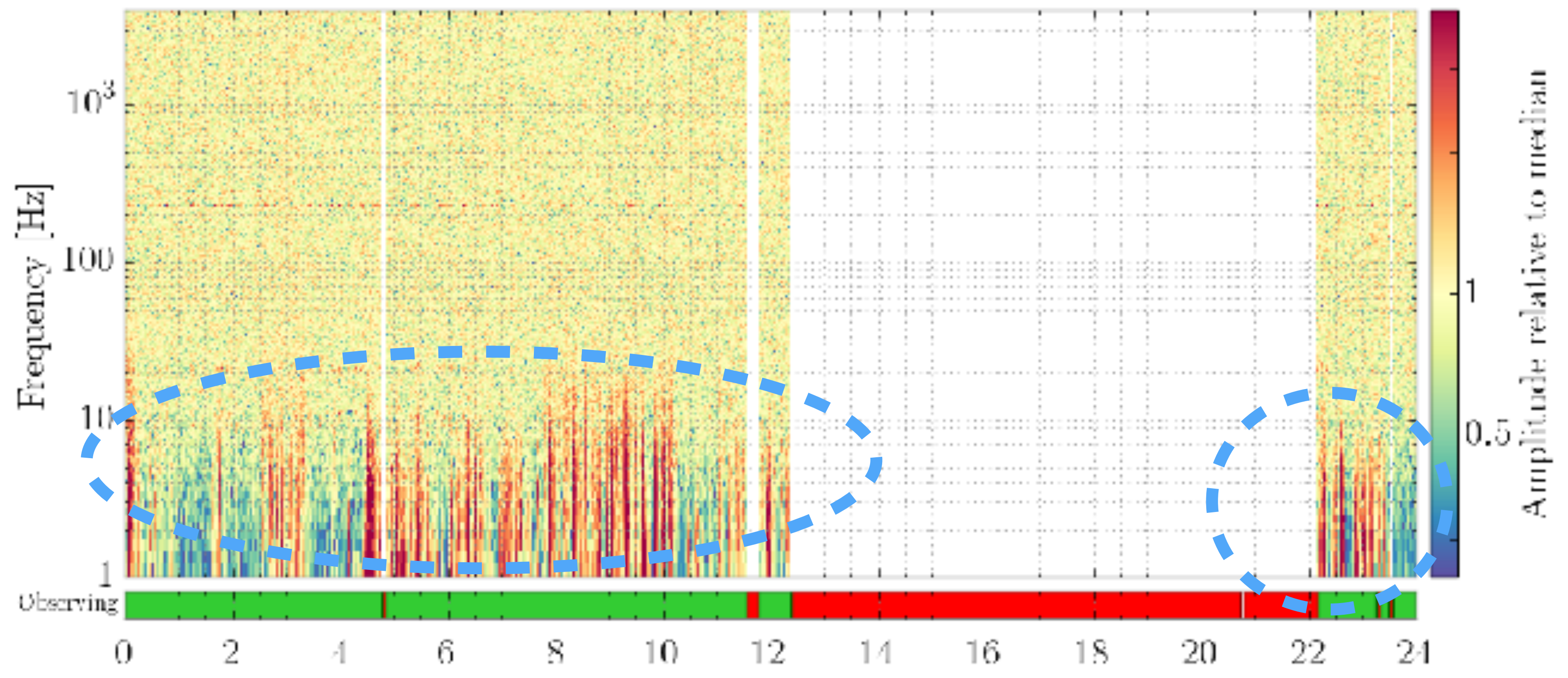

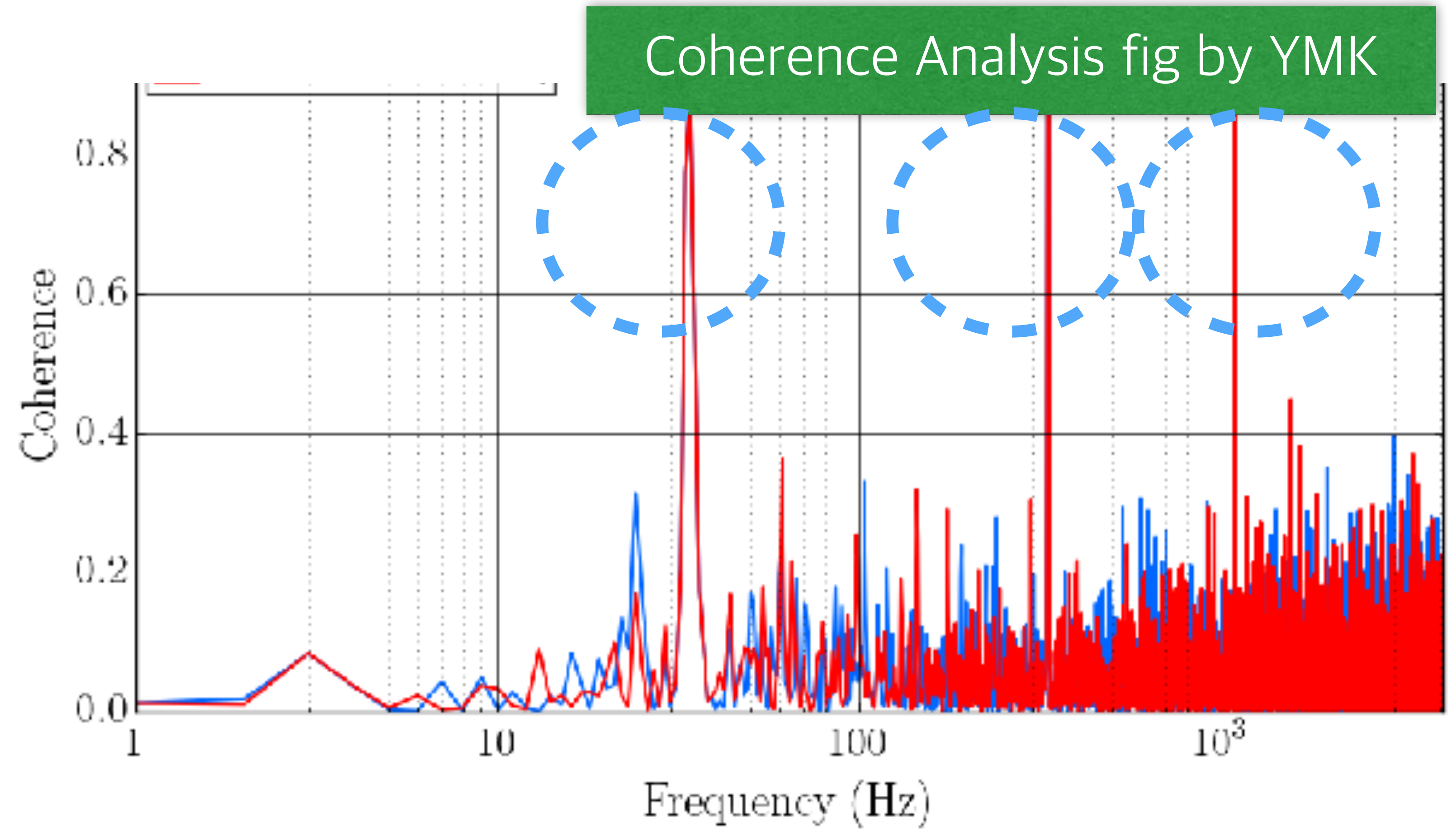

Strong Correlation between PCAL & GW channels, suspecting that it could be responsible for the noise during this observation period

e-CAGMon Tool: Goal and Workflow

- Identifying (non-)linear association with GW channel and other auxiliary channels that monitor the environment / instrumental disturbance
- 200,000 aux. channels in LIGO/Virgo - wind, acceleration, seismic vibration, temperature, magnetic fields etc
- Use three correlation measures: Pearson's correlation coefficient (PCC), Kendall's tau coefficient (K-tau) / Maximal Information Coefficient (MIC)

$$\rho(x,y) = \frac{\sum (x_i - \bar{x})(y_i - \bar{y})}{\sqrt{\sum (x_i - \bar{x})^2 \sum (y_i - \bar{y})^2}}$$

$$\tau(x,y) = \frac{(c-d)}{{}_nC_2}$$

$$MICe(x,y,\alpha,c) = \max_{ab<B(n)} \left\{ \frac{\max I^{[*]}(S,k,l)}{log_2 \min(k,l)} \right\}$$

$$I(x;y) = \sum_{x,y} p_{xy}(x,y) \log \frac{p_{xy}(x,y)}{p_x(x)p_y(y)}$$

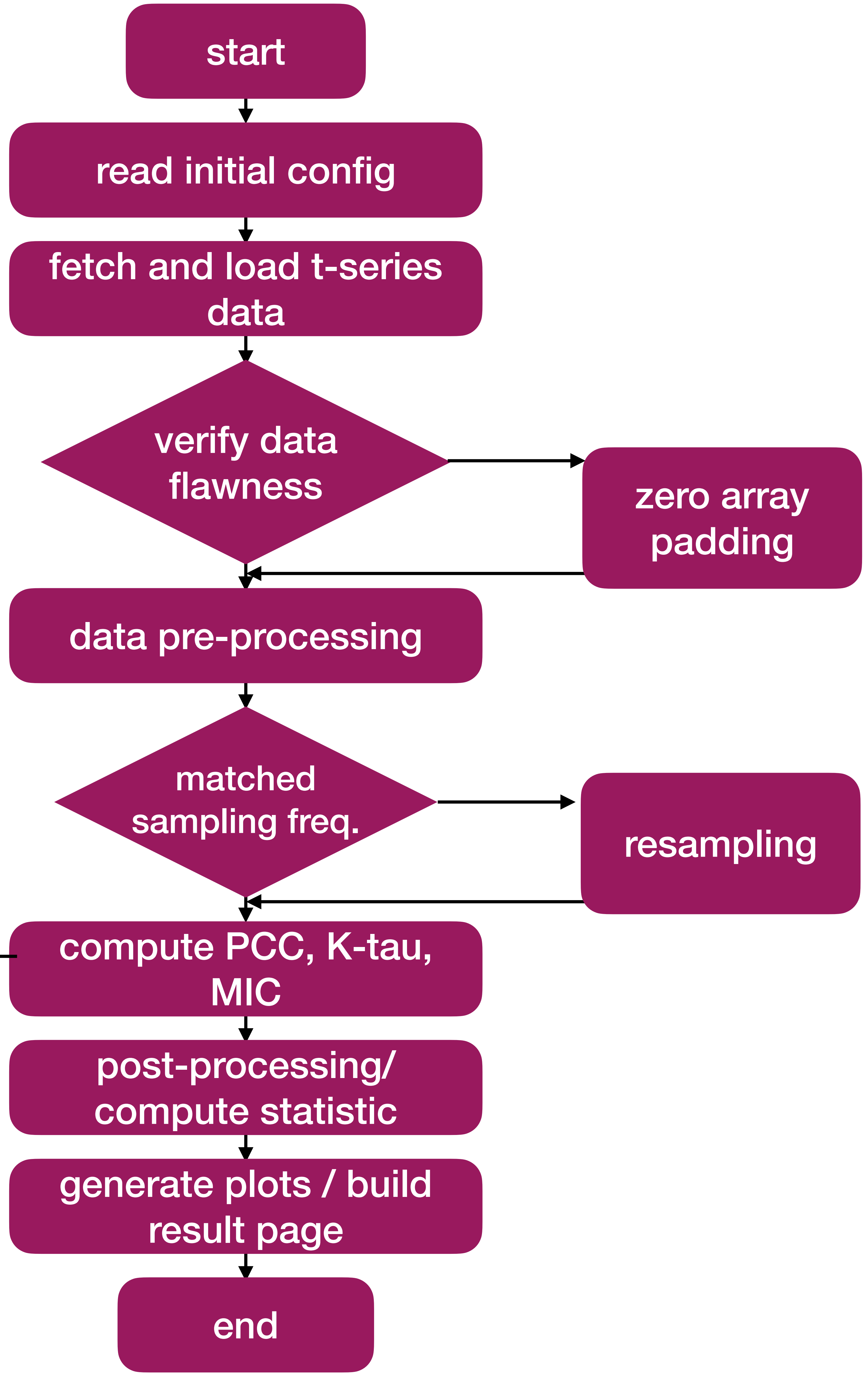

e-CAGMon Tool: Code Test

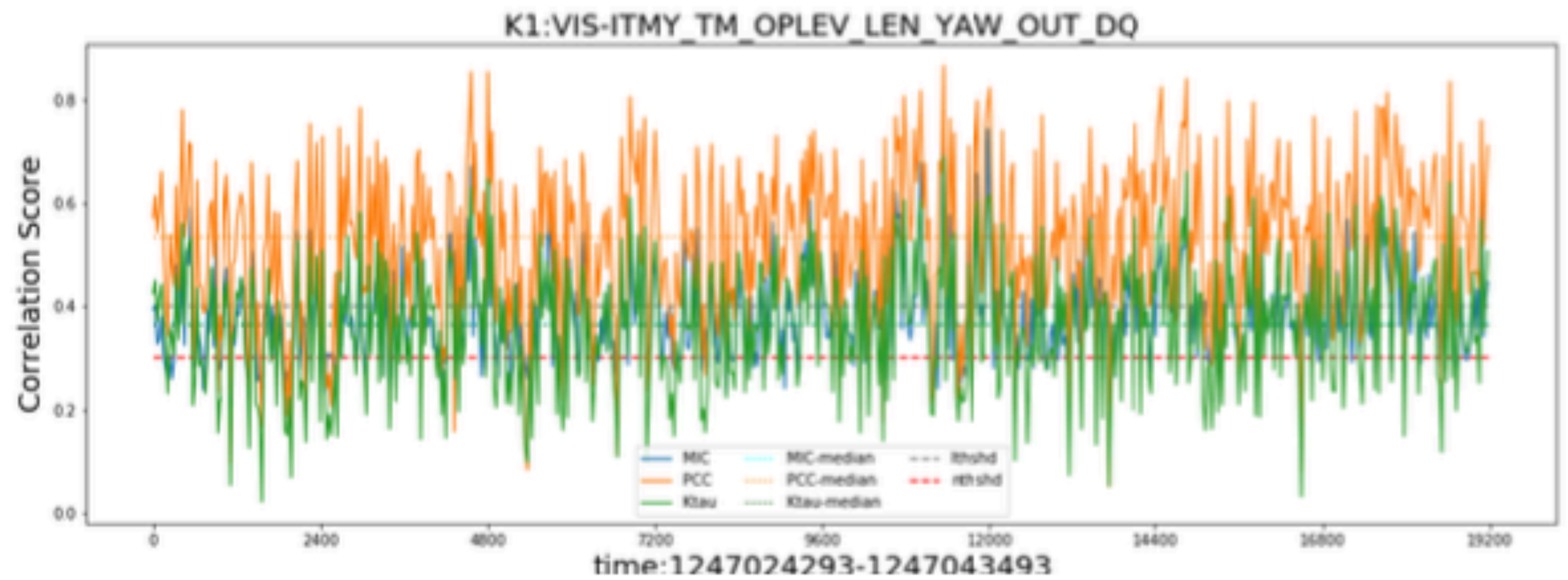

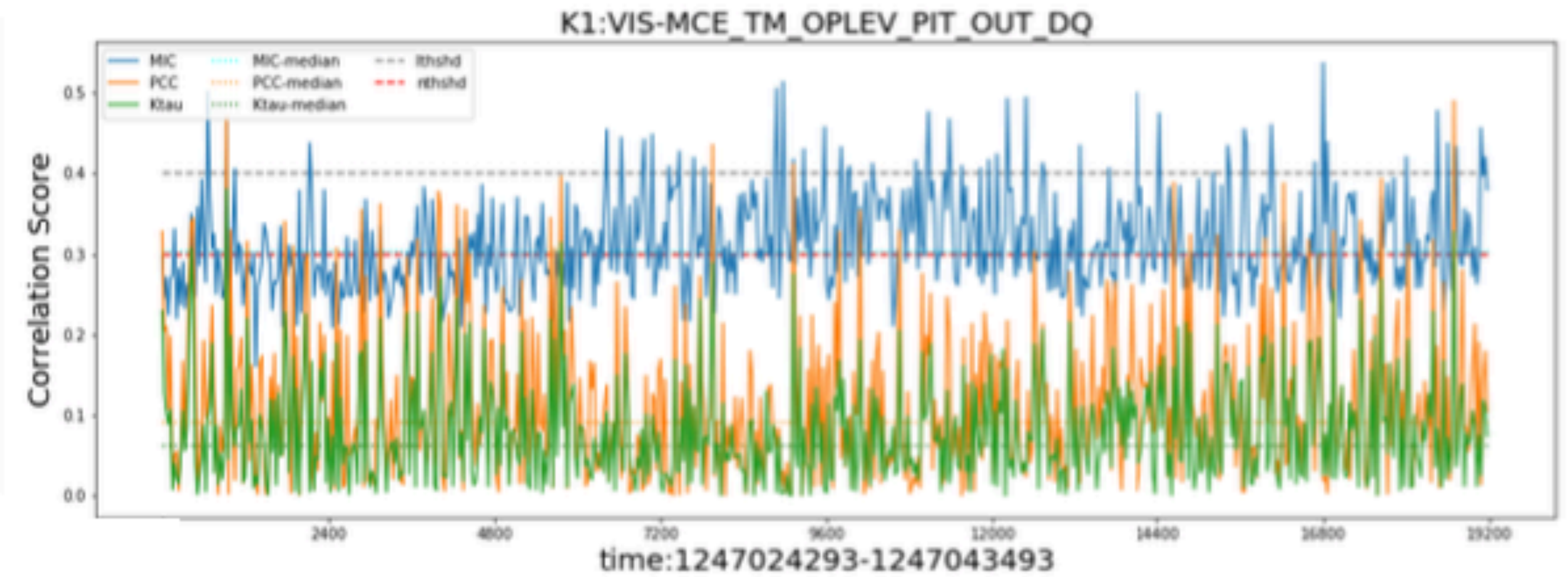

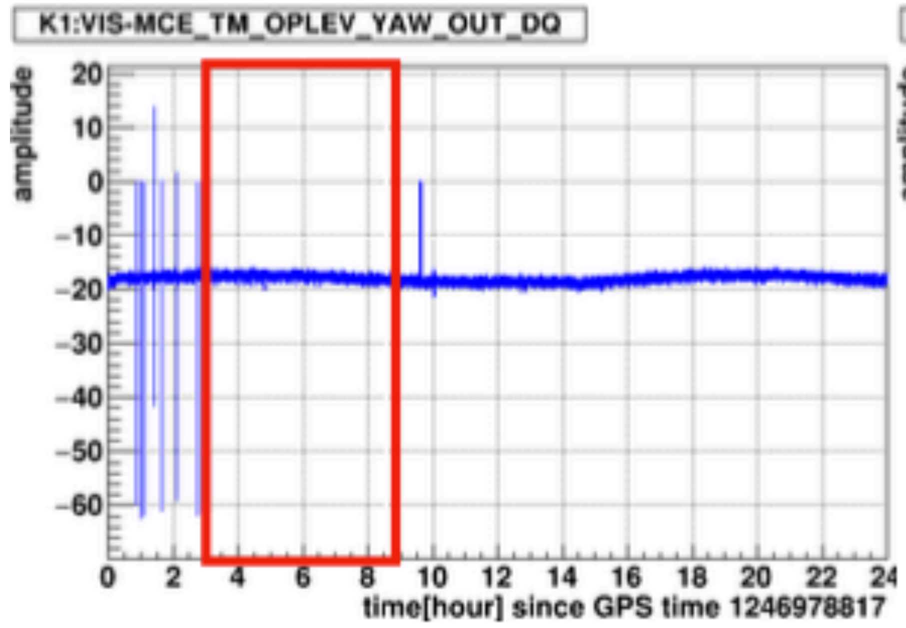

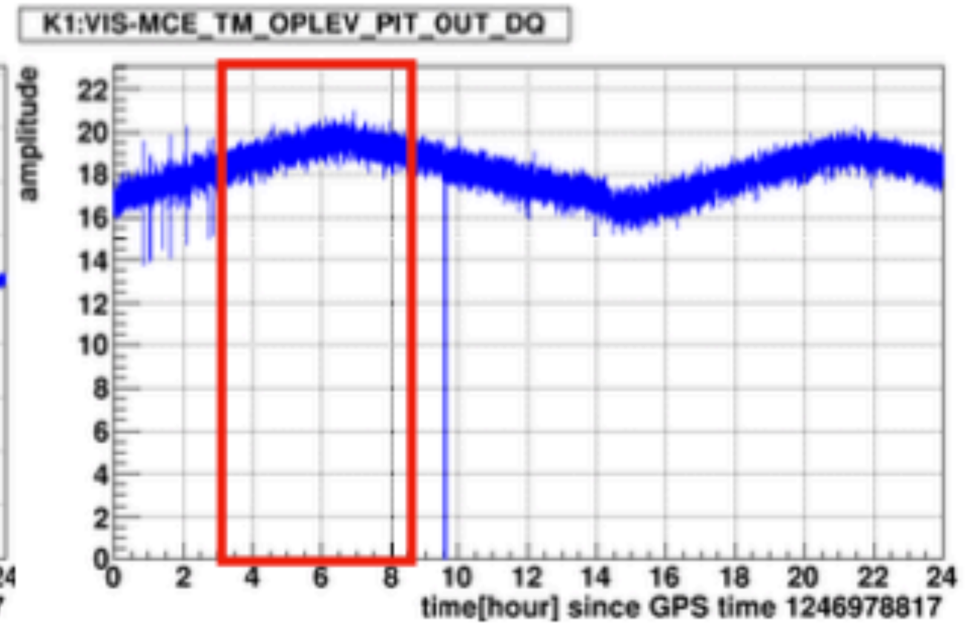

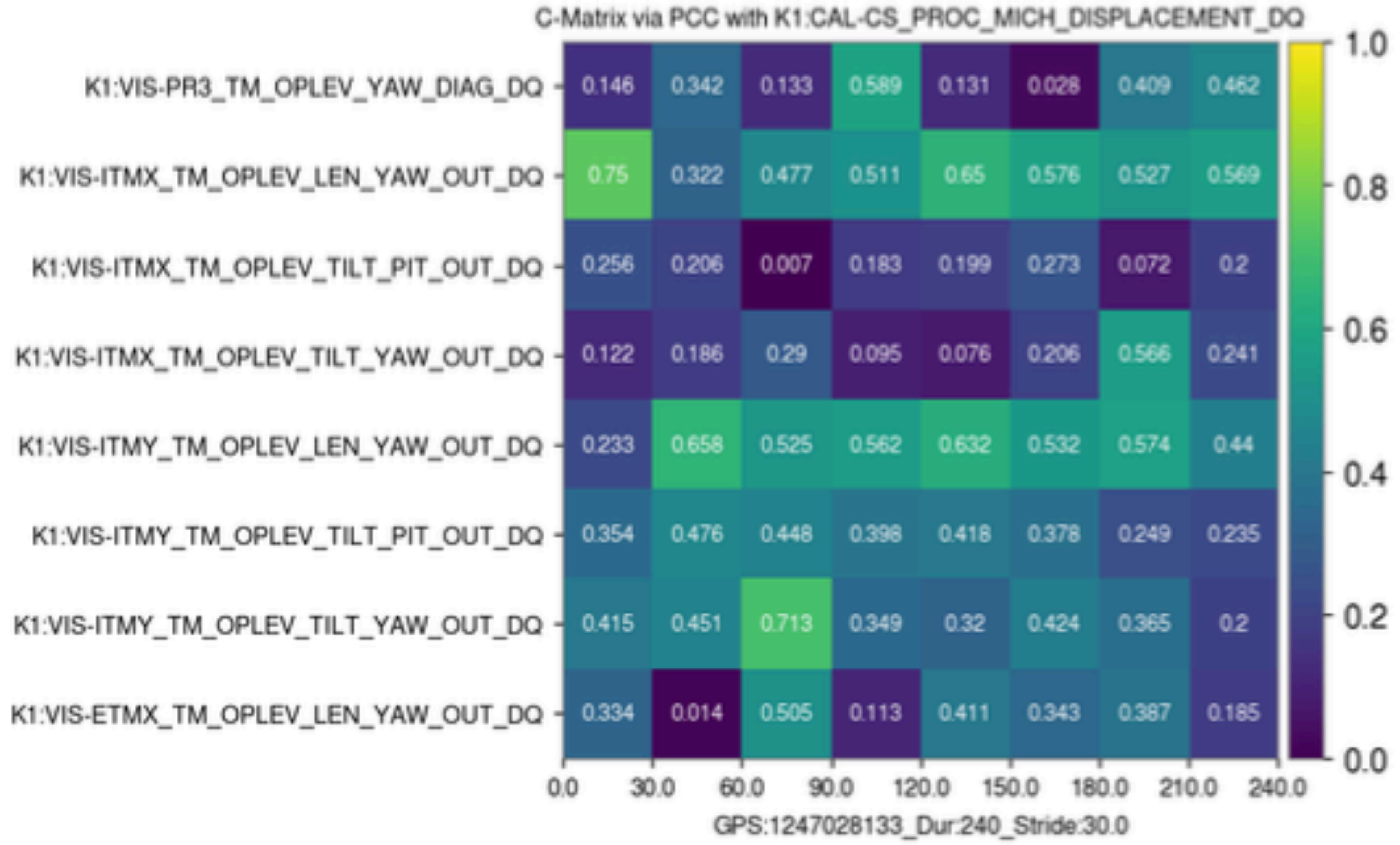

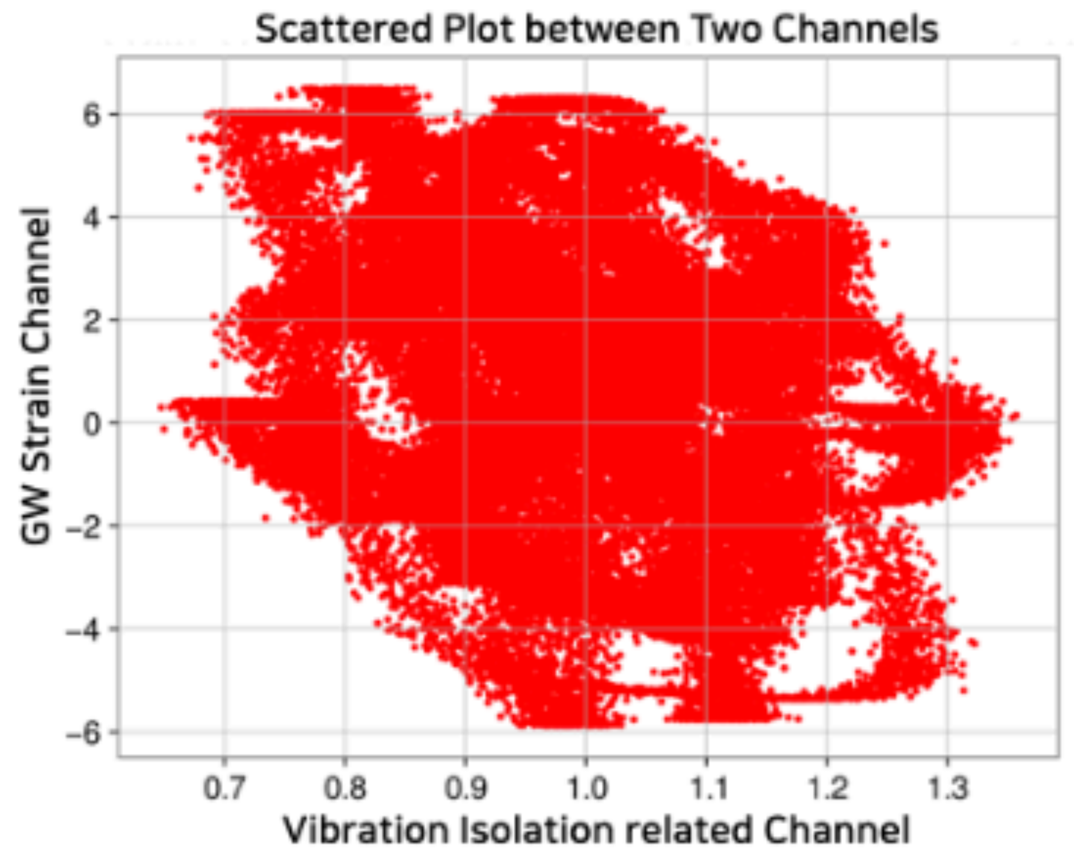

b) Scattered Plot

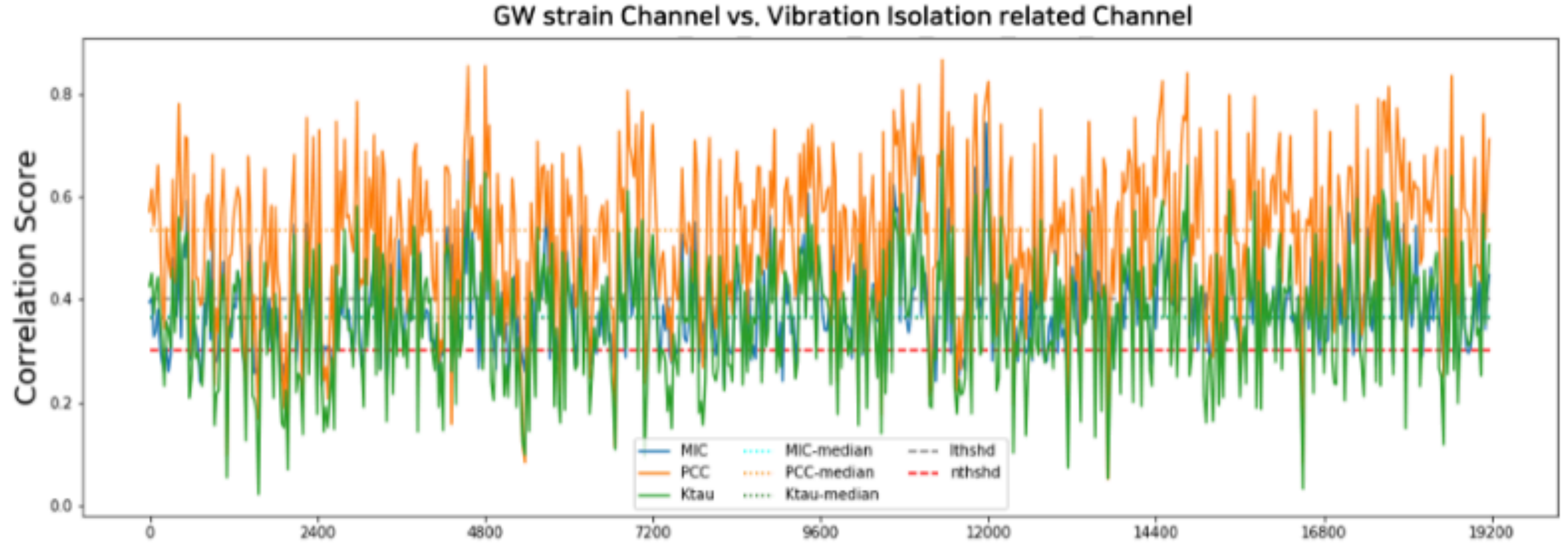

c) Correlation Trend Plot during 5.3 Hours

e-CAGMon Tool: MIC Parameter Optimization

- **Practical issues while computing and interpreting the MIC:**

1. How is the MIC value differently varied under the different types of background noises in data?

2. What is the reliable sampling rate and data size? How do they influence the computing cost?

3. When we handle the data from multi-channel devices with different sampling rates, does the resampling process affect MIC results? If so, what is the best way of resampling to obtain a reliable MIC score?

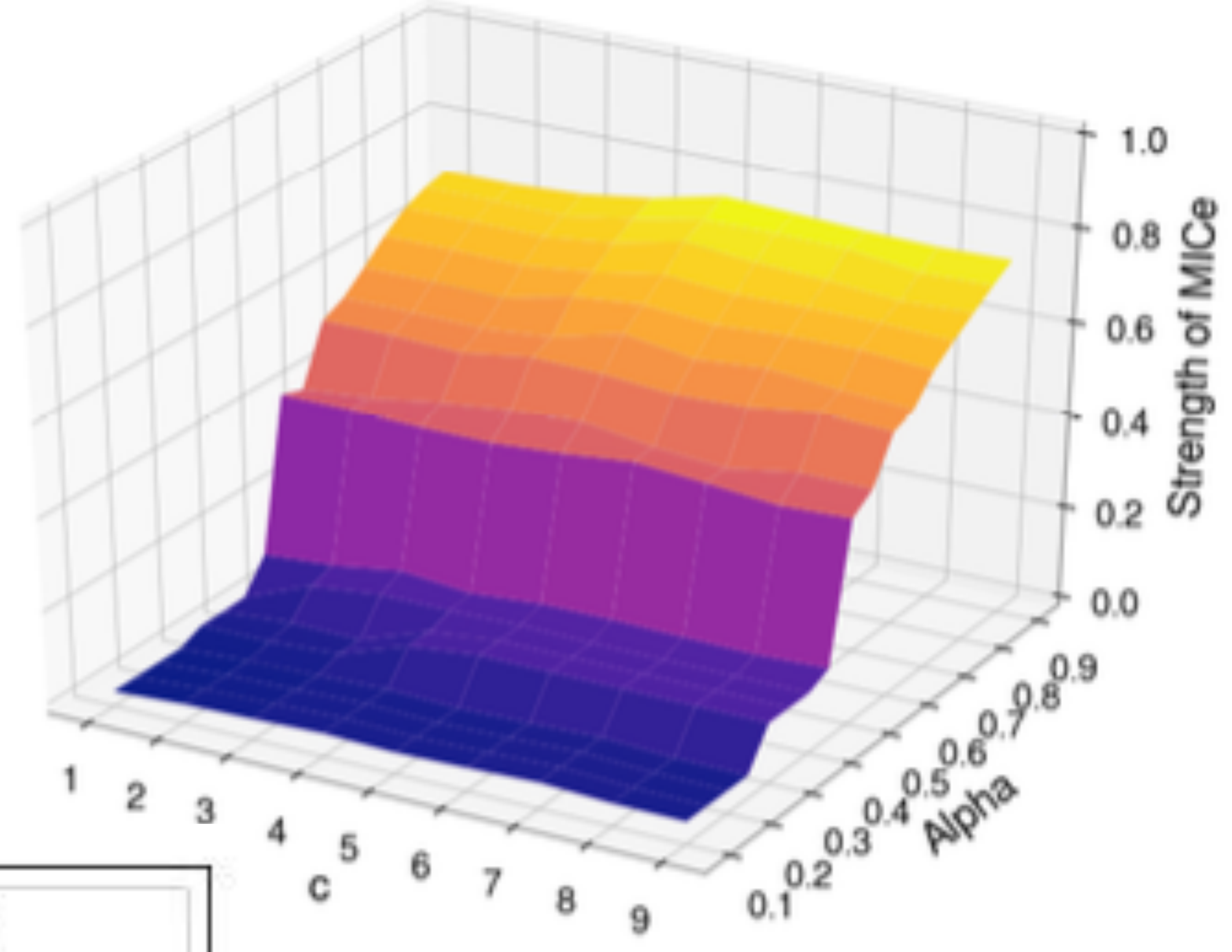

Optimizing $\{\alpha, c\}$

- **EX)** For any two random variables, the correlation should vanish, but MIC does not, depending upon the sample size → at least 12,000 sample size recommended

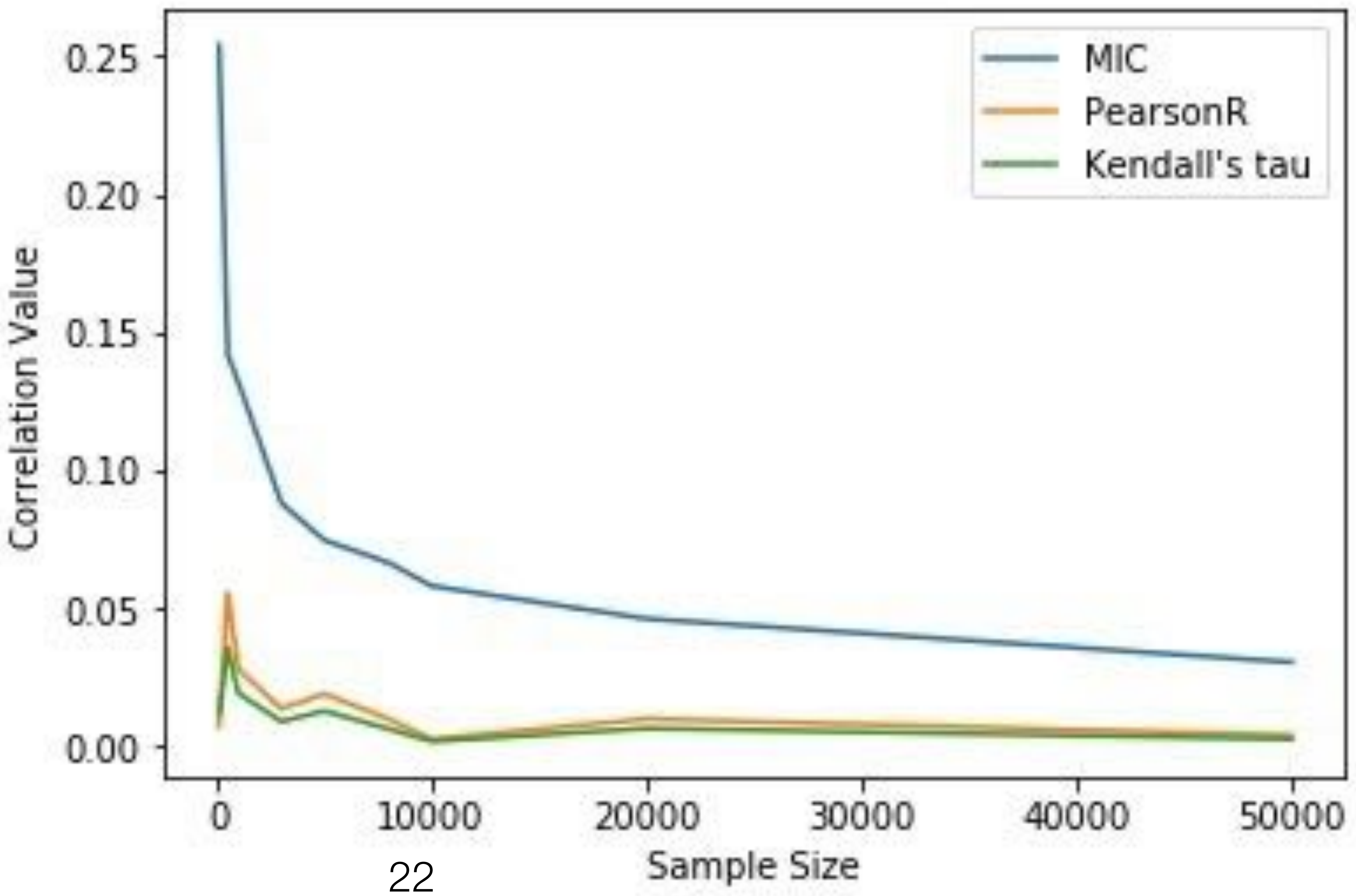

e-CAGMon Tool: MIC Parameter Optimization

- **Functionally associated two data samples:**

Association type	Function
Linear	$Y(X) = X$
Quadratic	$Y(X) = 4(X - \frac{1}{4})^2$
Cubic	$Y(X) = 128(X-\frac{1}{3})^3-48(X-\frac{1}{3})^2-12(X-\frac{1}{3})$
Sinusoidal: period 1/2	$Y(X) = \sin(4\pi X)$
Sinusoidal: period 1/4	$Y(X) = \sin(16\pi X)$
Fourth-root	$Y(X) = X^{1/4}$
Circular	$Y(X) = \pm\sqrt{1-(2X-1)^2}$
Stepwise	$Y(X) = 0$ if $X \leq 1/2$ or 1 if $X > 1/2$

Y. Chen, Y. Zeng, F. Luo, and Z. Yuan, PLoS One **0157567**, 1 (2016).

$$Y(t) = F(X) + (RND(n,1) - 0.5) \times \mathcal{N} \times \mathcal{R}$$

functional relation in the table

random noise n in [0,1]

Relative weight of noise amplitude

$\mathcal{R}$: range of F

- **Null hypothesis:** H_0
- **Alternative hypothesis:** H_1
- **Given parameters of** $\epsilon = (\alpha, c)$ in $MIC^e(X, Y, \epsilon)$

  $S_1^{5\%}(\epsilon) \equiv \{MIC^e(X(t), Y(t), \epsilon) > D_0^{95\%}(\epsilon)\}$, where $D_0^{95\%}(\epsilon) \in S_0^{95\%}(\epsilon)$

  which are greater than an element of the set for the null hypothesis.

- **The statistical power** $\mathcal{P}^{MICe}$ **defined as the ratio between the # of true positive samples and the # of alternative samples:**

$$\mathcal{P}^{MICe}(\epsilon) \equiv \frac{N[D_1^{5\%}(\epsilon)]}{N_1}, \quad \text{where } D_1^{5\%}(\epsilon) \in S_1^{5\%}(\epsilon).$$

- **Computing cost of MICe:** $\mathcal{O}(c^2 B(N)^{5/2}) = \mathcal{O}(c^2 N^{5\alpha/2})$

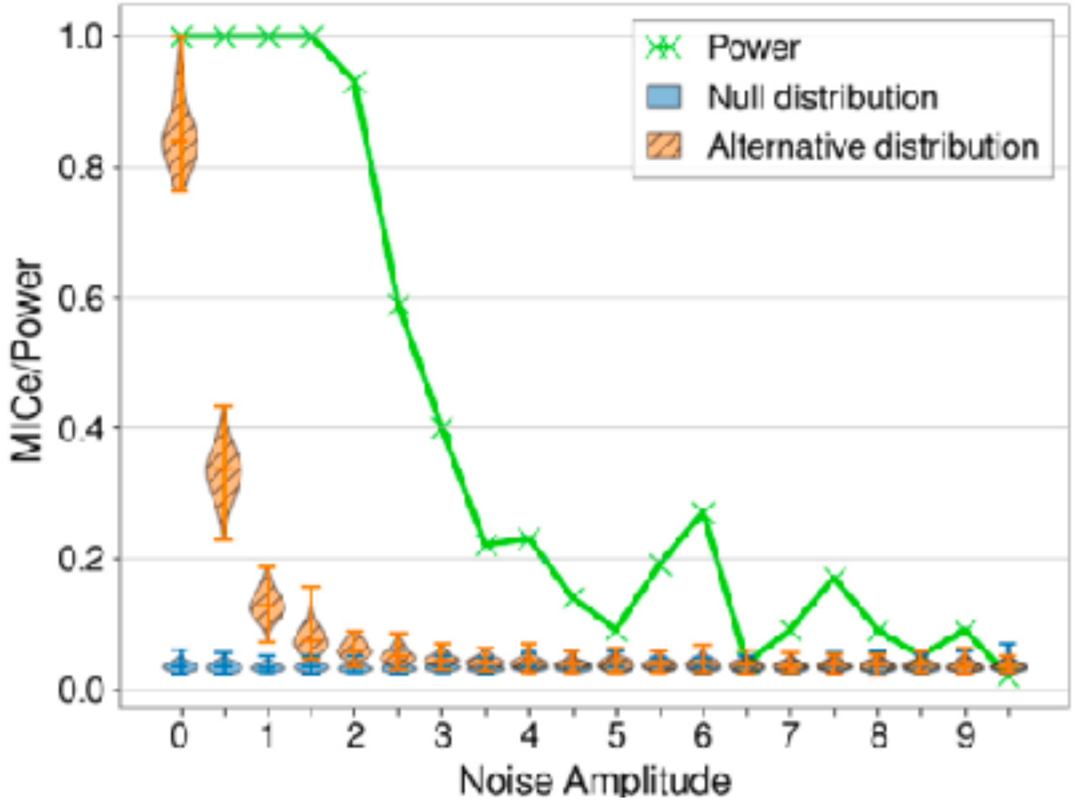

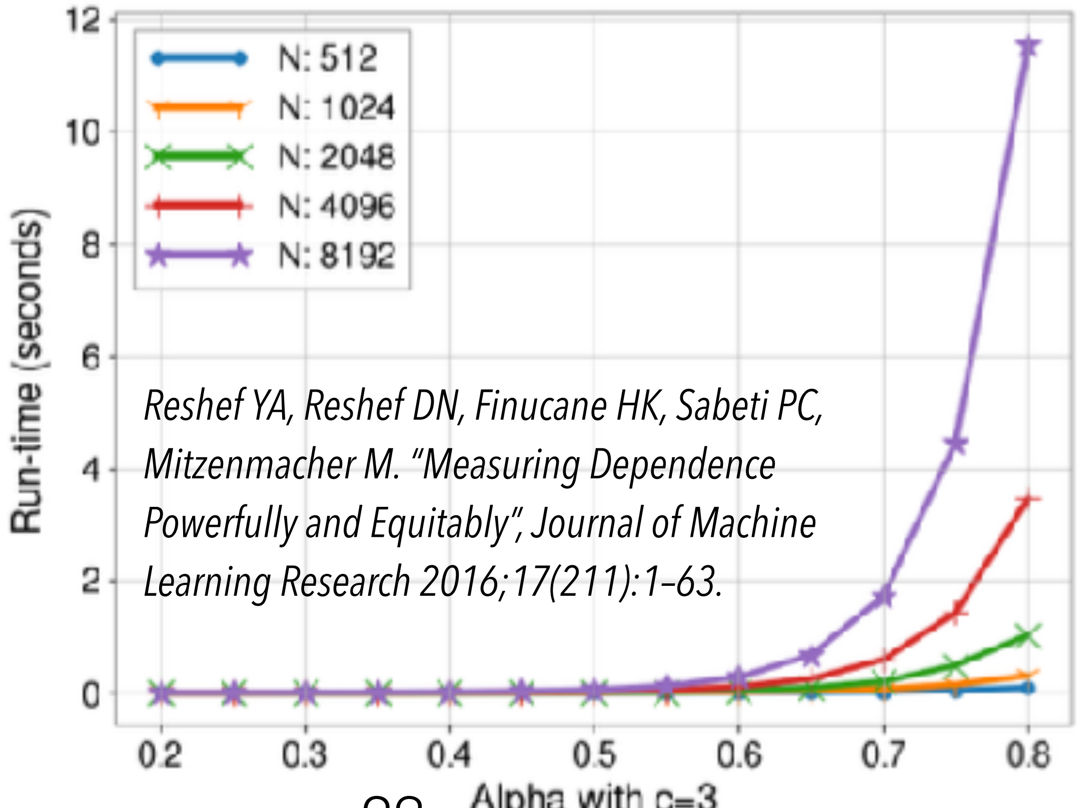

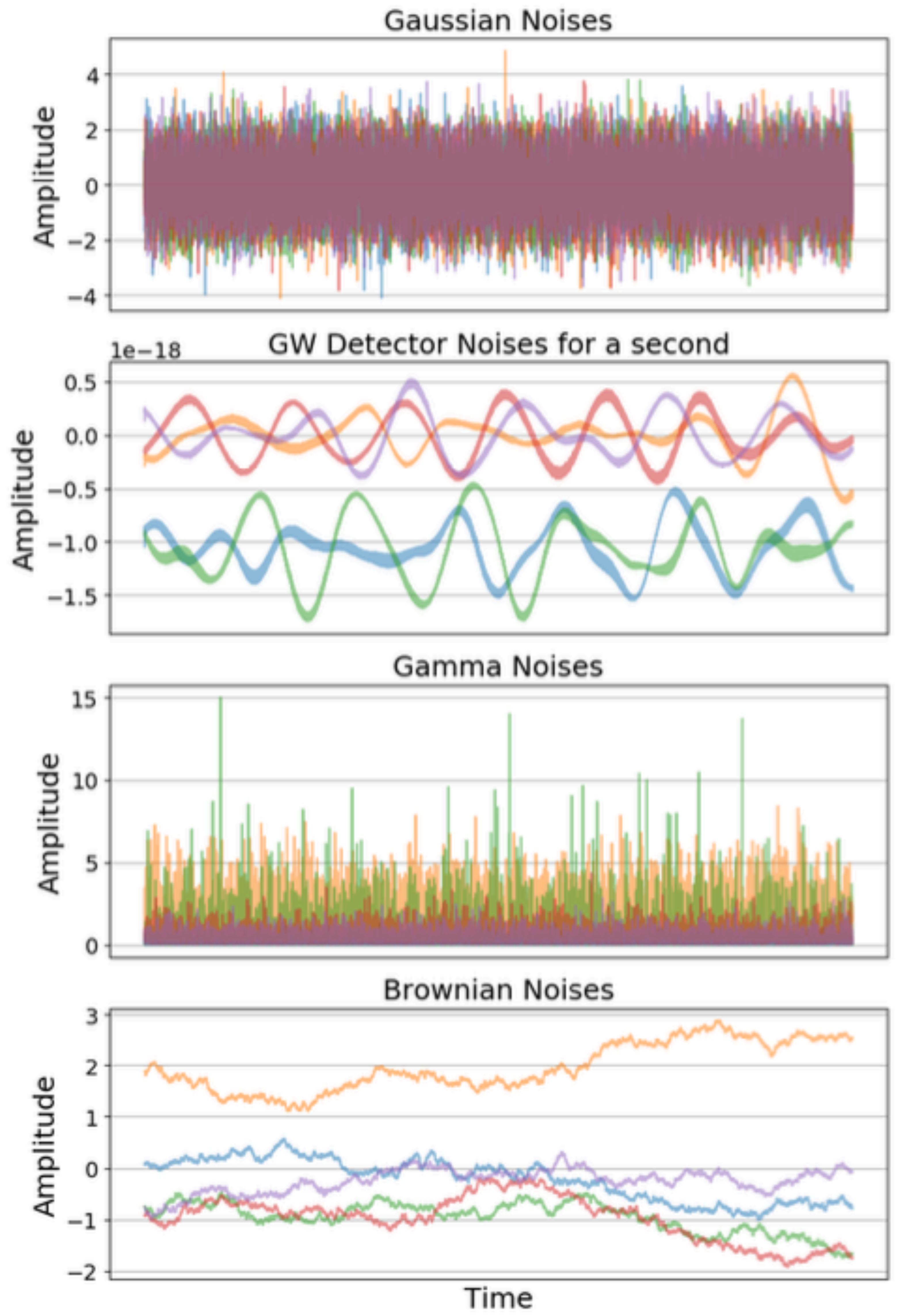

e-CAGMon Tool: MIC Parameter Optimization - Statistical Power

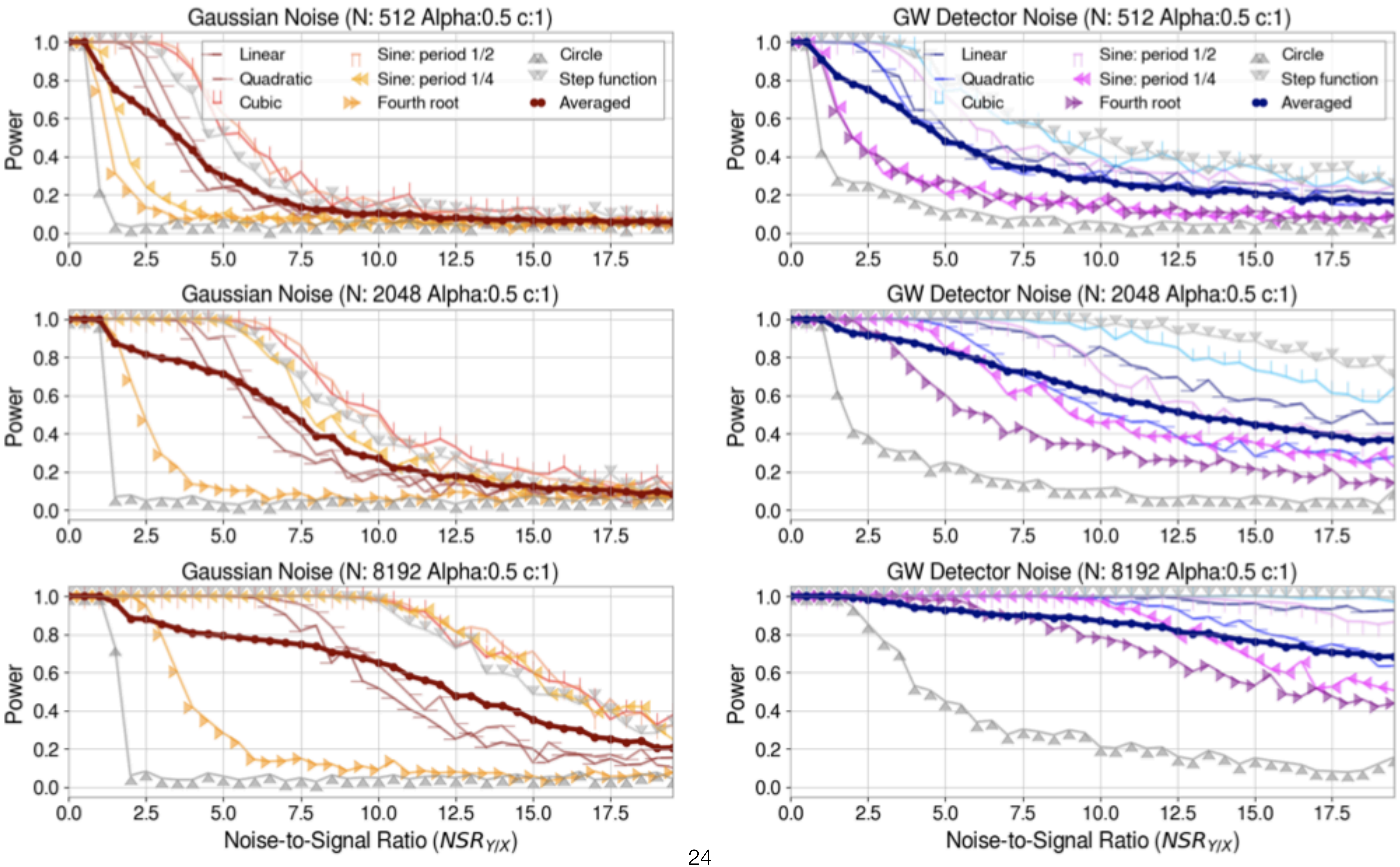

e-CAGMon Tool: MIC Parameter Optimization - Statistical Power

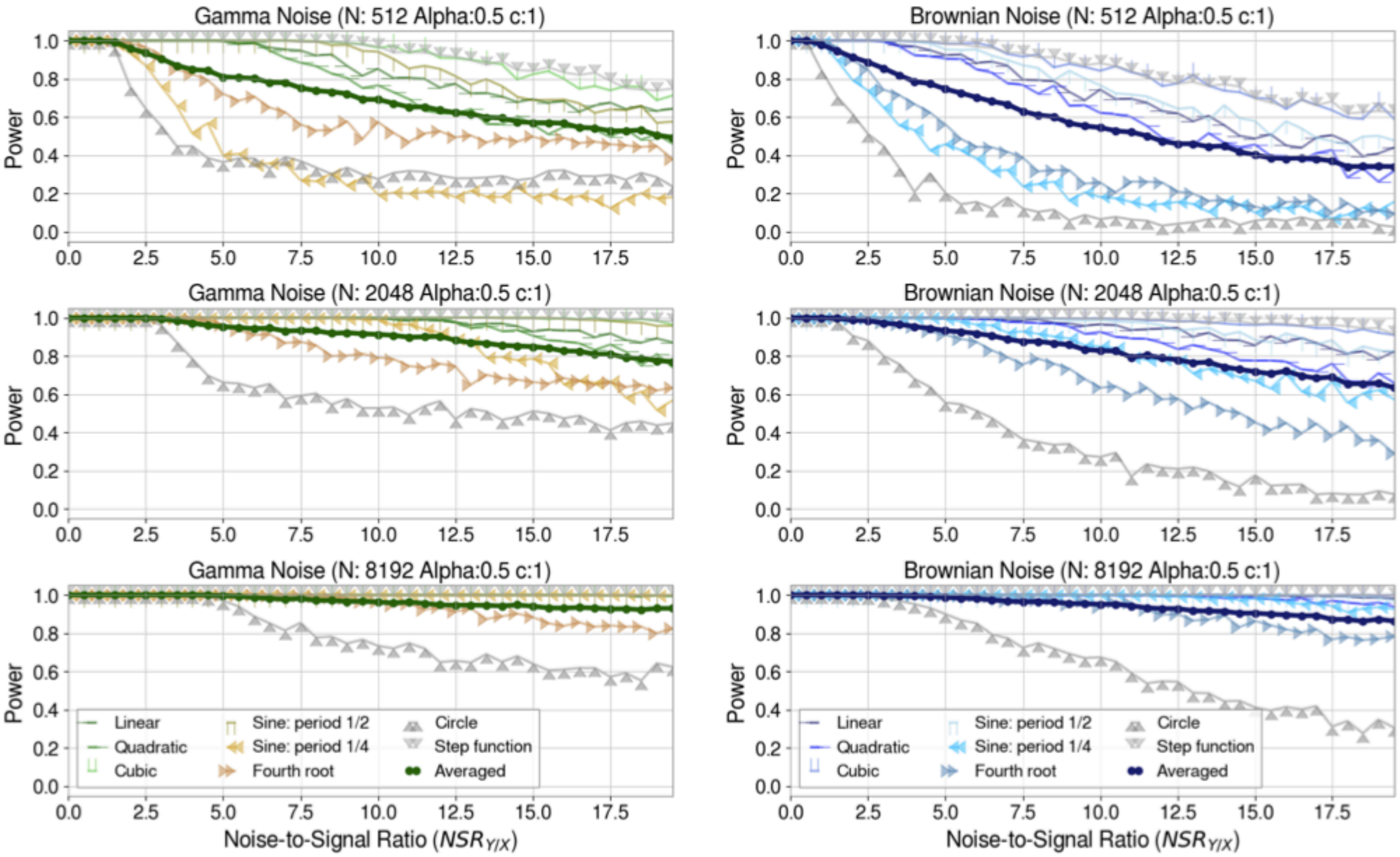

e-CAGMon Tool: MIC Parameter Optimization - Heatmap under AUPC

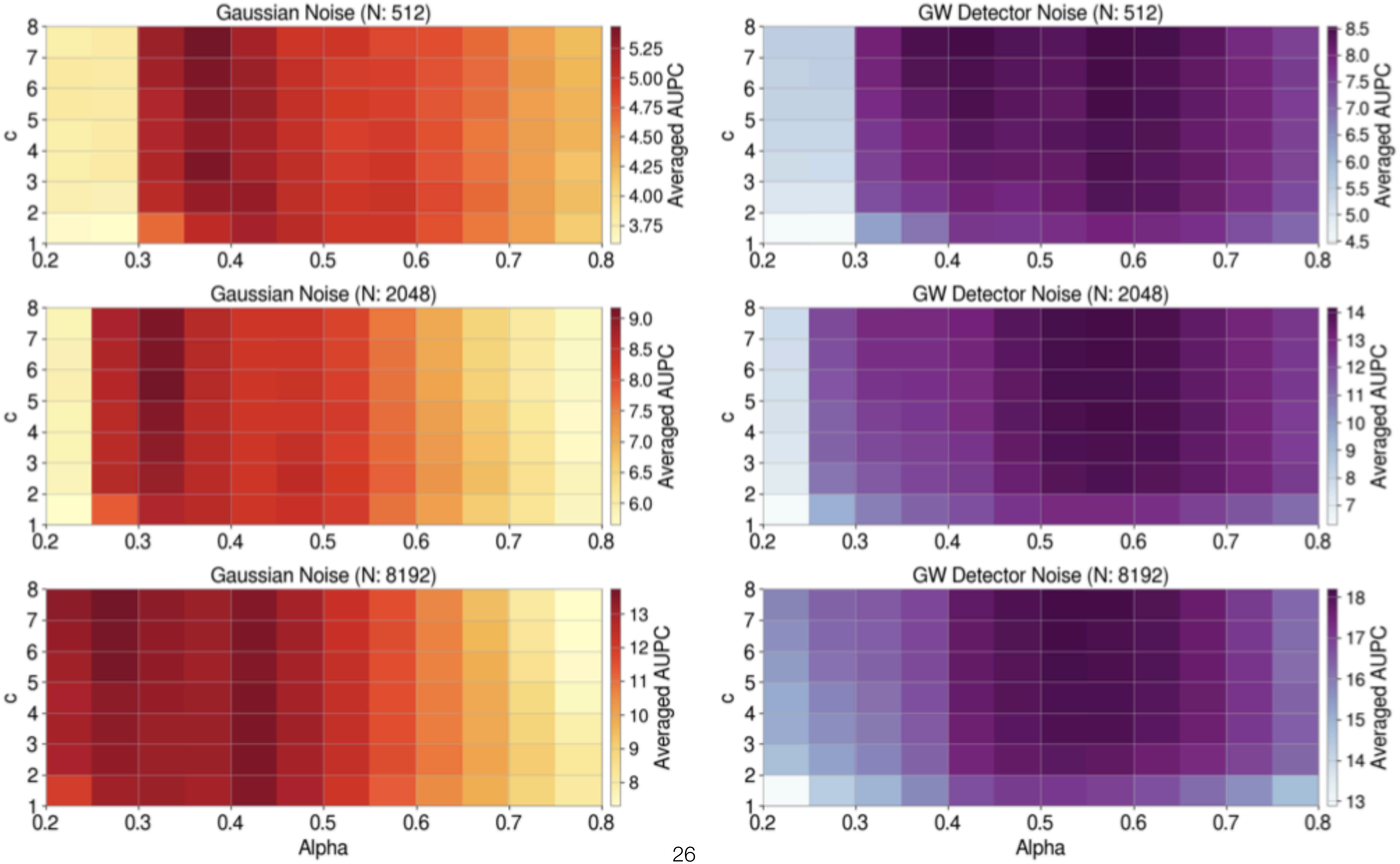

e-CAGMon Tool: MIC Parameter Optimization - Heatmap under AUPC

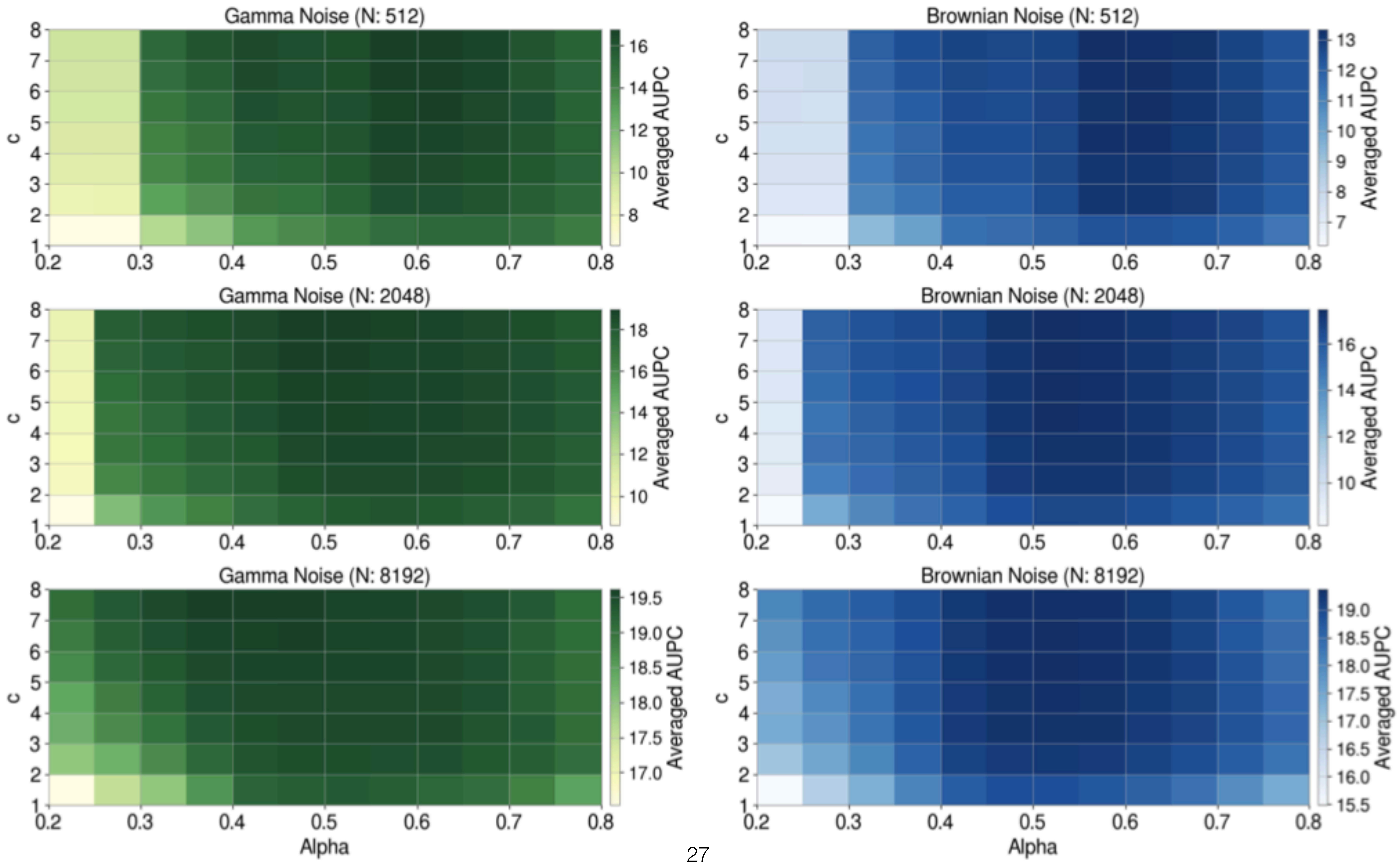

e-CAGMon Tool: MIC Parameter Optimization - MaxAUPC vs. MinComCost

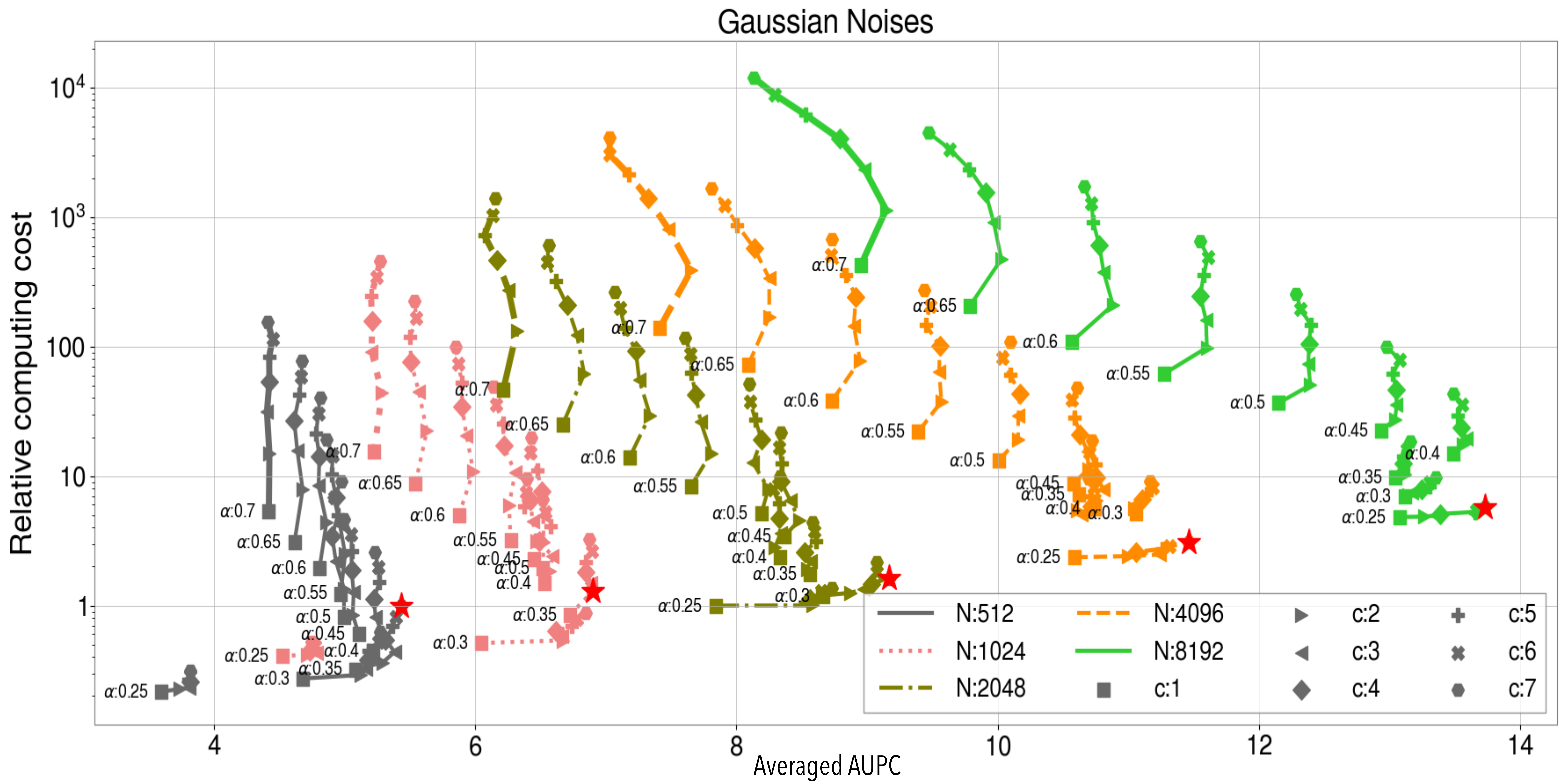

e-CAGMon Tool: MIC Parameter Optimization - MaxAUPC vs. MinComCost

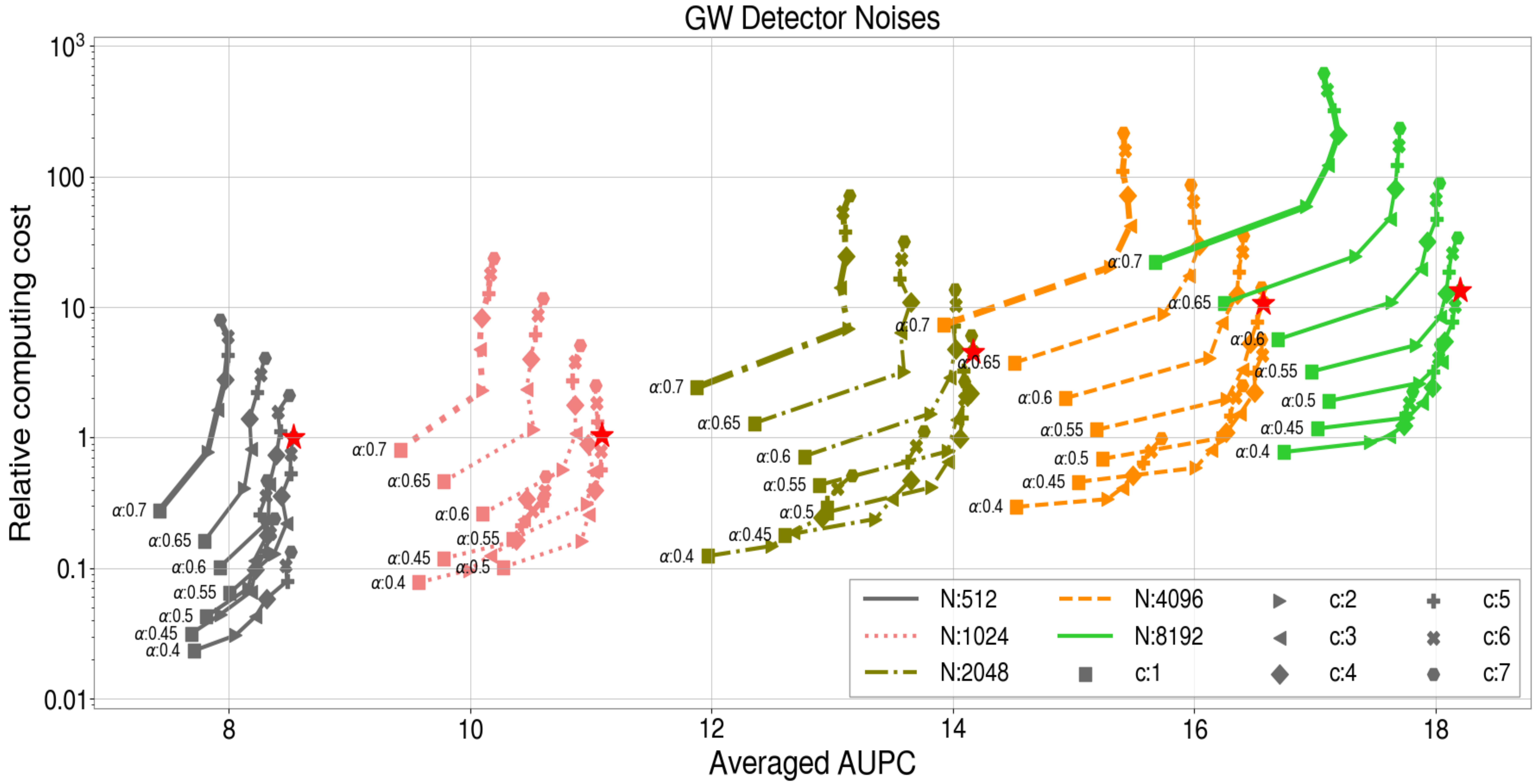

e-CAGMon Tool: MIC Parameter Optimization - MaxAUPC vs. MinComCost

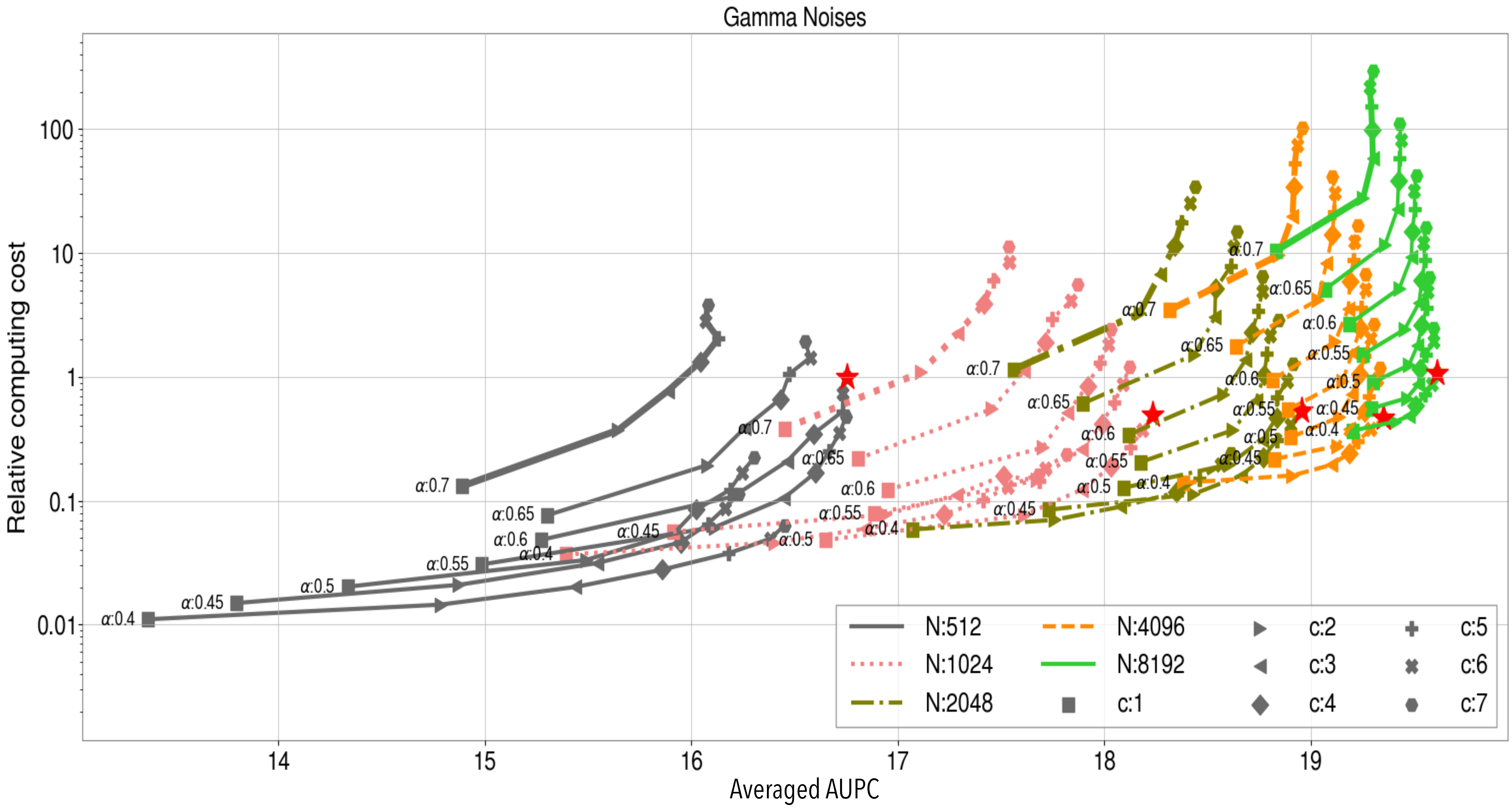

e-CAGMon Tool: MIC Parameter Optimization - MaxAUPC vs. MinComCost

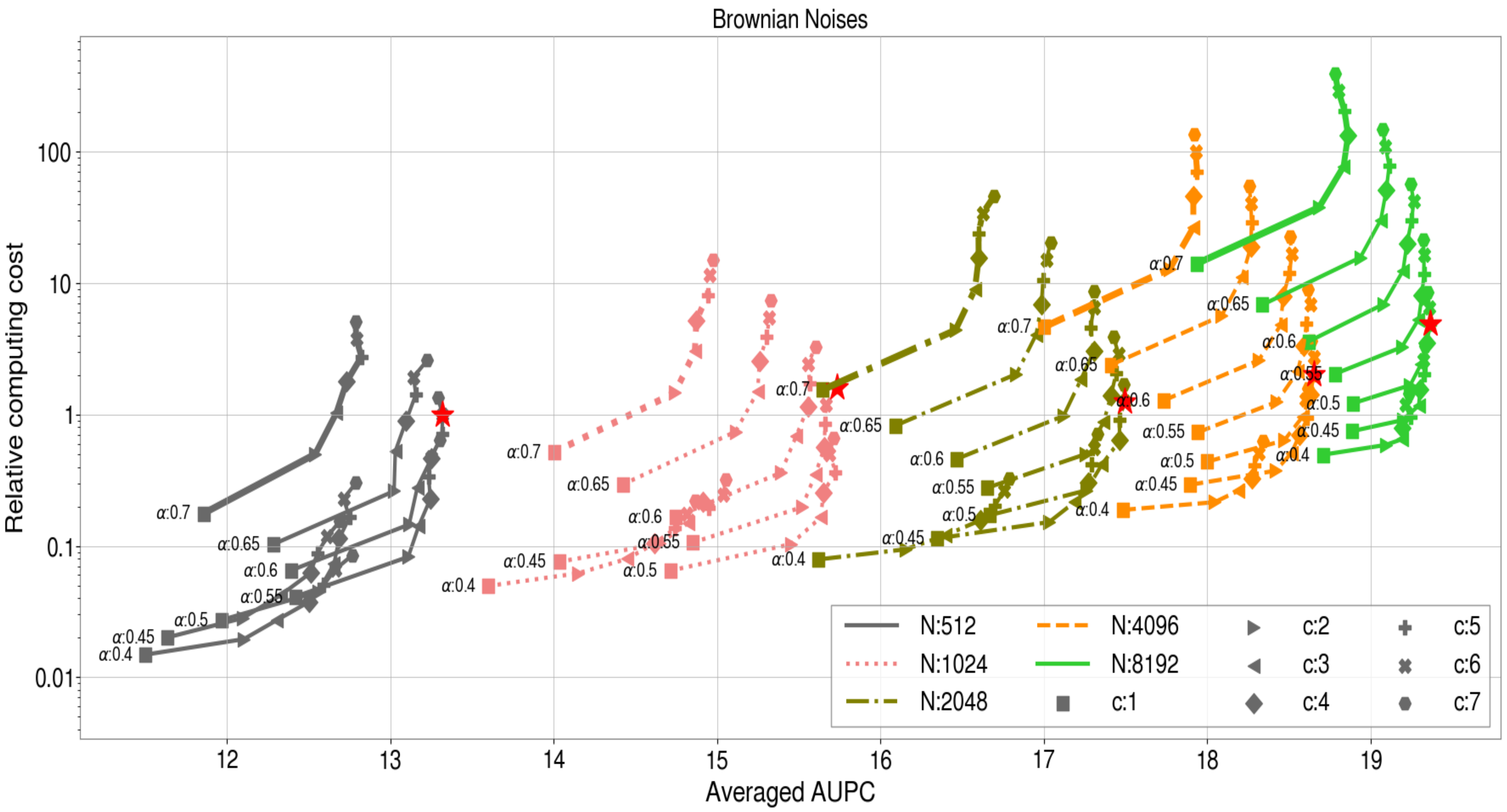

e-CAGMon Tool: MIC Parameter Optimization

Table 2. Table of proposed optimal parameters of $\epsilon = (\alpha, c)$ for data samples (N) under various background noises. The selected parameters provide the best averaged AUPC. The relative computational cost is the relative value calculated based on the computational time of each noise with $N = 512$. The runtime solely depends on the selected α, N, and c, regardless of the choice of the noise type.

Noise Type	N	α	c	Averaged AUPC	Relative Computing Cost	Runtime (sec)
Gaussian Noise	512	0.35	7.0	5.434	1.000	$7.2779\times10^{-4} \pm 5.1360\times10^{-6}$
	1024	0.35	2.0	6.899	1.286	$9.4907\times10^{-4} \pm 5.3110\times10^{-5}$
	2048	0.30	5.0	9.166	1.625	$1.1988\times10^{-3} \pm 3.5905\times10^{-5}$
	4096	0.25	7.0	11.465	3.069	$2.2643\times10^{-3} \pm 5.1274\times10^{-5}$
	8192	0.25	7.0	13.742	5.694	$4.2009\times10^{-3} \pm 1.5290\times10^{-5}$
GW Detector Noise	512	0.55	7.0	8.535	1.000	$1.4158\times10^{-2} \pm 5.4217\times10^{-5}$
	1024	0.50	7.0	11.092	1.040	$1.4721\times10^{-2} \pm 6.6200\times10^{-5}$
	2048	0.55	6.0	14.164	4.561	$6.4571\times10^{-2} \pm 5.8023\times10^{-4}$
	4096	0.55	6.0	16.566	10.781	$1.5264\times10^{-1} \pm 4.1442\times10^{-3}$
	8192	0.50	7.0	18.199	13.330	$1.8872\times10^{-1} \pm 3.7194\times10^{-4}$
Gamma Noise	512	0.6	7.0	16.752	1.000	$2.9842\times10^{-2} \pm 8.6986\times10^{-5}$
	1024	0.50	7.0	18.234	0.493	$1.4721\times10^{-2} \pm 6.6200\times10^{-5}$
	2048	0.45	7.0	18.955	0.531	$1.5858\times10^{-2} \pm 9.5062\times10^{-5}$
	4096	0.40	7.0	19.346	0.466	$1.3906\times10^{-2} \pm 4.6712\times10^{-5}$
	8192	0.40	7.0	19.614	1.069	$3.1898\times10^{-2} \pm 4.4971\times10^{-5}$
Brownian Noise	512	0.60	6.0	13.320	1.000	$2.2202\times10^{-2} \pm 5.4714\times10^{-5}$
	1024	0.55	7.0	15.736	1.613	$3.5811\times10^{-2} \pm 2.3834\times10^{-3}$
	2048	0.50	6.0	17.495	1.252	$2.7804\times10^{-2} \pm 1.0220\times10^{-4}$
	4096	0.50	5.0	18.652	2.014	$4.4709\times10^{-2} \pm 8.6971\times10^{-5}$
	8192	0.50	5.0	19.367	4.886	$1.0848\times10^{-1} \pm 2.1029\times10^{-3}$

PTEP2022, 073H01 (2022)

e-CAGMon Tool: MIC Parameter Optimization

Table 2. Table of proposed optimal parameters of $\epsilon = (\alpha, c)$ for data samples (N) under various background noises. The selected parameters provide the best averaged AUPC. The relative computational cost is the relative value calculated based on the computational time of each noise with $N = 512$. The runtime solely depends on the selected α, N, and c, regardless of the choice of the noise type.

Noise Type	N	α	c	Averaged AUPC	Relative Computing Cost	Runtime (sec)
Gaussian Noise	512	0.35	7.0	5.434	1.000	$7.2779\times10^{-4} \pm 5.1360\times10^{-6}$
	1024	0.35	2.0	6.899	1.286	$9.4907\times10^{-4} \pm 5.3110\times10^{-5}$
	2048	0.30	5.0	9.166	1.625	$1.1988\times10^{-3} \pm 3.5905\times10^{-5}$
	4096	0.25	7.0	11.465	3.069	$2.2643\times10^{-3} \pm 5.1274\times10^{-5}$
	8192	0.25	7.0	13.742	5.694	$4.2009\times10^{-3} \pm 1.5290\times10^{-5}$
GW Detector Noise	512	0.55	7.0	8.535	1.000	$1.4158\times10^{-2} \pm 5.4217\times10^{-5}$
	1024	0.50	7.0	11.092	1.040	$1.4721\times10^{-2} \pm 6.6200\times10^{-5}$
	2048	0.55	6.0	14.164	4.561	$6.4571\times10^{-2} \pm 5.8023\times10^{-4}$
	4096	0.55	6.0	16.566	10.781	$1.5264\times10^{-1} \pm 4.1442\times10^{-3}$
	8192	0.50	7.0	18.199	13.330	$1.8872\times10^{-1} \pm 3.7194\times10^{-4}$
Gamma Noise	512	0.6	7.0	16.752	1.000	$2.9842\times10^{-2} \pm 8.6986\times10^{-5}$
	1024	0.50	7.0	18.234	0.493	$1.4721\times10^{-2} \pm 6.6200\times10^{-5}$
	2048	0.45	7.0	18.955	0.531	$1.5858\times10^{-2} \pm 9.5062\times10^{-5}$
	4096	0.40	7.0	19.346	0.466	$1.3906\times10^{-2} \pm 4.6712\times10^{-5}$
	8192	0.40	7.0	19.614	1.069	$3.1898\times10^{-2} \pm 4.4971\times10^{-5}$
Brownian Noise	512	0.60	6.0	13.320	1.000	$2.2202\times10^{-2} \pm 5.4714\times10^{-5}$
	1024	0.55	7.0	15.736	1.613	$3.5811\times10^{-2} \pm 2.3834\times10^{-3}$
	2048	0.50	6.0	17.495	1.252	$2.7804\times10^{-2} \pm 1.0220\times10^{-4}$
	4096	0.50	5.0	18.652	2.014	$4.4709\times10^{-2} \pm 8.6971\times10^{-5}$
	8192	0.50	5.0	19.367	4.886	$1.0848\times10^{-1} \pm 2.1029\times10^{-3}$

PTEP2022, 073H01 (2022)

Application to GW Data I : Lightning Strokes

PRD 106, 042010 (2022)

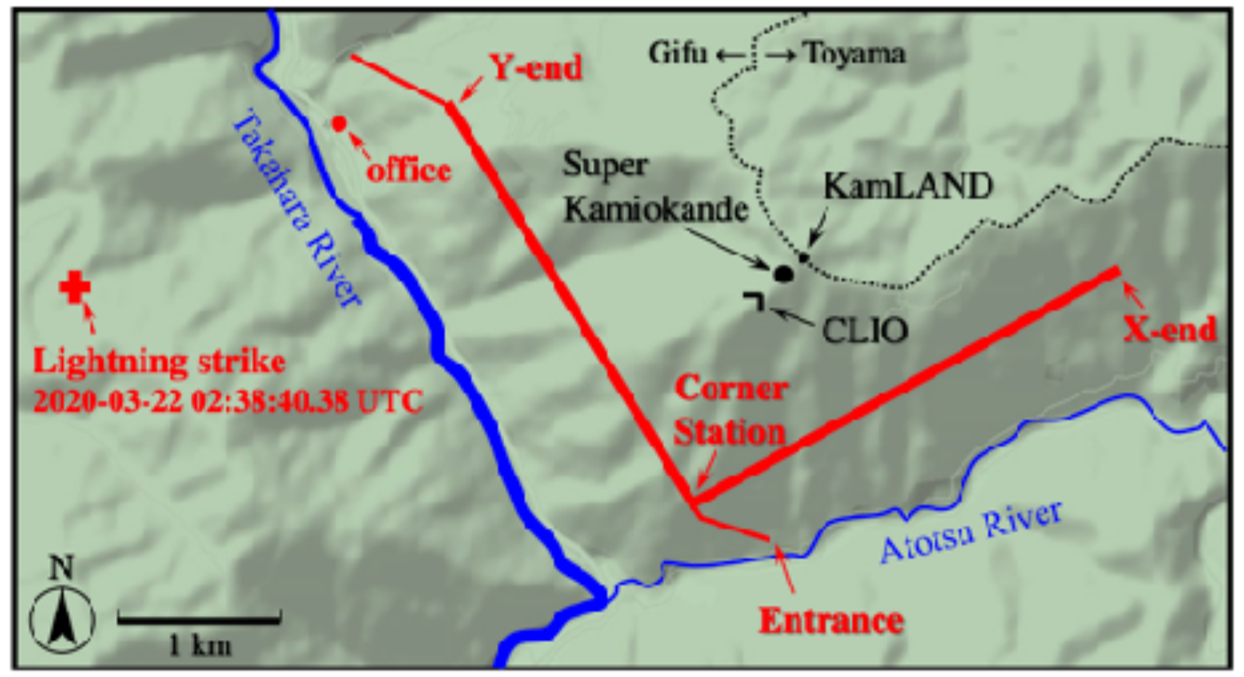

T. Washimi et al. JINST 16 P07033 (2021)

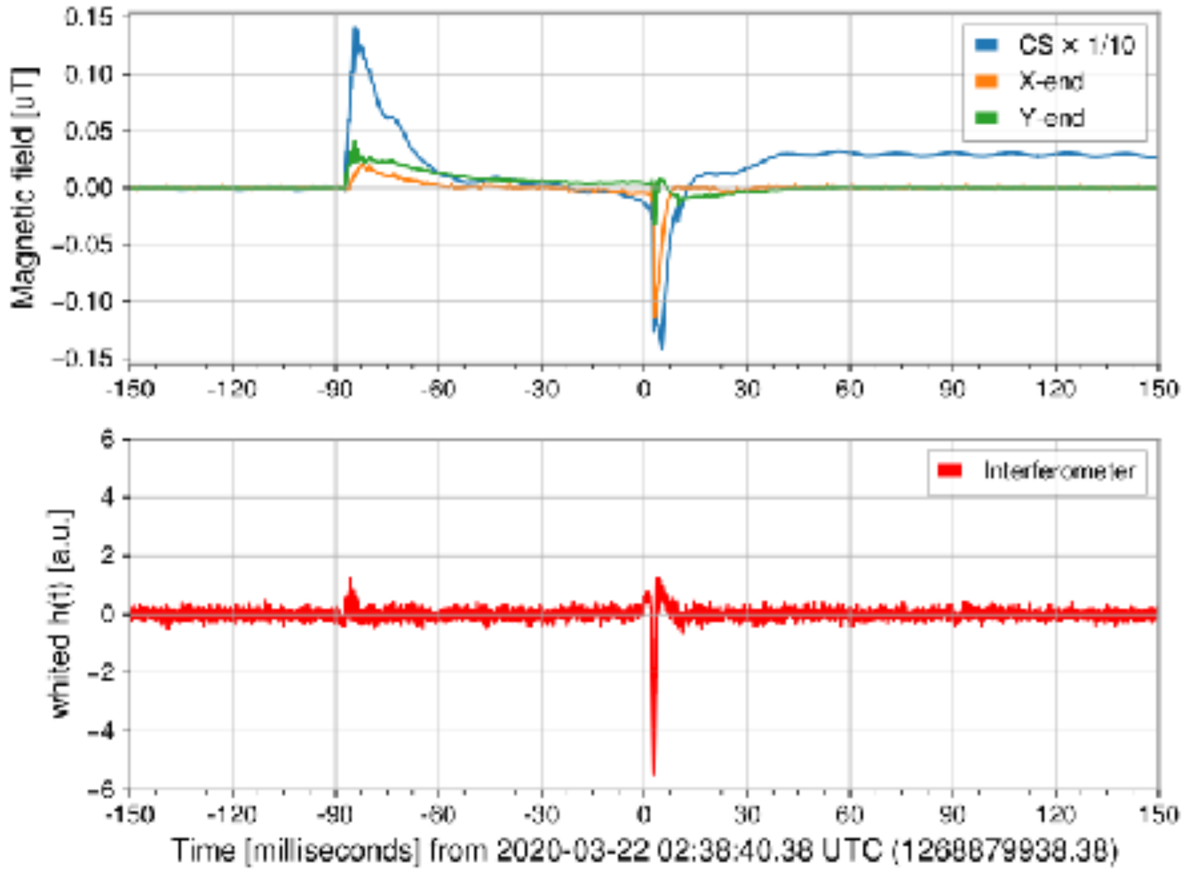

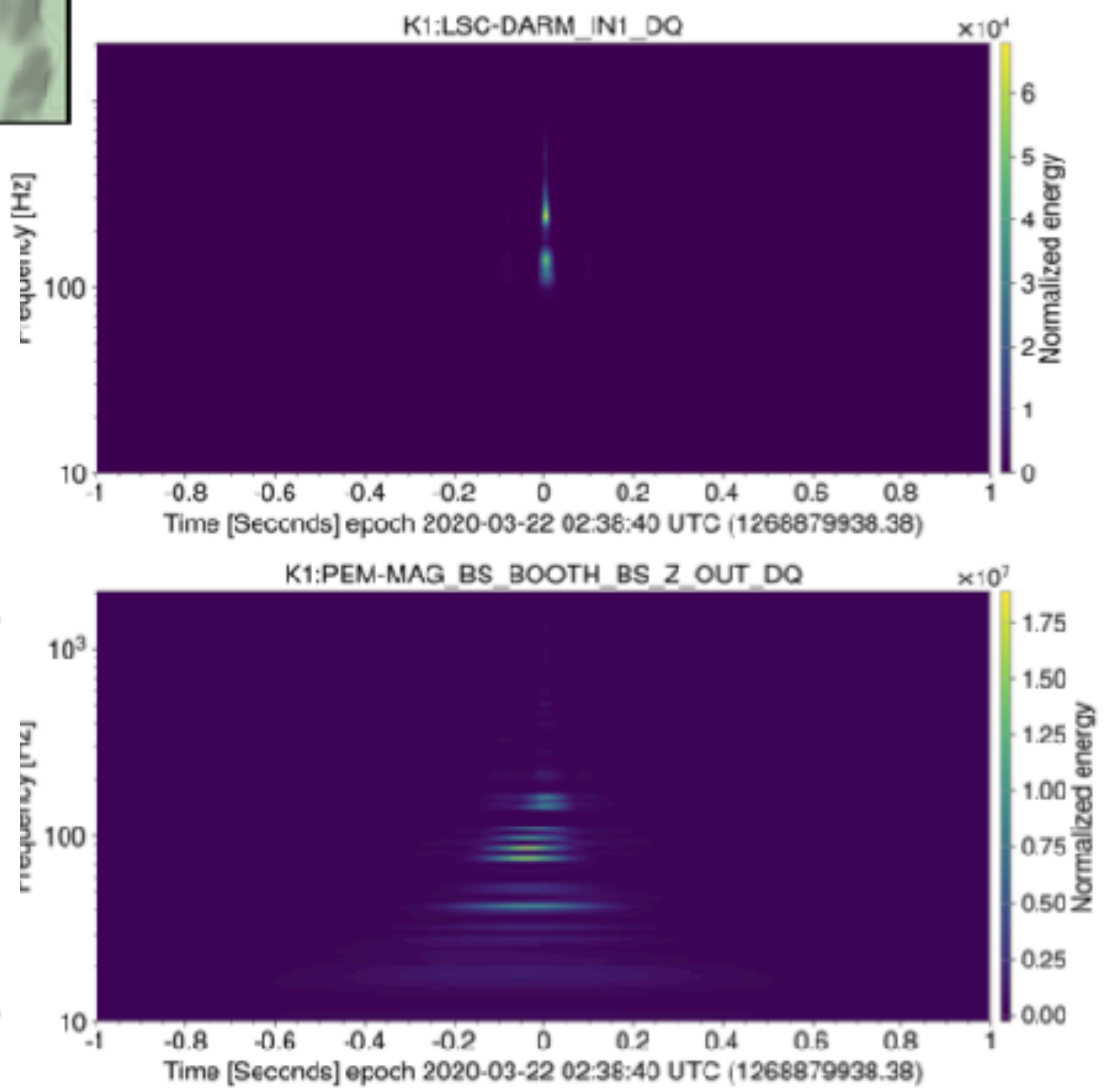

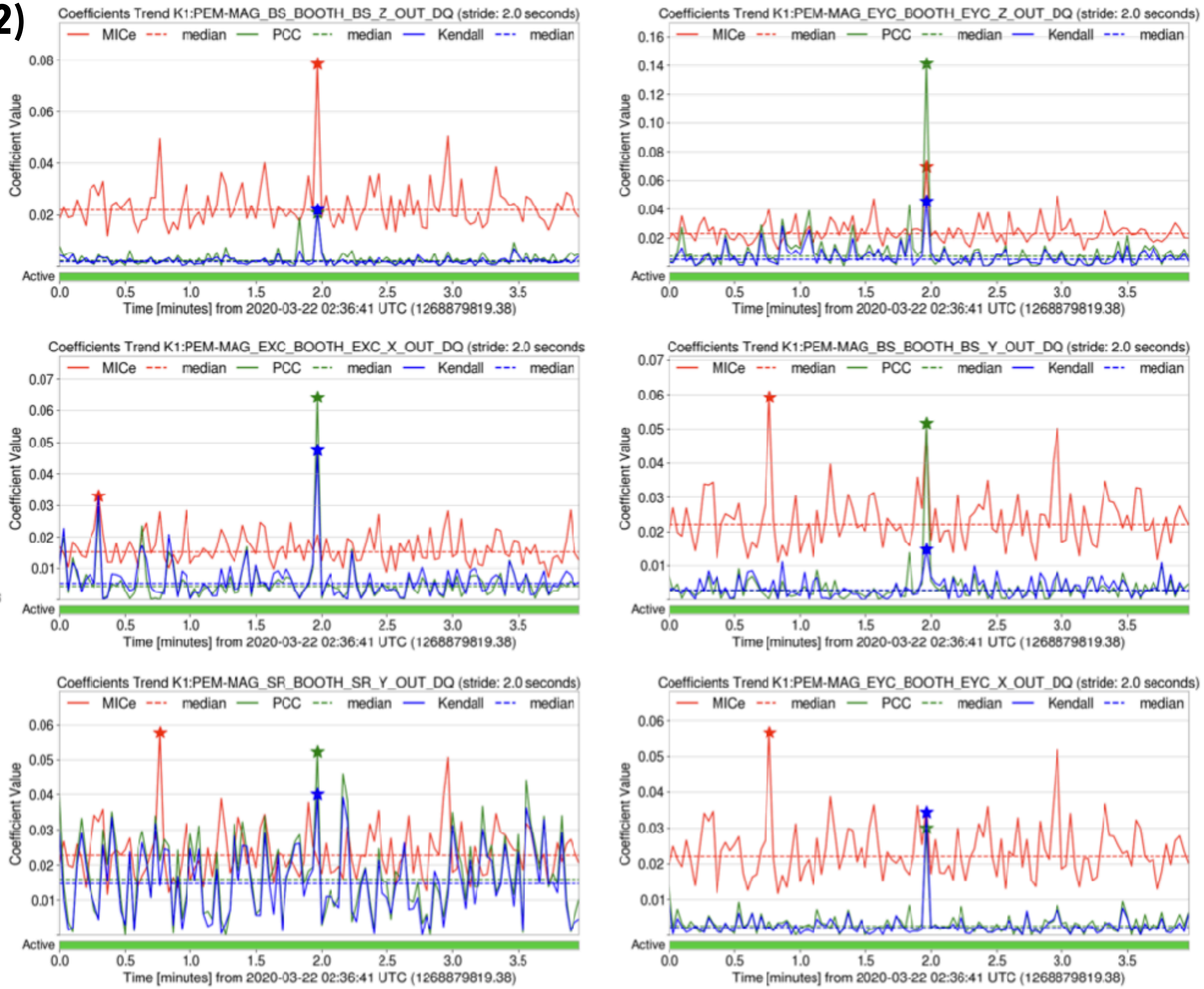

Event time (GPS)	Associated auxiliary channels[a]	MICe	Med(MICe)[b] (10^{-2})	ρ	Med(ρ)(10^{-2})	τ	Med(τ)(10^{-2})
	K1:PEM[c]-MAG_BS_BOOTH_BS_Z_OUT_DQ	0.079	2.210	0.021	0.212	0.022	0.172
March 22, 2020	K1:PEM-MAG_BS_BOOTH_BS_Y_OUT_DQ	0.050	2.210	0.052	0.250	0.015	0.275
02:38:39-41UTC	K1:PEM-MAG_BS_BOOTH_BS_X_OUT_DQ	0.026	2.188	0.040	0.266	0.001	0.197
(1268879937.38	K1:PEM-MAG_EXC_BOOTH_EXC_X_OUT_DQ	0.021	1.499	0.064	0.423	0.047	0.521
-1268879939.38)	K1:PEM-MAG_EYC_BOOTH_EYC_Z_OUT_DQ	0.069	2.309	0.141	0.709	0.045	0.474
	K1:PEM-MAG_SR_BOOTH_SR_Z_OUT_DQ	0.022	2.271	0.052	1.595	0.040	1.458

Application to GW Data II : Air Compressor Noises

PRD 106, 042010 (2022)

- **Correlated peaks with a harmonic f=26.5Hz in 2.58hours/day**
- **New discovery in KAGRA – should be handled for noise mitigation**

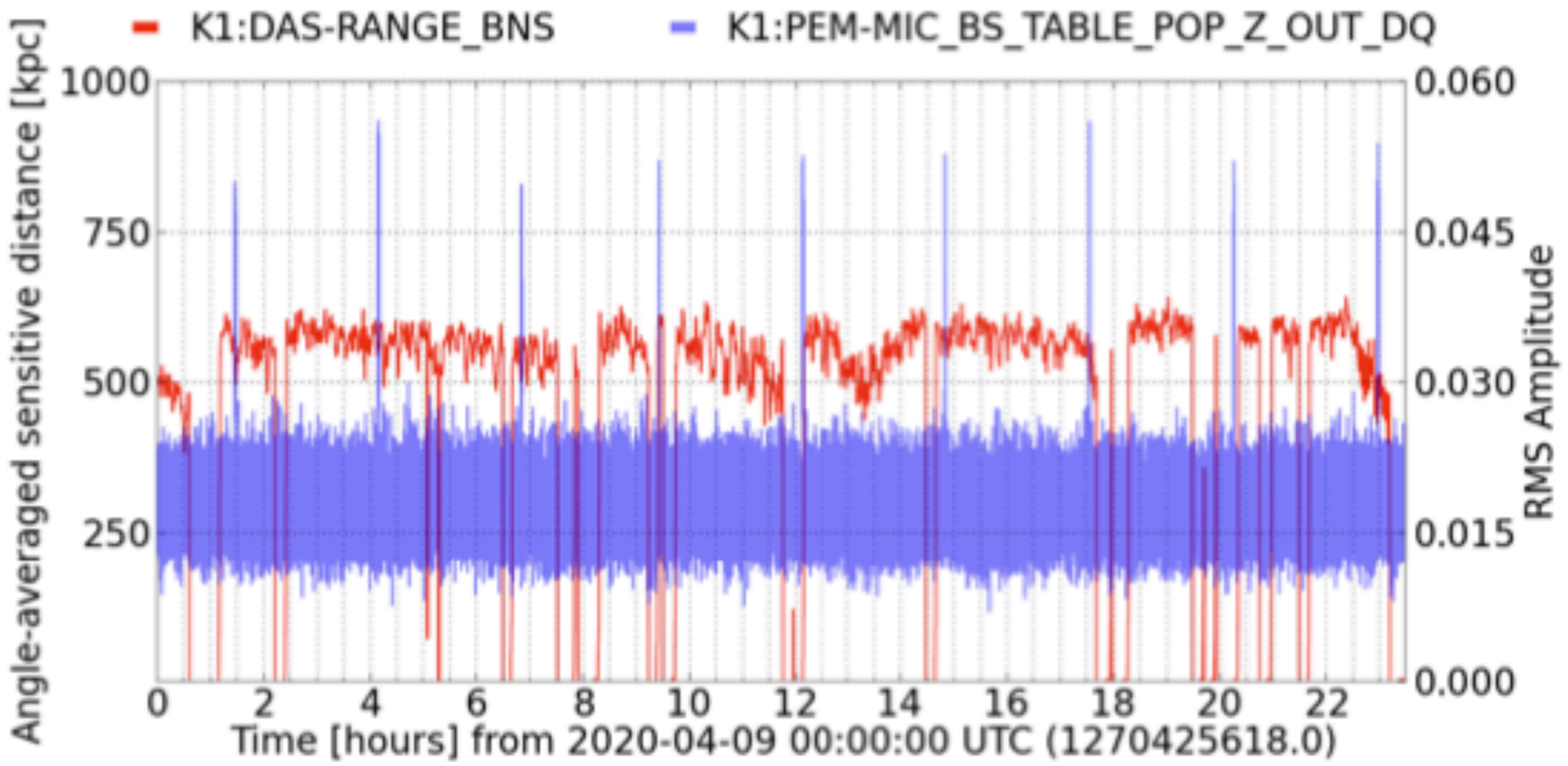

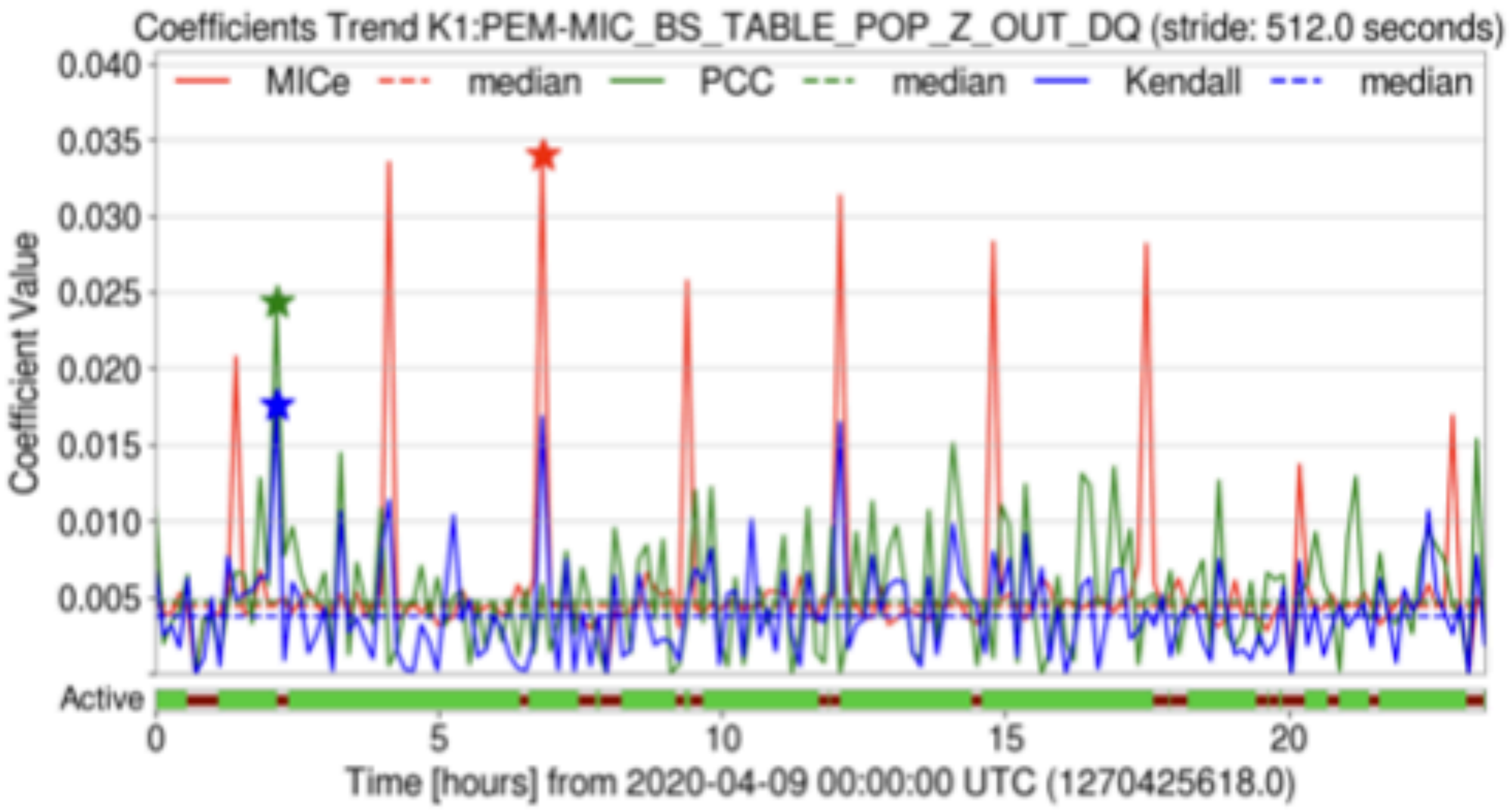

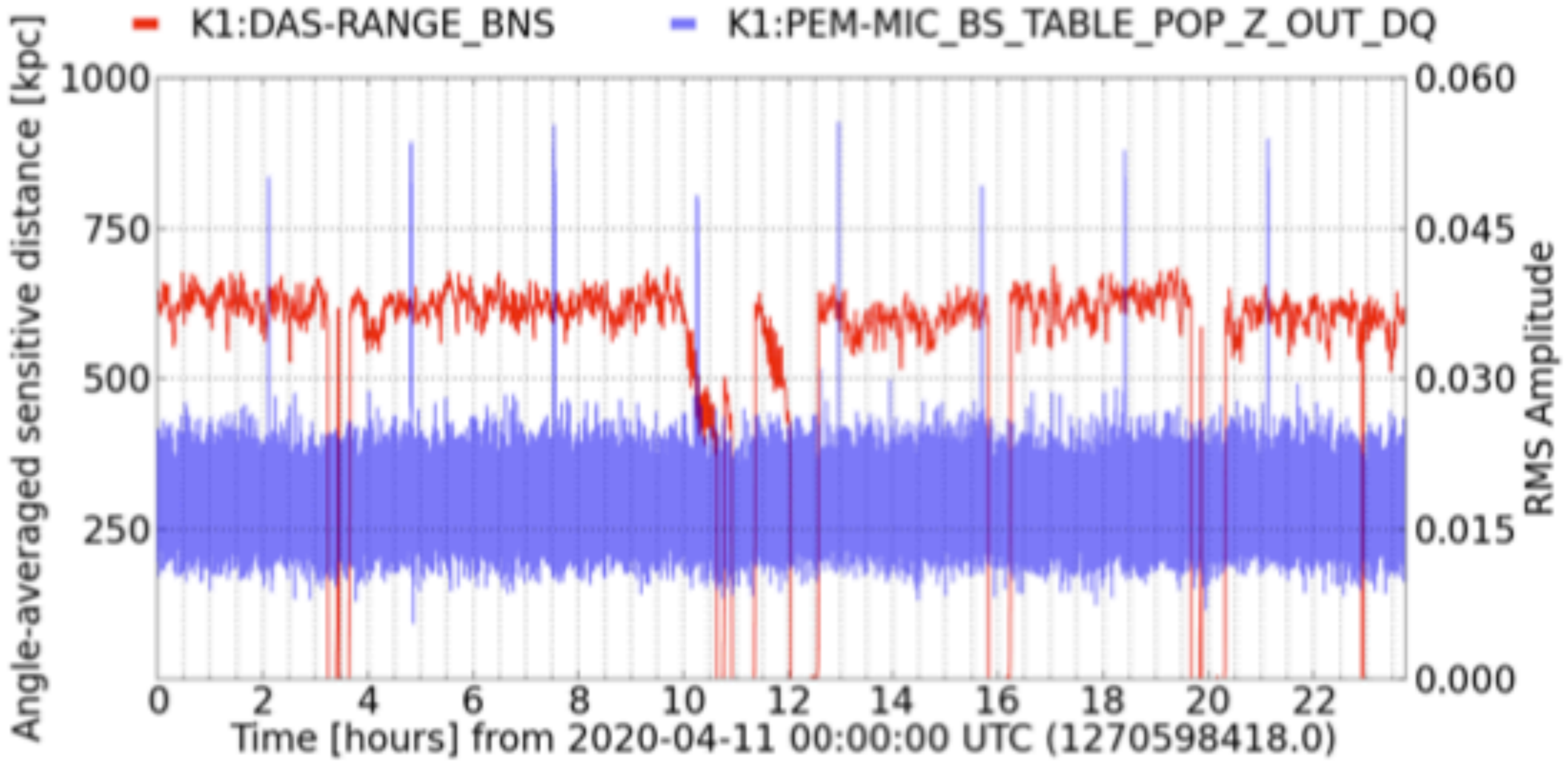

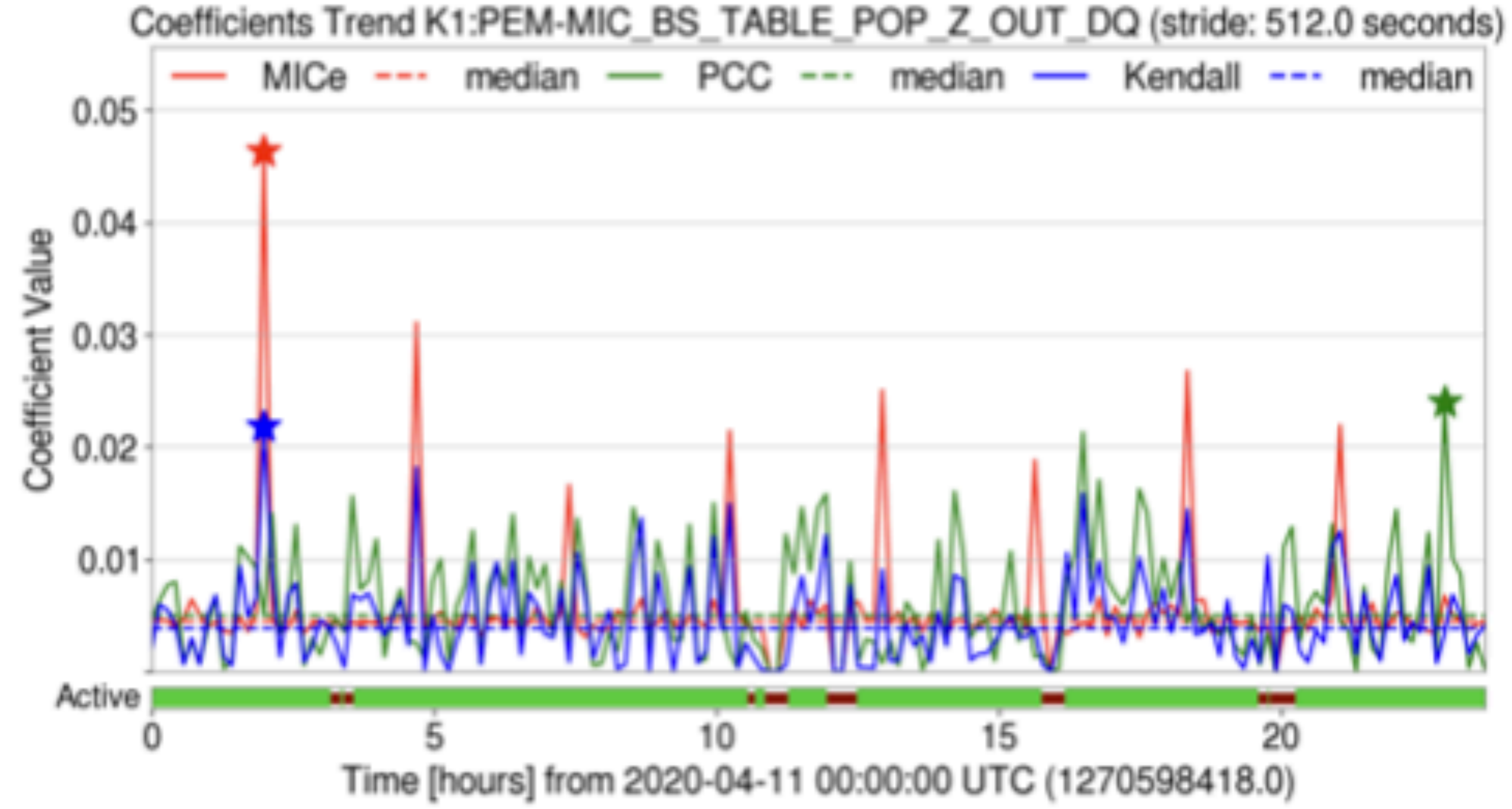

Application to GW Data III : Gravity Gradient Noise from Winds

PRD 106, 042010 (2022)

- **Strong winds found in day time (9AM-7PM) between valley of IKENO Mt.**
- **PEM MIC channels are affected by this wind effects in the underground facilities**
- **Strong non-linear correlations between MIC-GW channels**

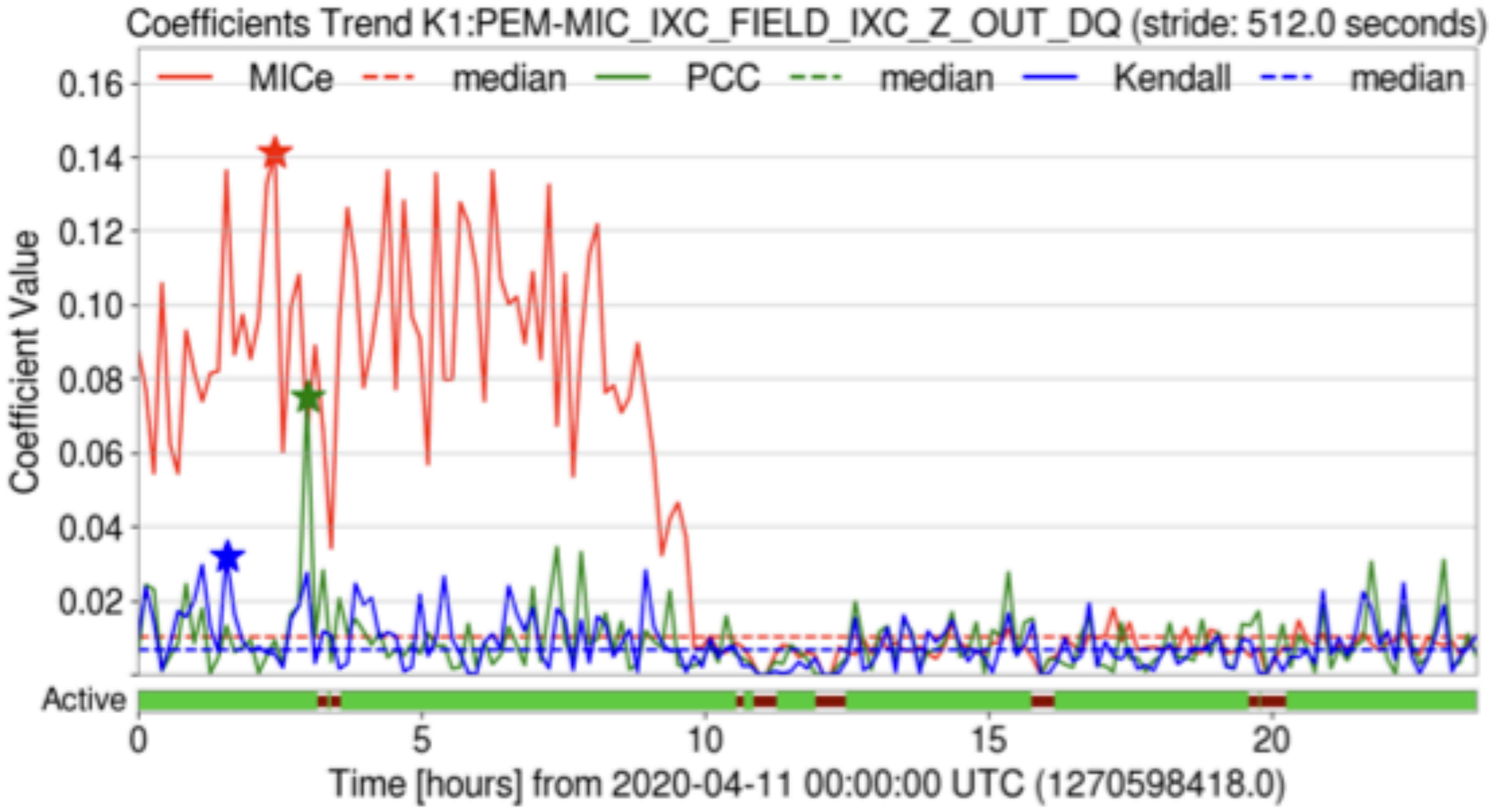

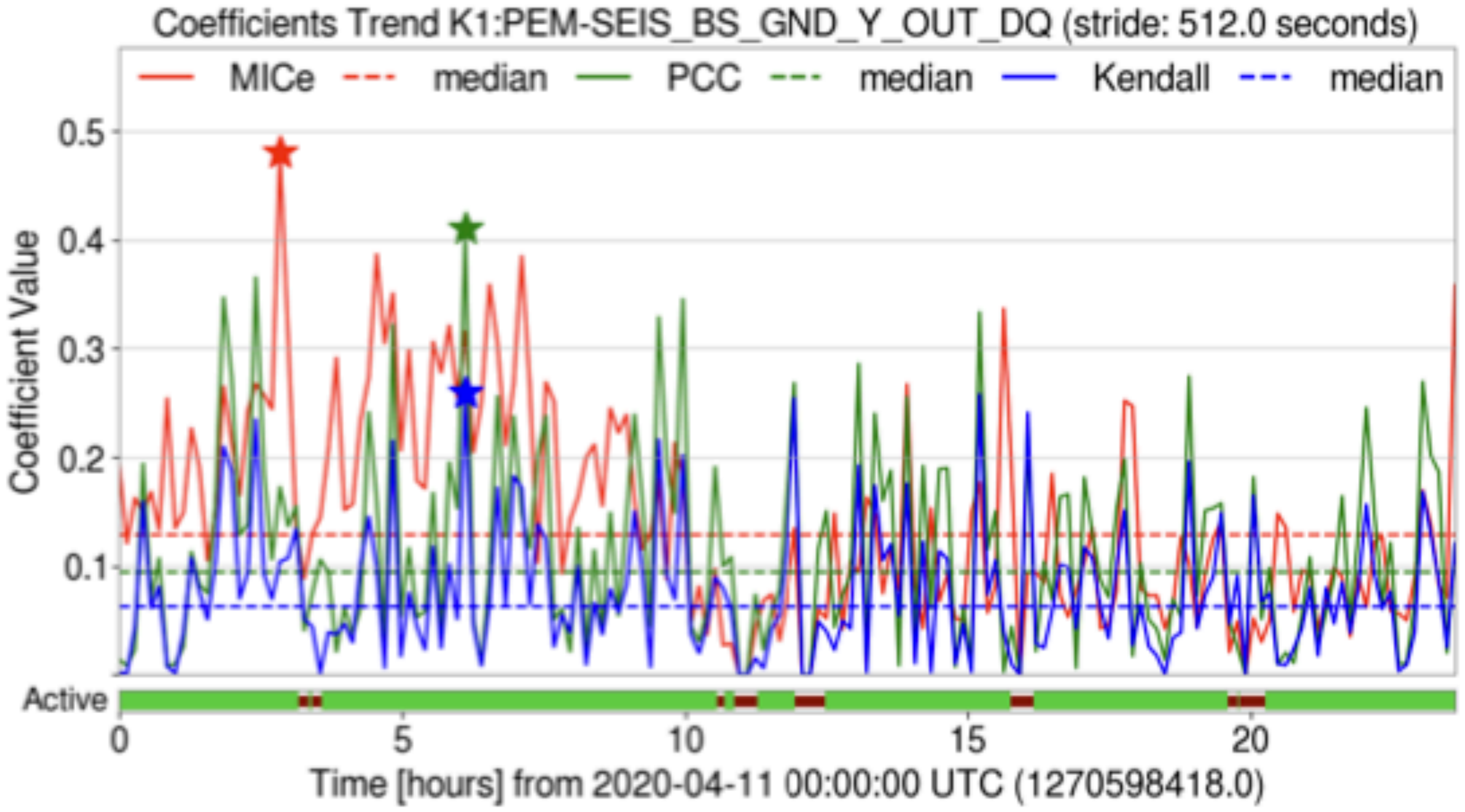

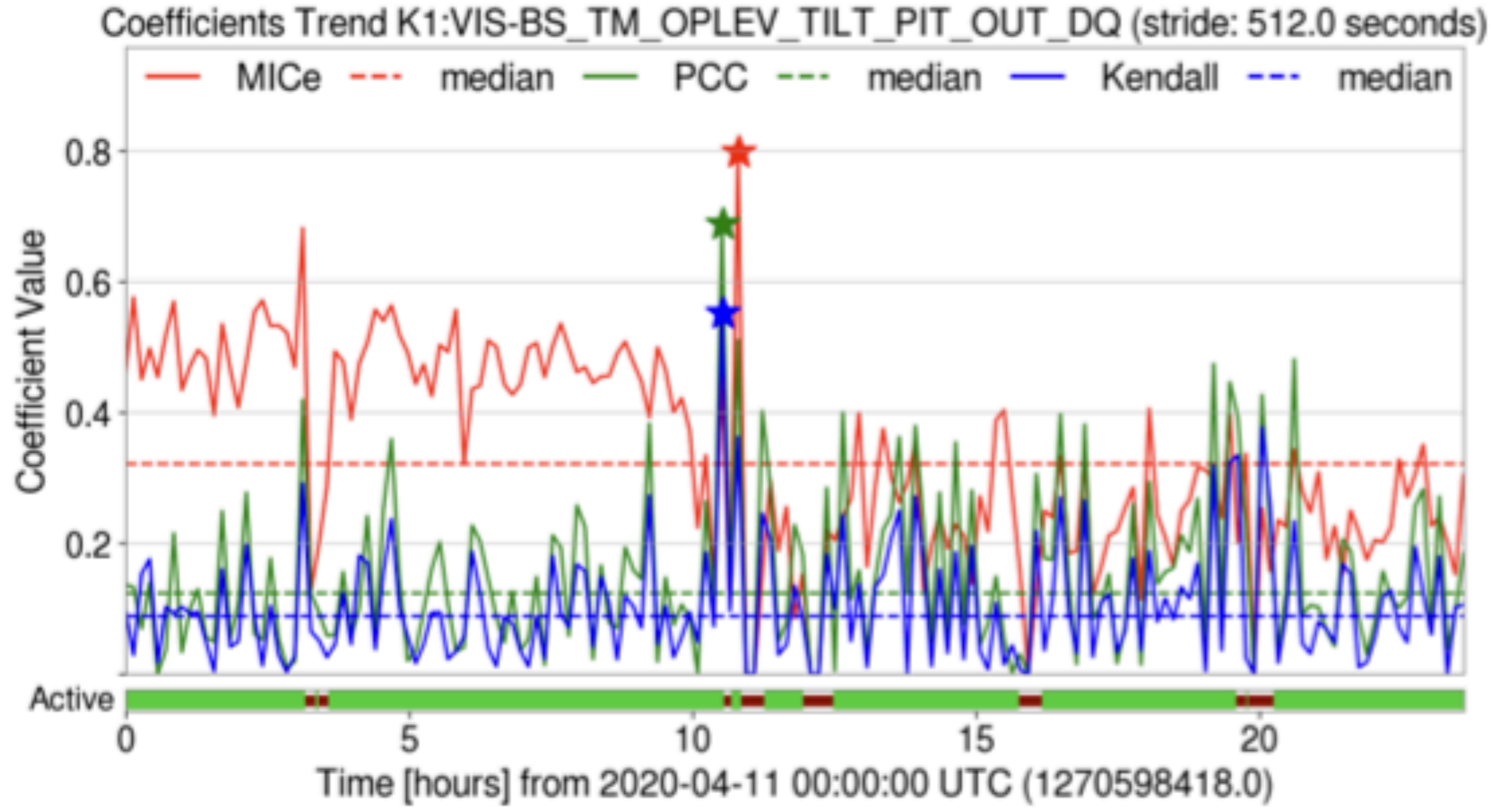

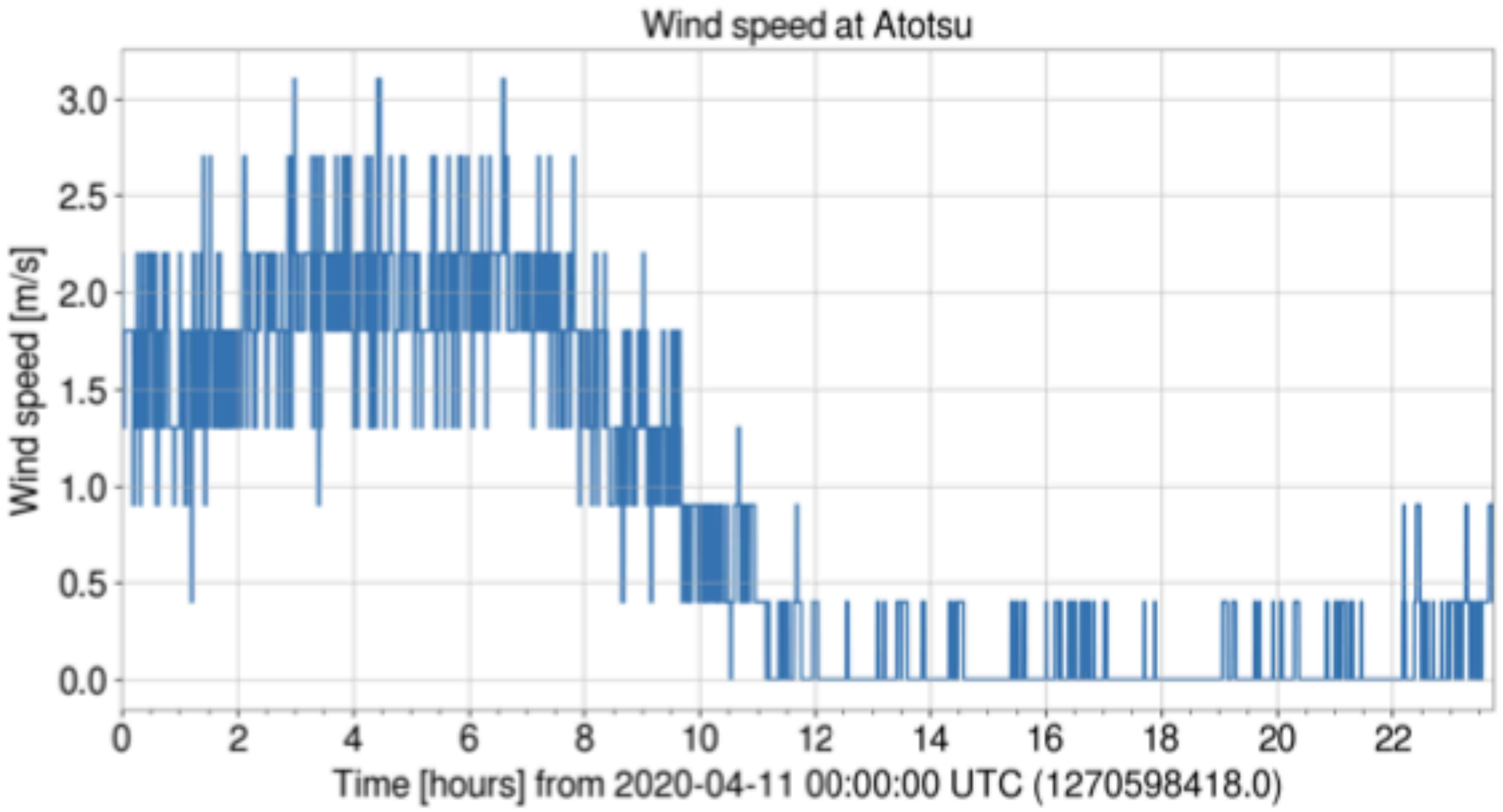

Application to GW Data III : Gravity Gradient Noise from Winds

PRD 106, 042010 (2022)

- **Strong winds found in day time (9AM-7PM) between valley of IKENO Mt.**
- **PEM MIC channels are affected by this wind effects in the underground facilities**
- **Strong non-linear correlations between MIC-GW channels**

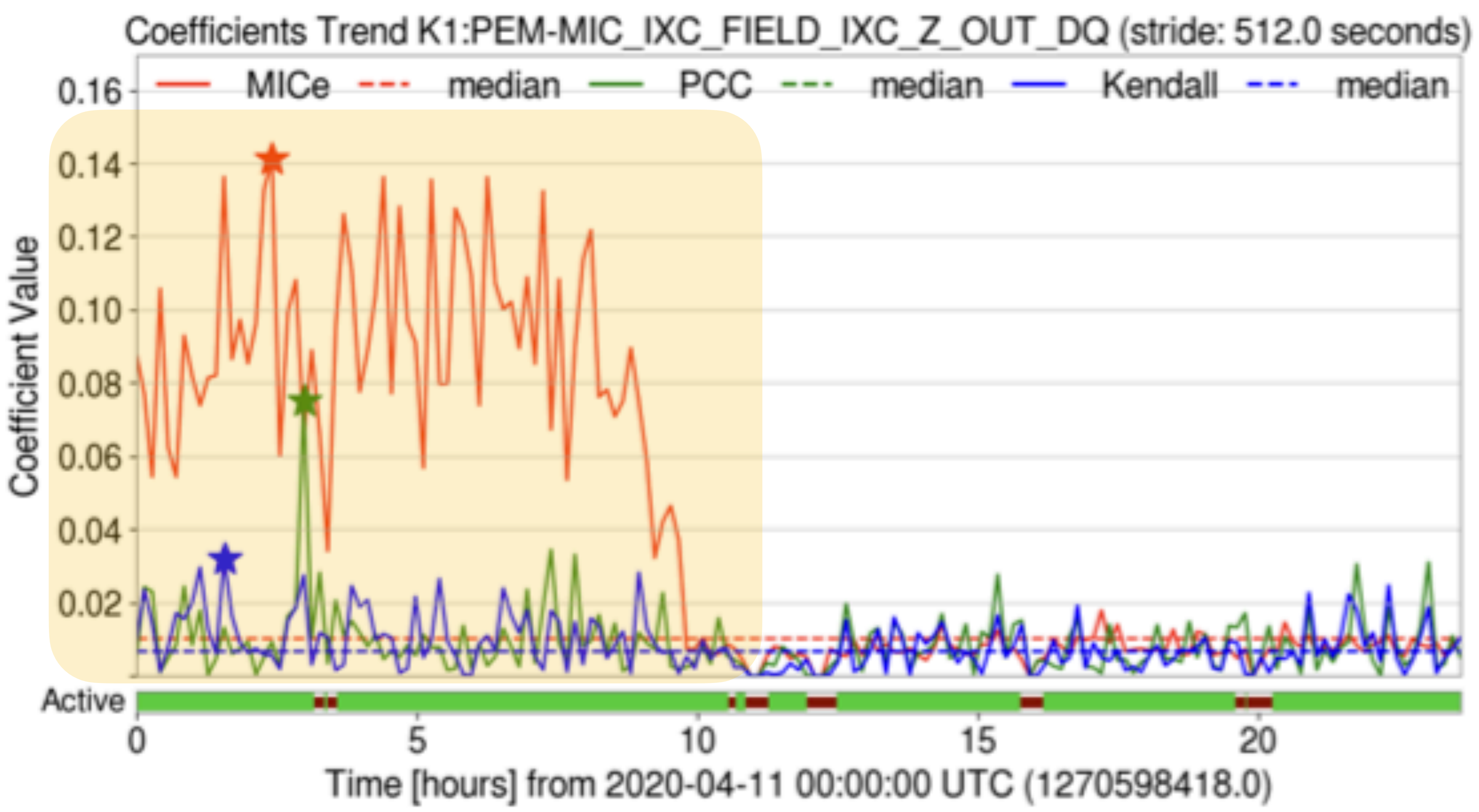

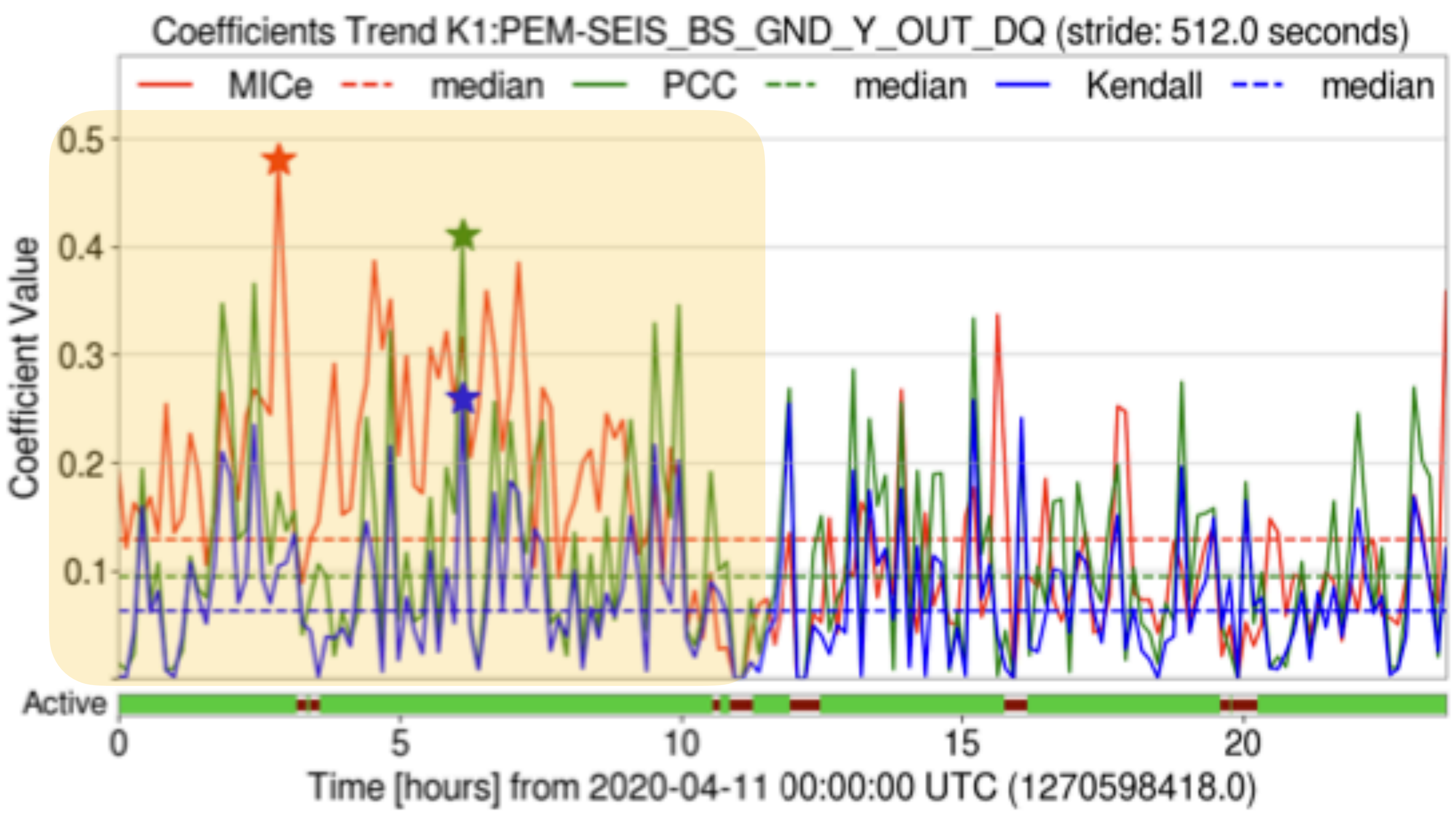

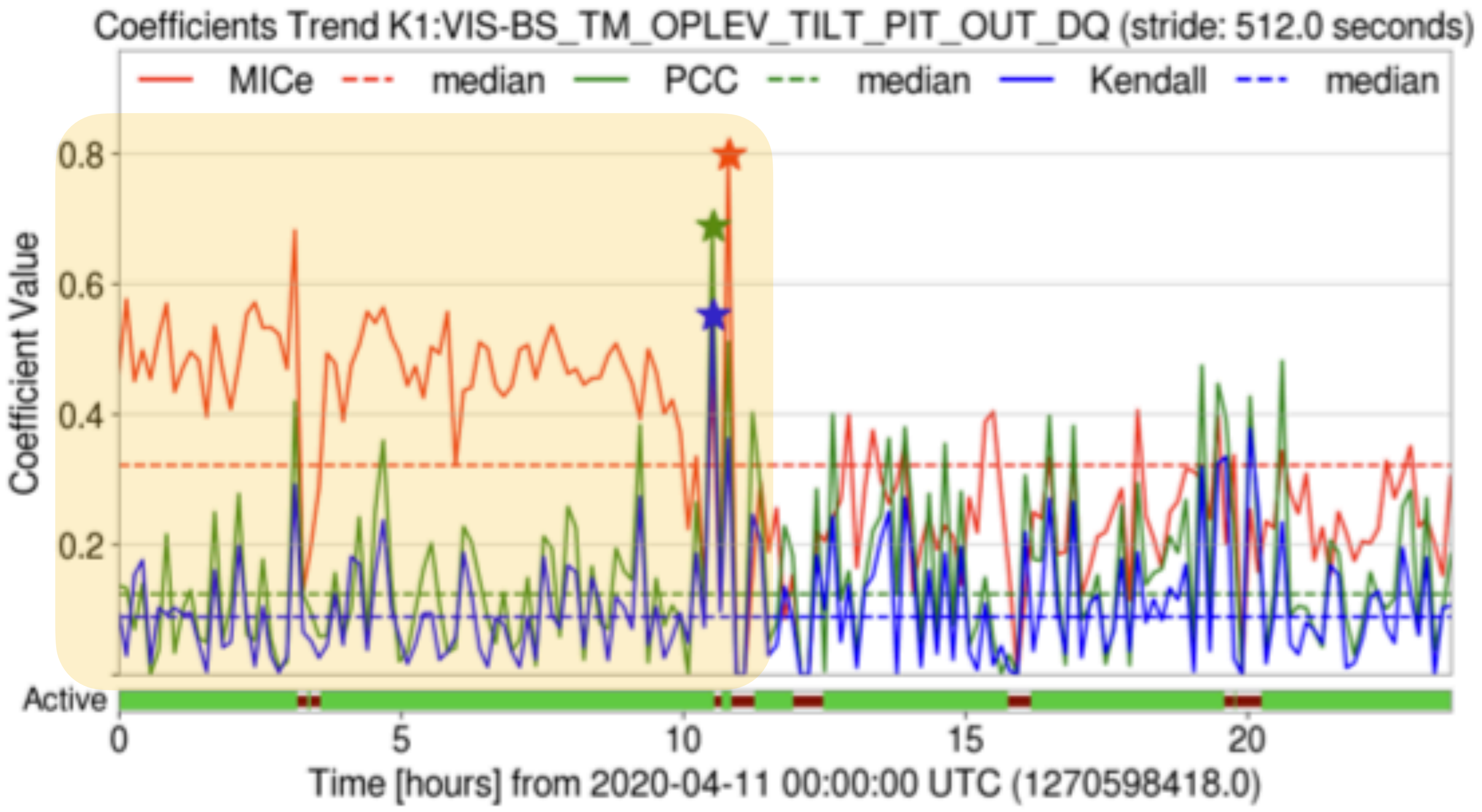

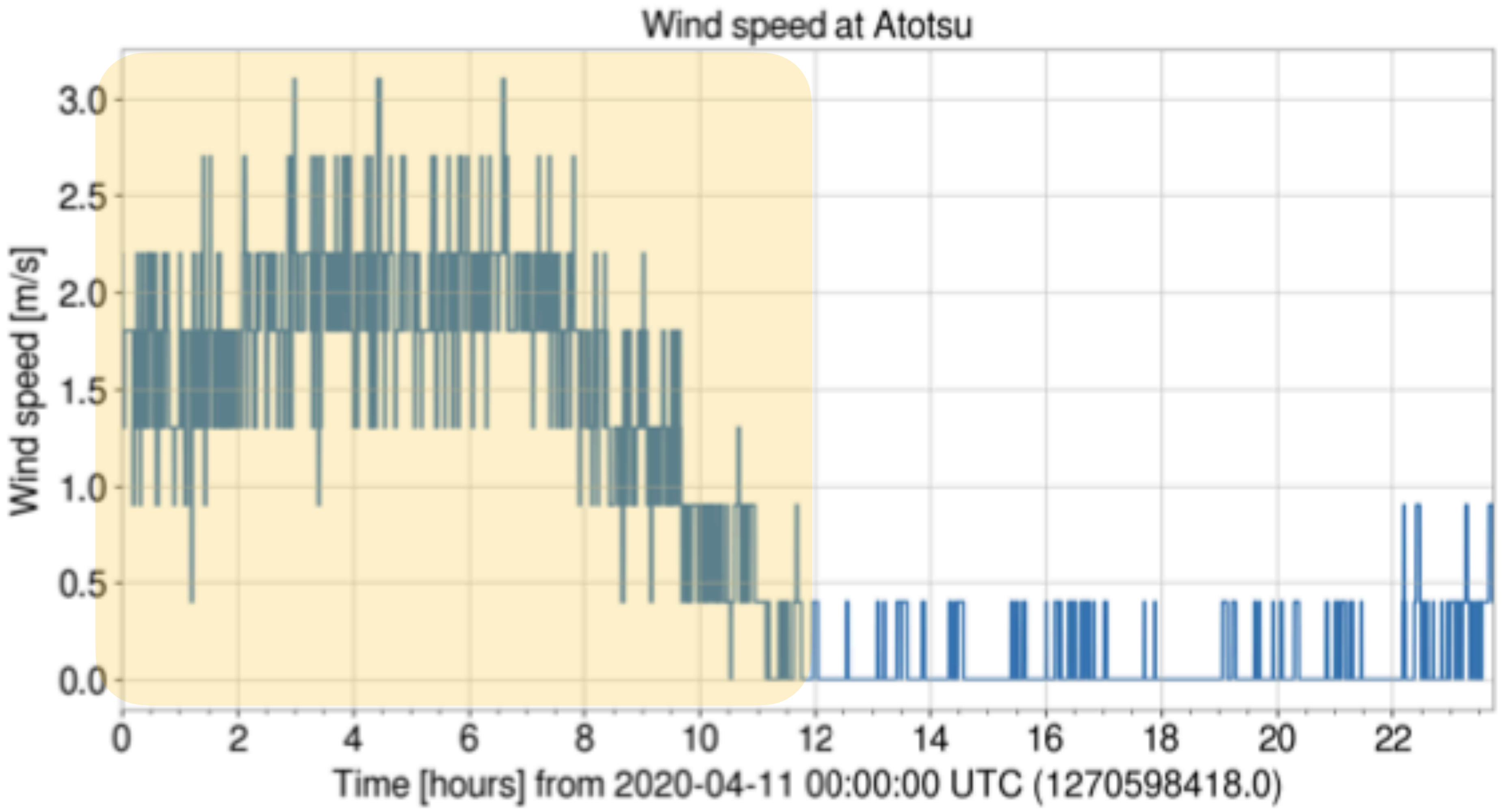

Application to GW Data III : Scenario & Simulation

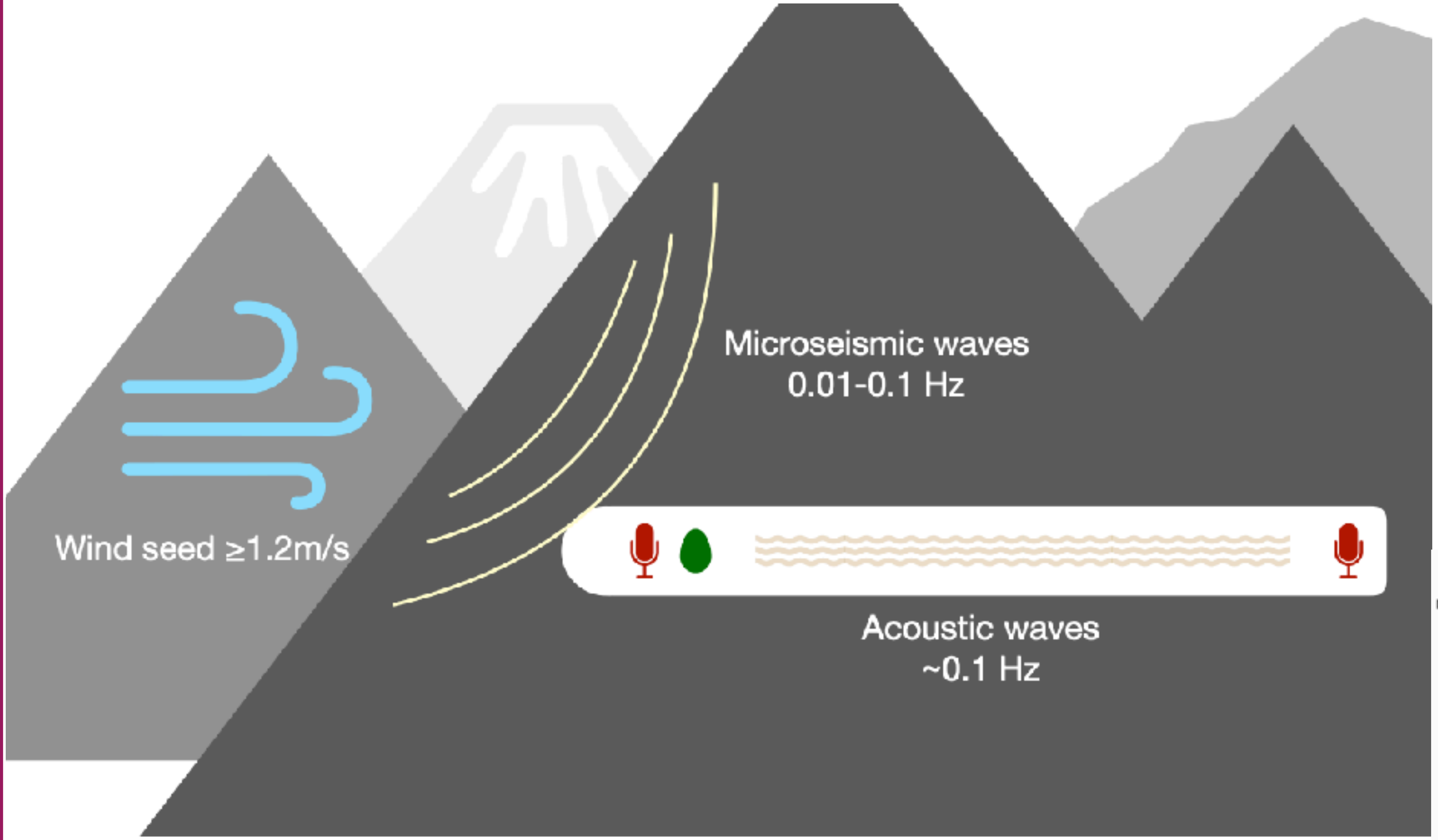

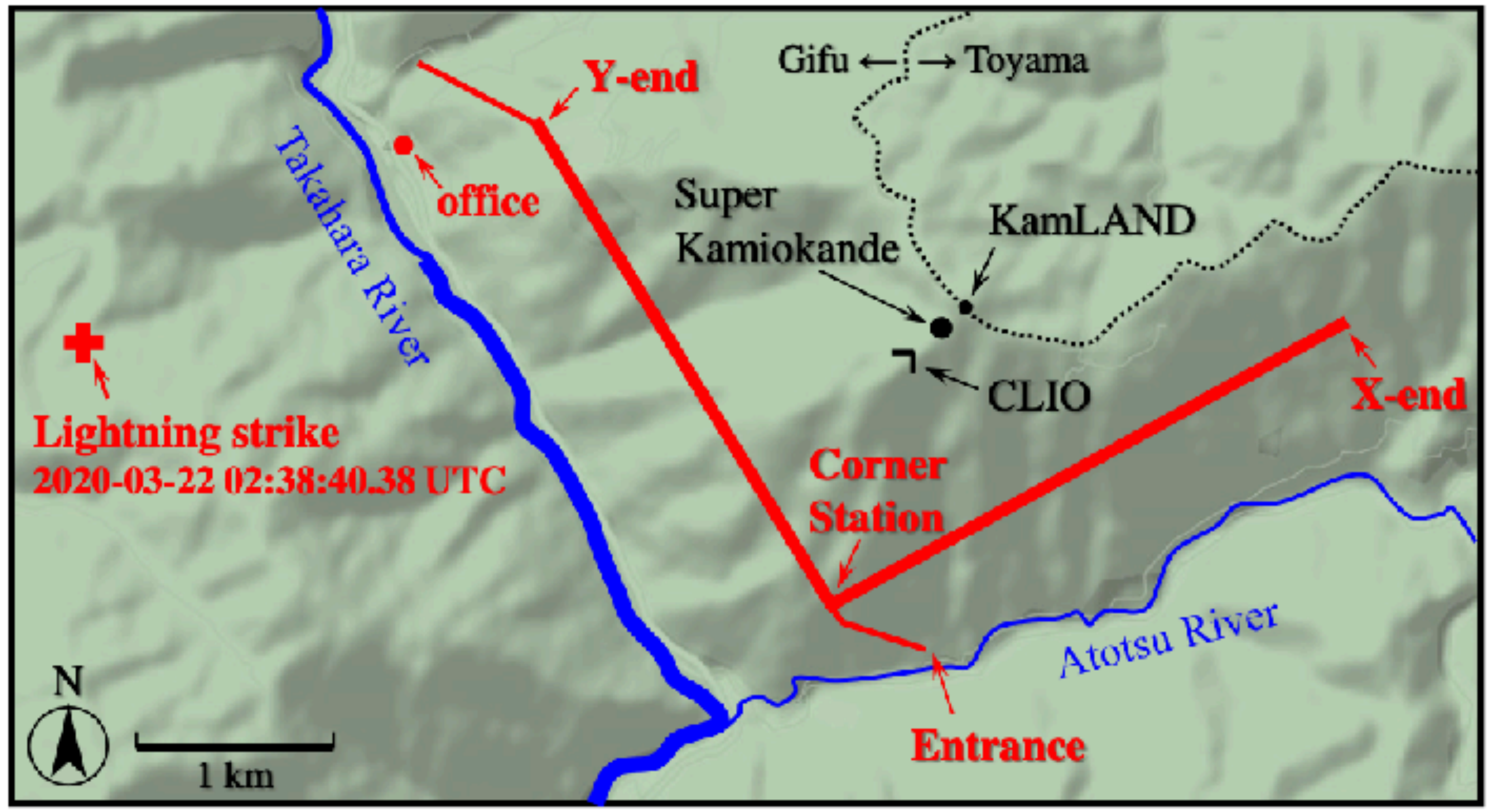

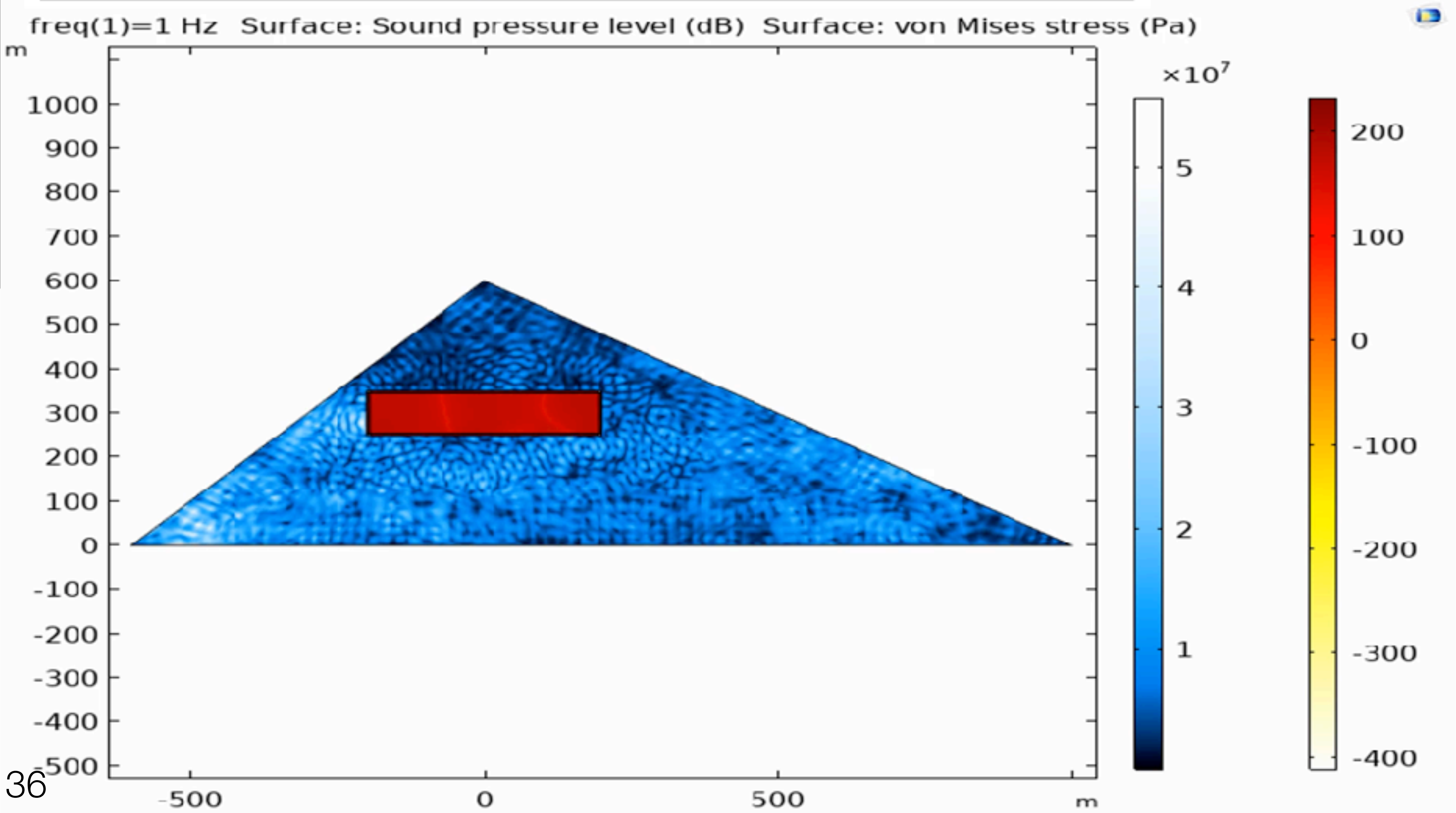

- Low sound pressure level at deep inside the tunnel
- Seismic vibration propagates to the tunnel, then excites the acoustic pressure level
- 2D simulation (RHS) coincides with the acoustic noise measurement in the tunnel of the X-arm

PRD 106, 042010 (2022)

Application to GW Data III : Scenario & Simulation

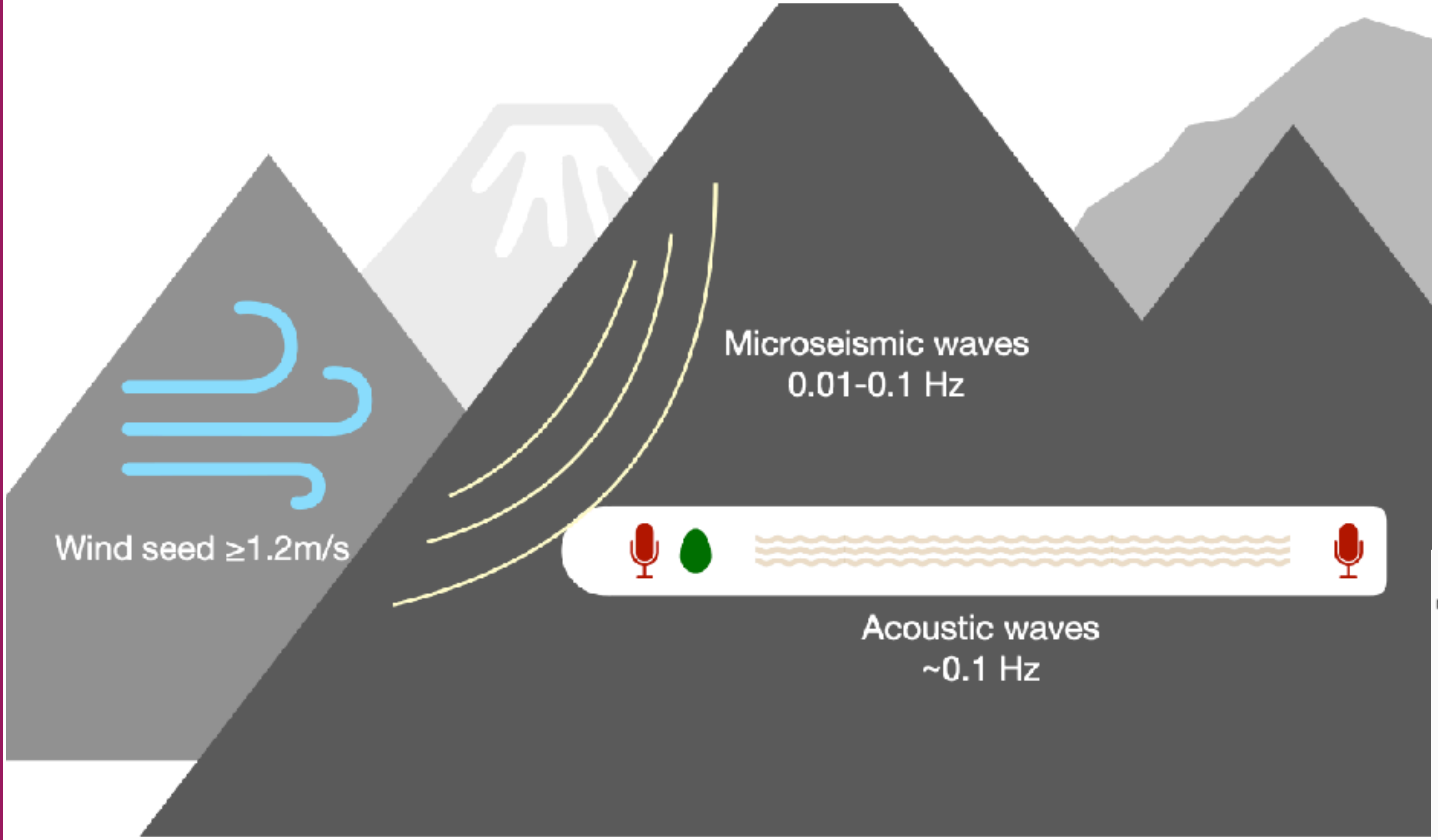

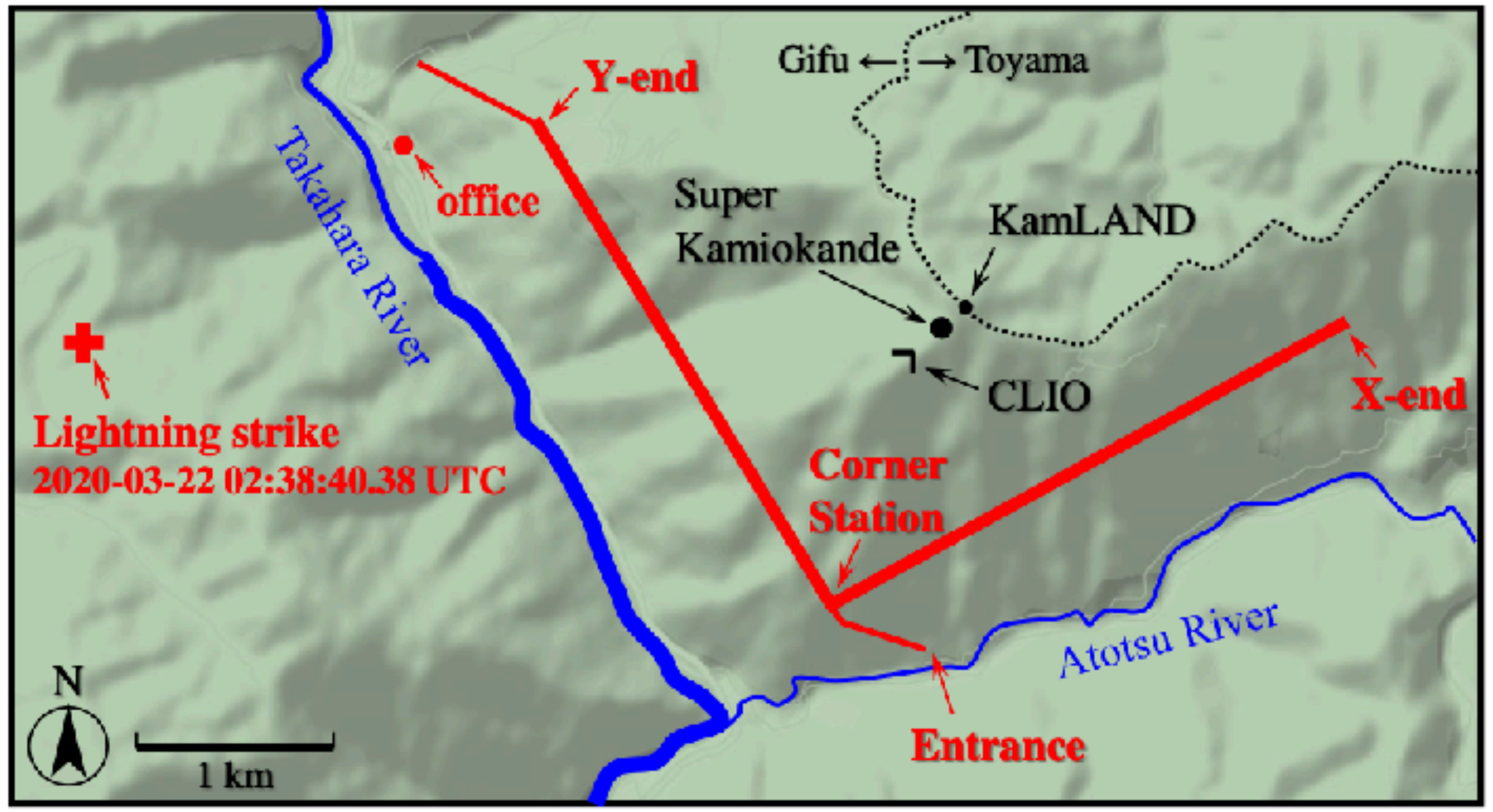

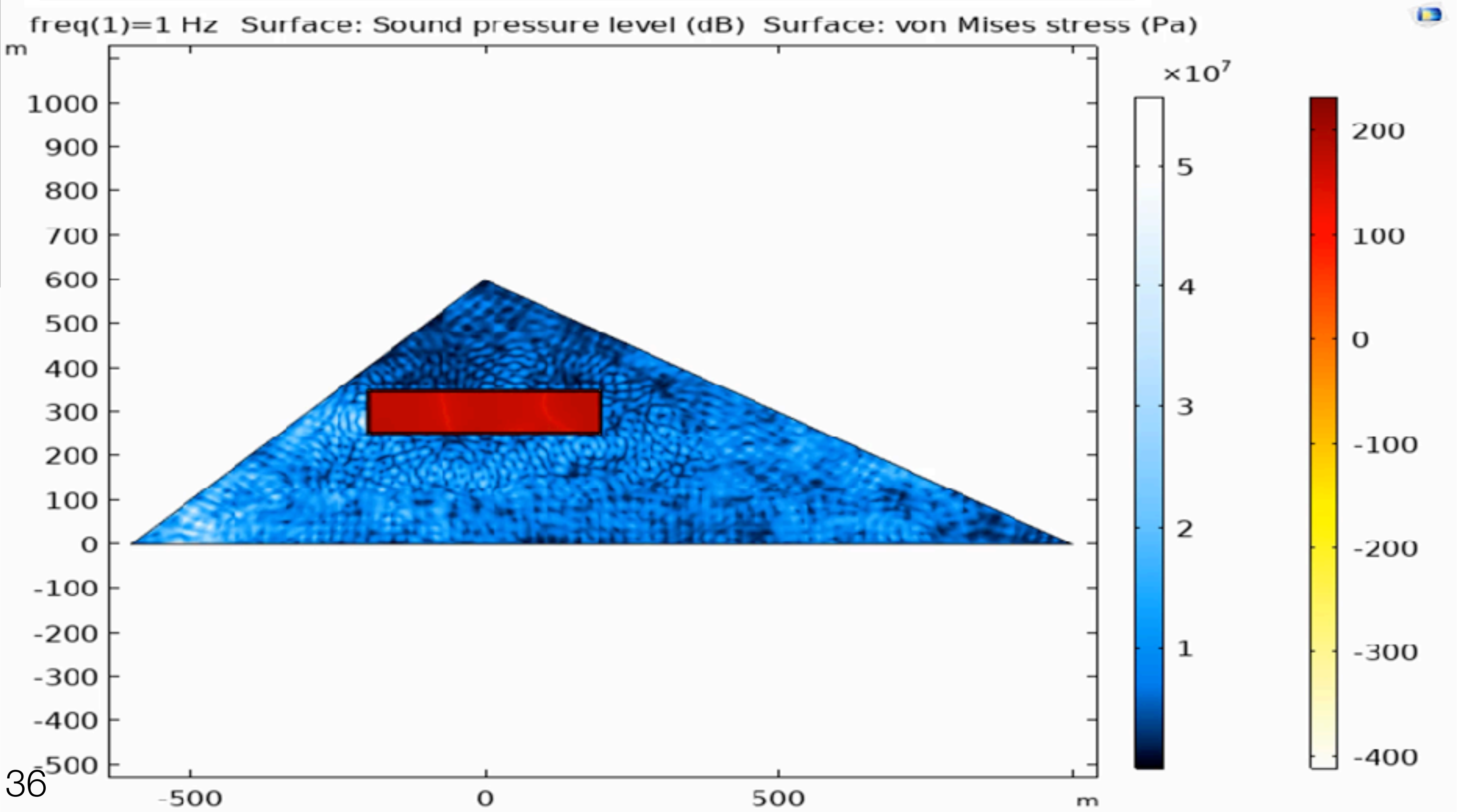

- Low sound pressure level at deep inside the tunnel
- Seismic vibration propagates to the tunnel, then excites the acoustic pressure level
- 2D simulation (RHS) coincides with the acoustic noise measurement in the tunnel of the X-arm

PRD 106, 042010 (2022)

Application to GW Data III : Scenario & Simulation

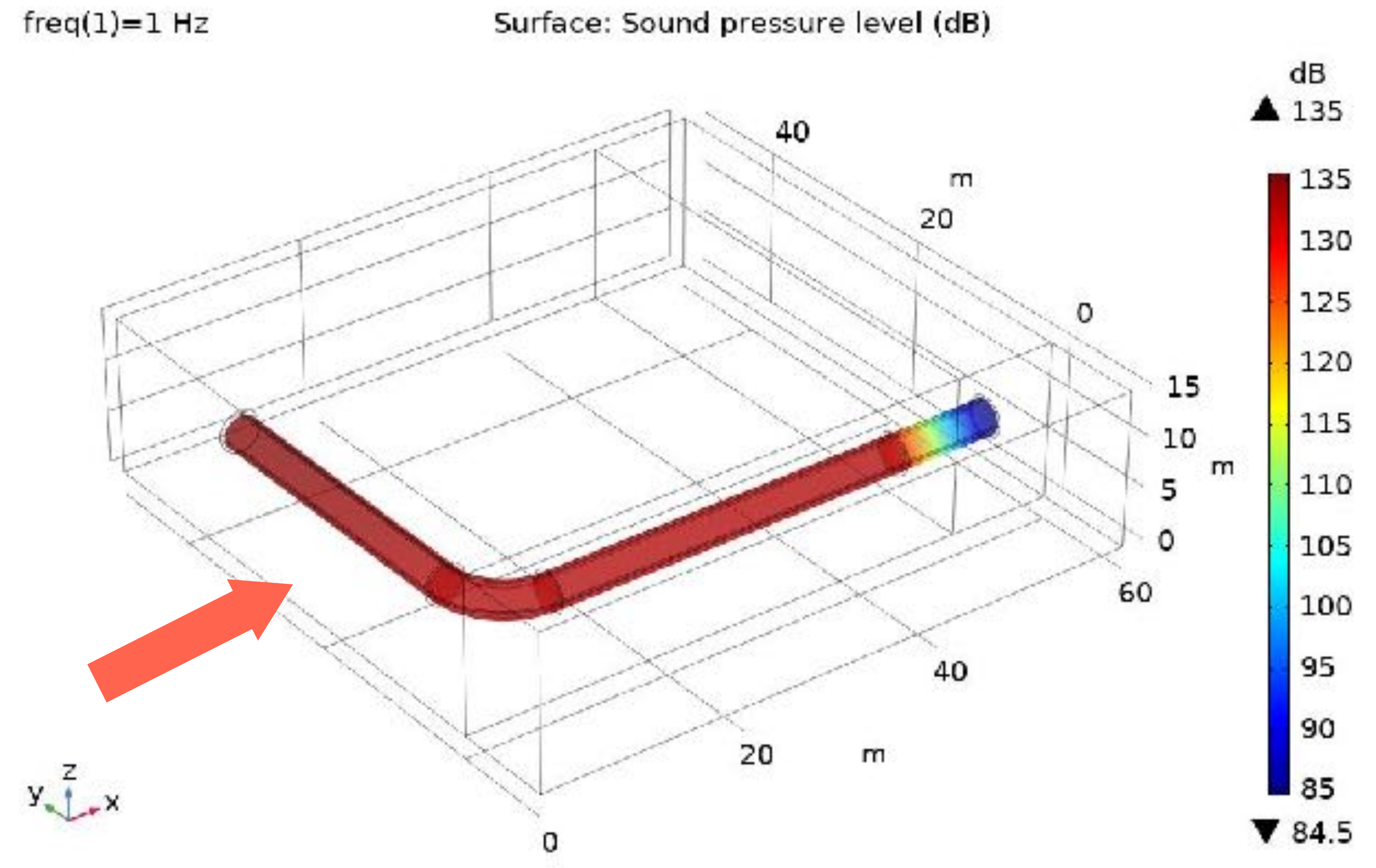

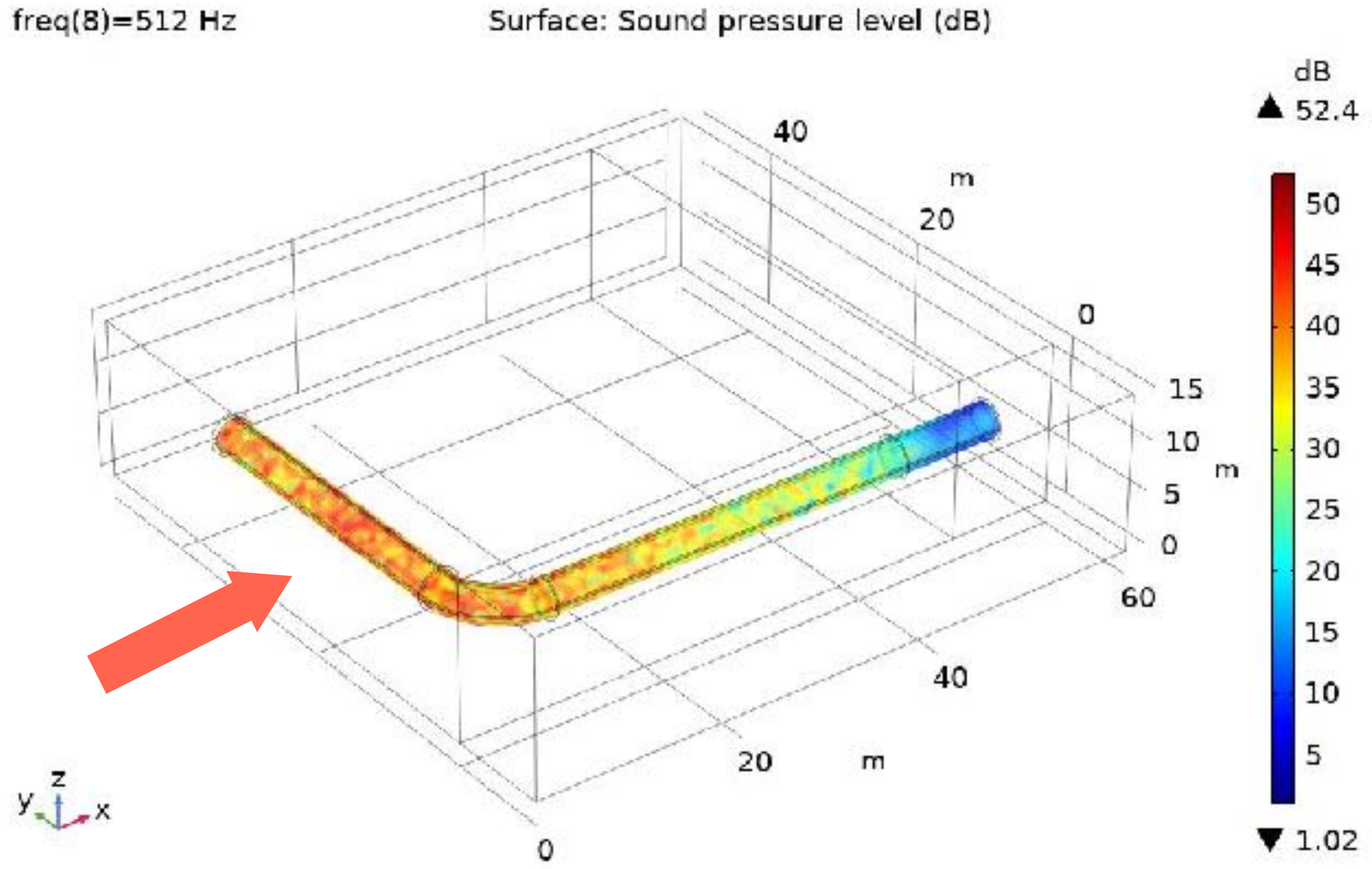

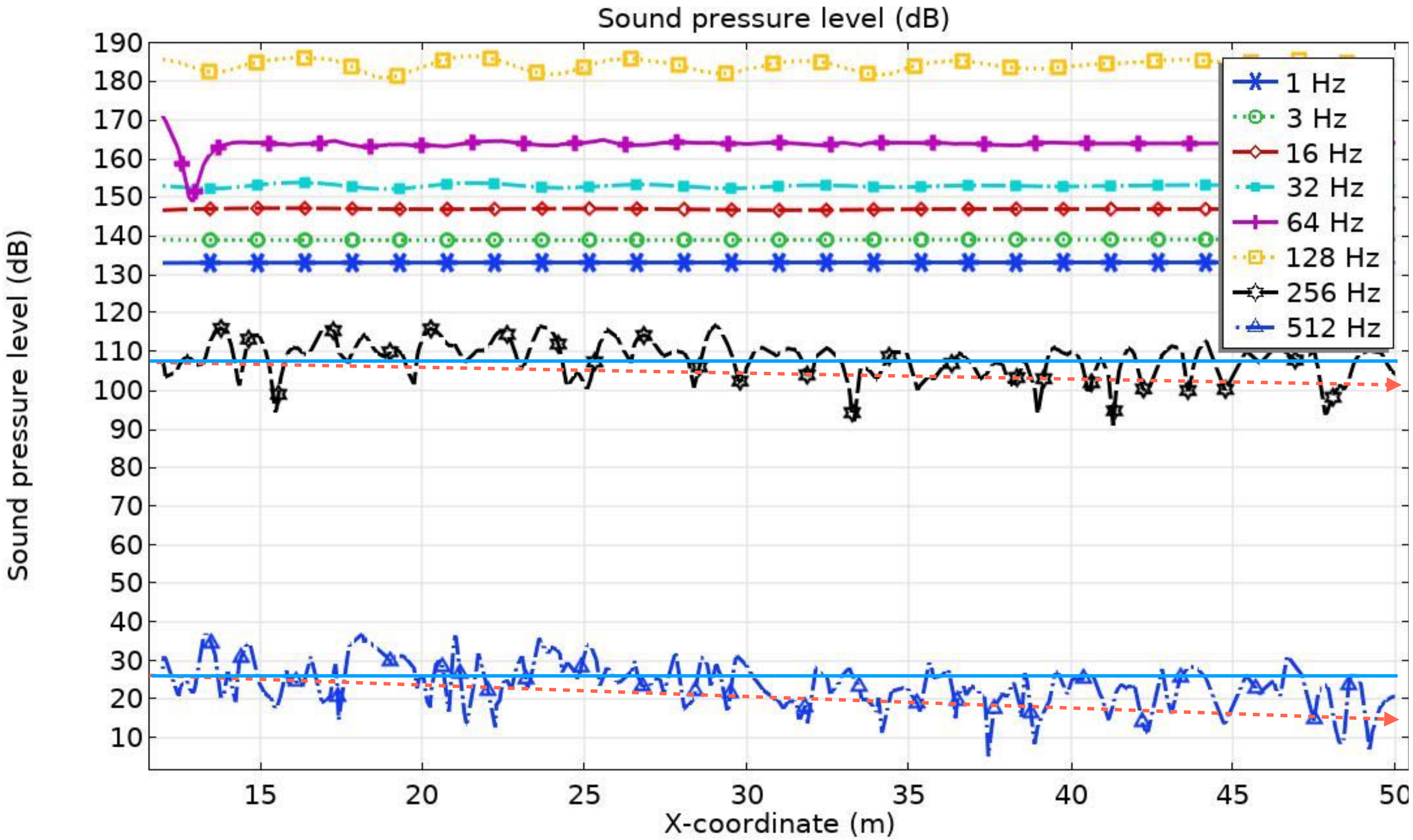

PRD 106, 042010 (2022)

Mitigation of Low-Frequency Noise by using Bandgap Engineering

D. J. Griffiths, 'Introduction to Quantum Mechanics'

- Let us consider a periodic potential in one-dimensional space: $V(x) = V(x+a)$

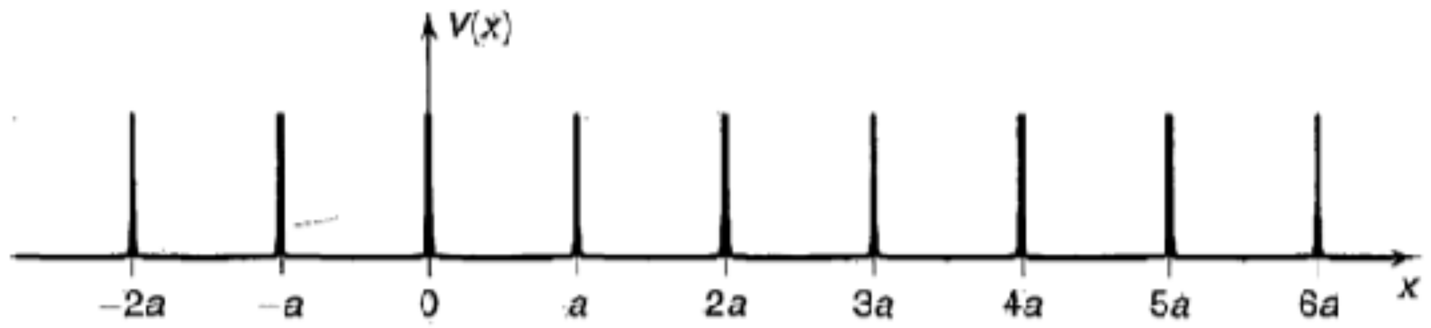

then, Bloch's theorem: the solution to the Schrödinger's eqn,

$$-\frac{\hbar^2}{2m}\frac{d^2\psi}{dx^2} + V(x)\psi = E\psi$$

can be taken to satisfy the condition: $\psi(x+a) = e^{iKa}\psi(x)$

for some constant K

- At $x = 0$, ψ must be continuous, then:

1) $B = e^{-iKa}[A\sin(ka) + B\cos(ka)]$

- And for the derivatives,

$$\lim_{\epsilon\to 0}\left(\frac{d\psi}{dx}\bigg|_{+\epsilon} - \frac{d\psi}{dx}\bigg|_{-\epsilon}\right) = \frac{2m\alpha}{\hbar^2}\psi(0)$$

2) $\rightarrow kA - e^{-iKa}[kA\cos(ka) - kB\sin(ka)] = \frac{2m\alpha}{\hbar^2}B$

Combining 1) and 2) gives:

$$\cos Ka = \cos ka + \frac{m\alpha}{\hbar^2 k}\sin ka$$

Let $z \equiv kz$, $\beta \equiv \frac{m\alpha a}{\hbar^2}$, then

$$f(z) \equiv \cos(z) + \beta\frac{\sin(z)}{z}$$

Mitigation of Low-Frequency Noise by using Bandgap Engineering

D. J. Griffiths, 'Introduction to Quantum Mechanics'

- Let us consider a periodic potential in one-dimensional space: $V(x) = V(x+a)$

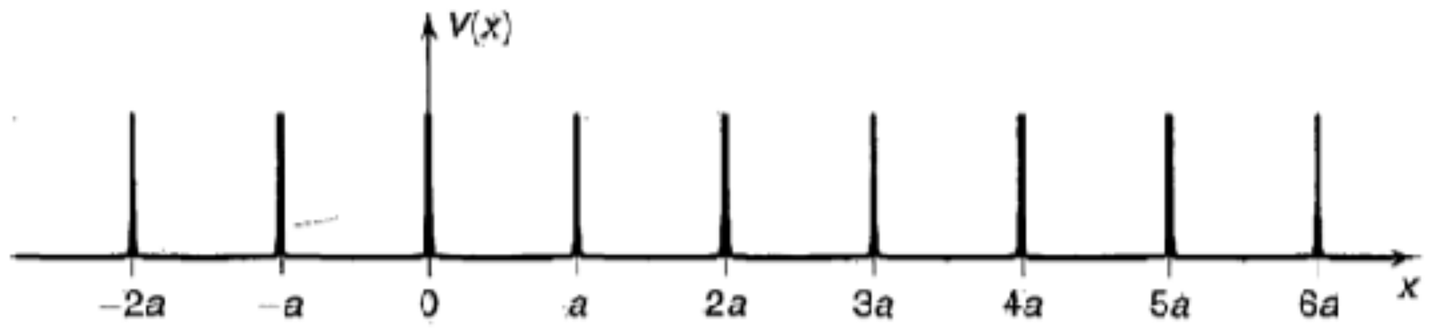

then, Bloch's theorem: the solution to the Schrödinger's eqn,

$$-\frac{\hbar^2}{2m}\frac{d^2\psi}{dx^2} + V(x)\psi = E\psi$$

can be taken to satisfy the condition: $\psi(x+a) = e^{iKa}\psi(x)$

for some constant K

- At $x = 0$, ψ must be continuous, then:

1) $B = e^{-iKa}[A\sin(ka) + B\cos(ka)]$

- And for the derivatives,

$$\lim_{\epsilon\to 0}\left(\left.\frac{d\psi}{dx}\right|_{+\epsilon} - \left.\frac{d\psi}{dx}\right|_{-\epsilon}\right) = \frac{2m\alpha}{\hbar^2}\psi(0)$$

2) $\rightarrow kA - e^{-iKa}[kA\cos(ka) - kB\sin(ka)] = \frac{2m\alpha}{\hbar^2}B$

Combining 1) and 2) gives:

$$\cos Ka = \cos ka + \frac{m\alpha}{\hbar^2 k}\sin ka$$

Let $z \equiv kz$, $\beta \equiv \frac{m\alpha a}{\hbar^2}$, then

$$f(z) \equiv \cos(z) + \beta\frac{\sin(z)}{z}$$

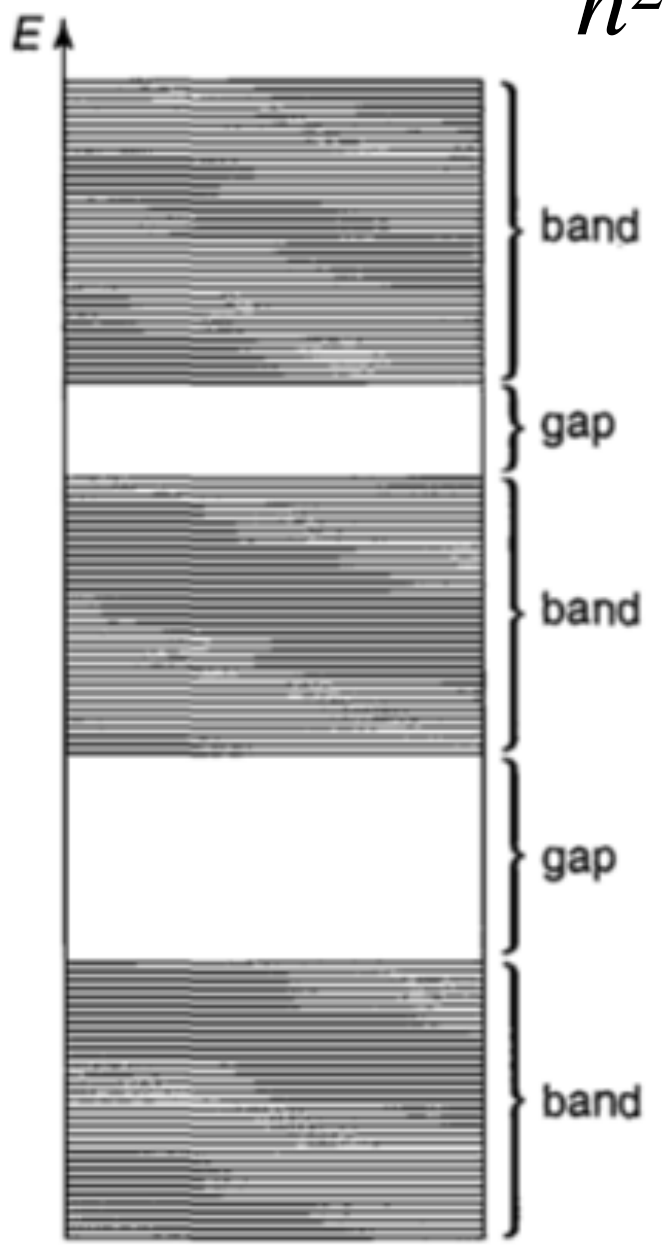

Mitigation of Low-Frequency Noise by using Bandgap Engineering

D. J. Griffiths, 'Introduction to Quantum Mechanics'

- Let us consider a periodic potential in one-dimensional space: $V(x) = V(x + a)$

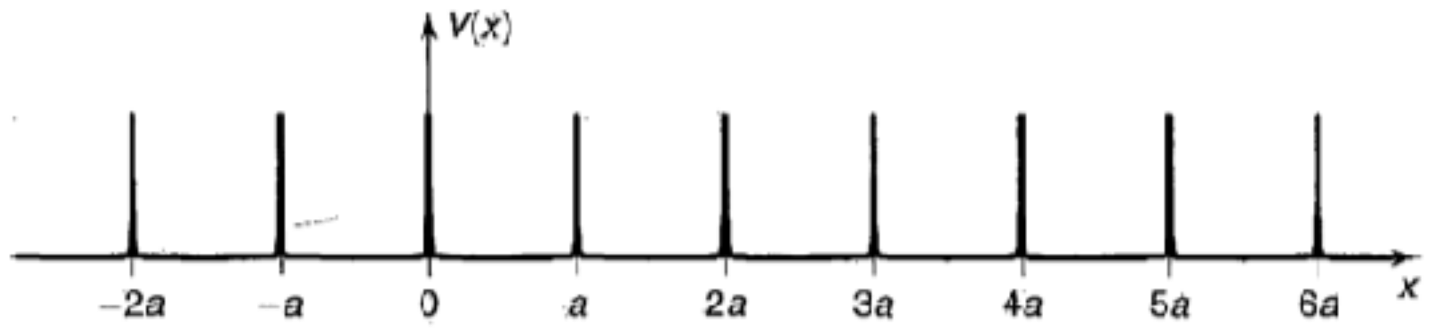

then, Bloch's theorem: the solution to the Schrödinger's eqn,

$$-\frac{\hbar^2}{2m}\frac{d^2\psi}{dx^2} + V(x)\psi = E\psi$$

can be taken to satisfy the condition: $\psi(x + a) = e^{iKa}\psi(x)$

for some constant K

$$E_k = \frac{\hbar^2 k^2}{2m}$$

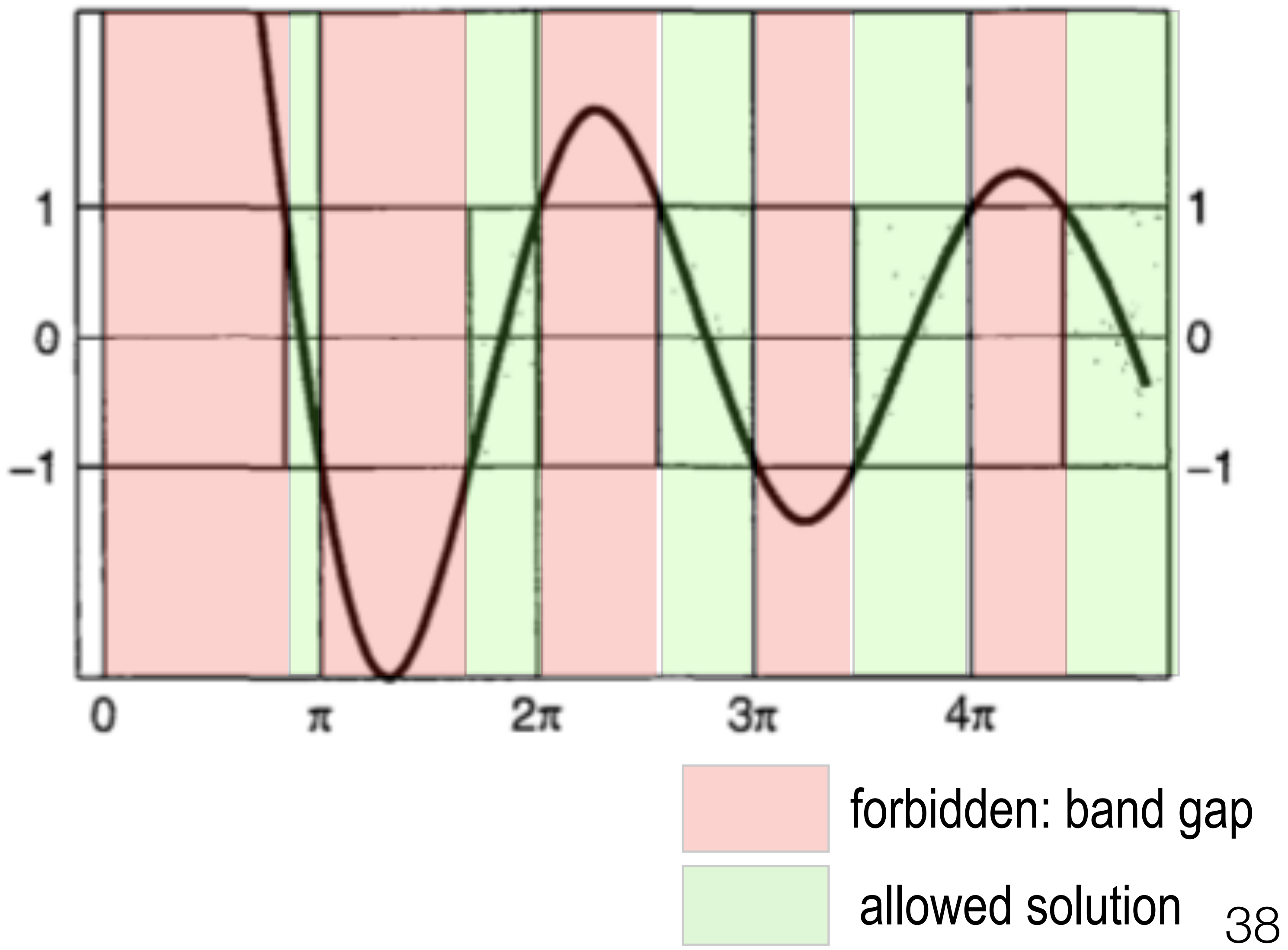

- At $x = 0$, ψ must be continuous, then:

1) $B = e^{-iKa}[A\sin(ka) + B\cos(ka)]$

- And for the derivatives,

$$\lim_{\epsilon\to 0}\left(\frac{d\psi}{dx}\bigg|_{+\epsilon} - \frac{d\psi}{dx}\bigg|_{-\epsilon}\right) = \frac{2m\alpha}{\hbar^2}\psi(0)$$

2) $\rightarrow kA - e^{-iKa}[kA\cos(ka) - kB\sin(ka)] = \frac{2m\alpha}{\hbar^2}B$

Combining 1) and 2) gives:

$$\cos Ka = \cos ka + \frac{m\alpha}{\hbar^2 k}\sin ka$$

Let $z \equiv kz$, $\beta \equiv \frac{m\alpha a}{\hbar^2}$, then

$$f(z) \equiv \cos(z) + \beta\frac{\sin(z)}{z}$$

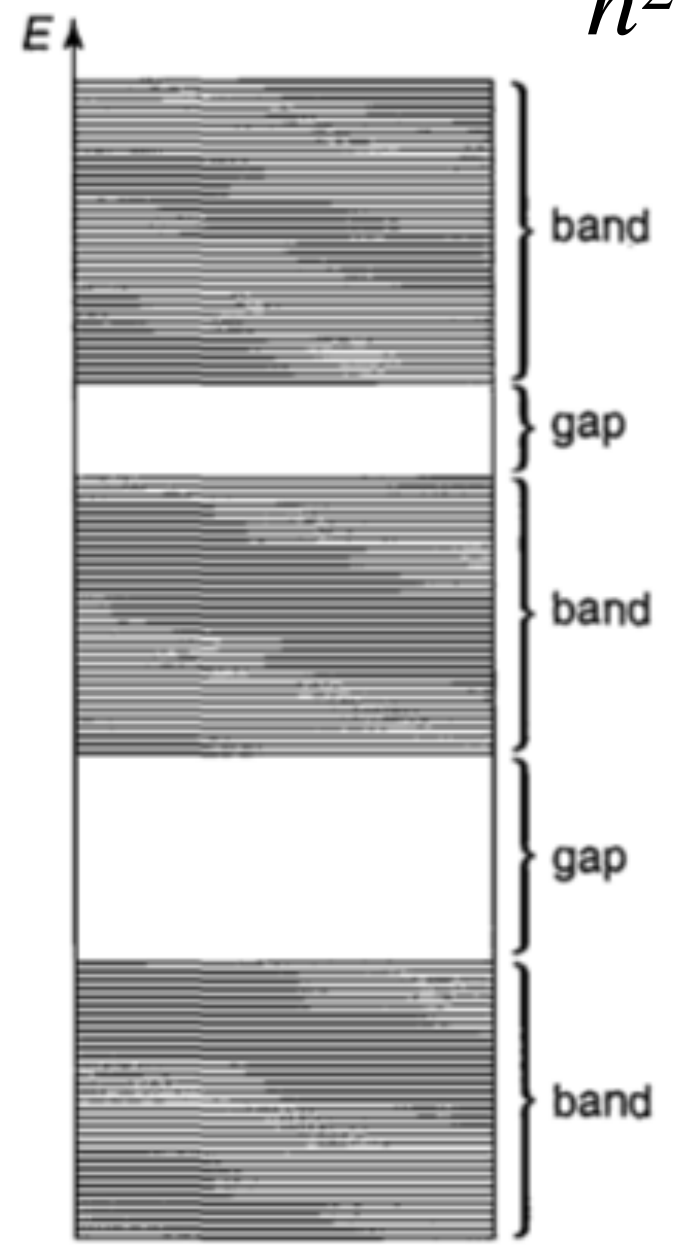

Eigen value problem on IBZ: 2D bandgap structure

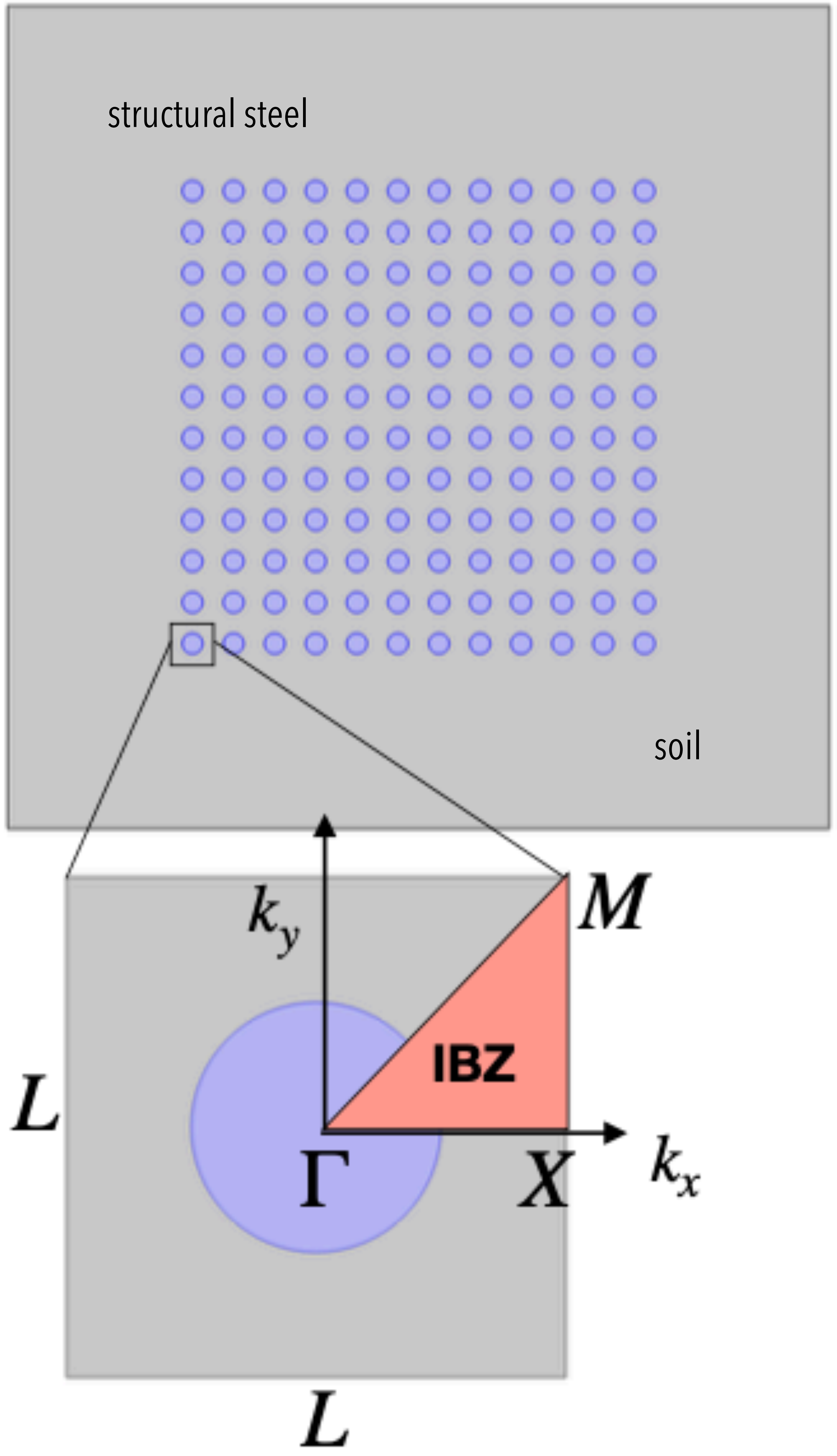

- **Solid Mechanics:**

$$\rho \frac{\partial^2 \mathbf{u}}{\partial t^2} = \mathbf{F}_v - \nabla_X \cdot \mathbf{P}^T$$

$\mathbf{P}$ is the 1st Piola-Kirchhoff stress tensor
$\mathbf{F}$ is the deformation gradient

- **Eigenvalue Equation on irreducible Brillouin zone (IBZ):**

$$\nabla^2 u_z + \frac{\rho}{\mathfrak{m}} \omega^2 u_z = 0$$

$\mathfrak{m}$ **:** Lame constant

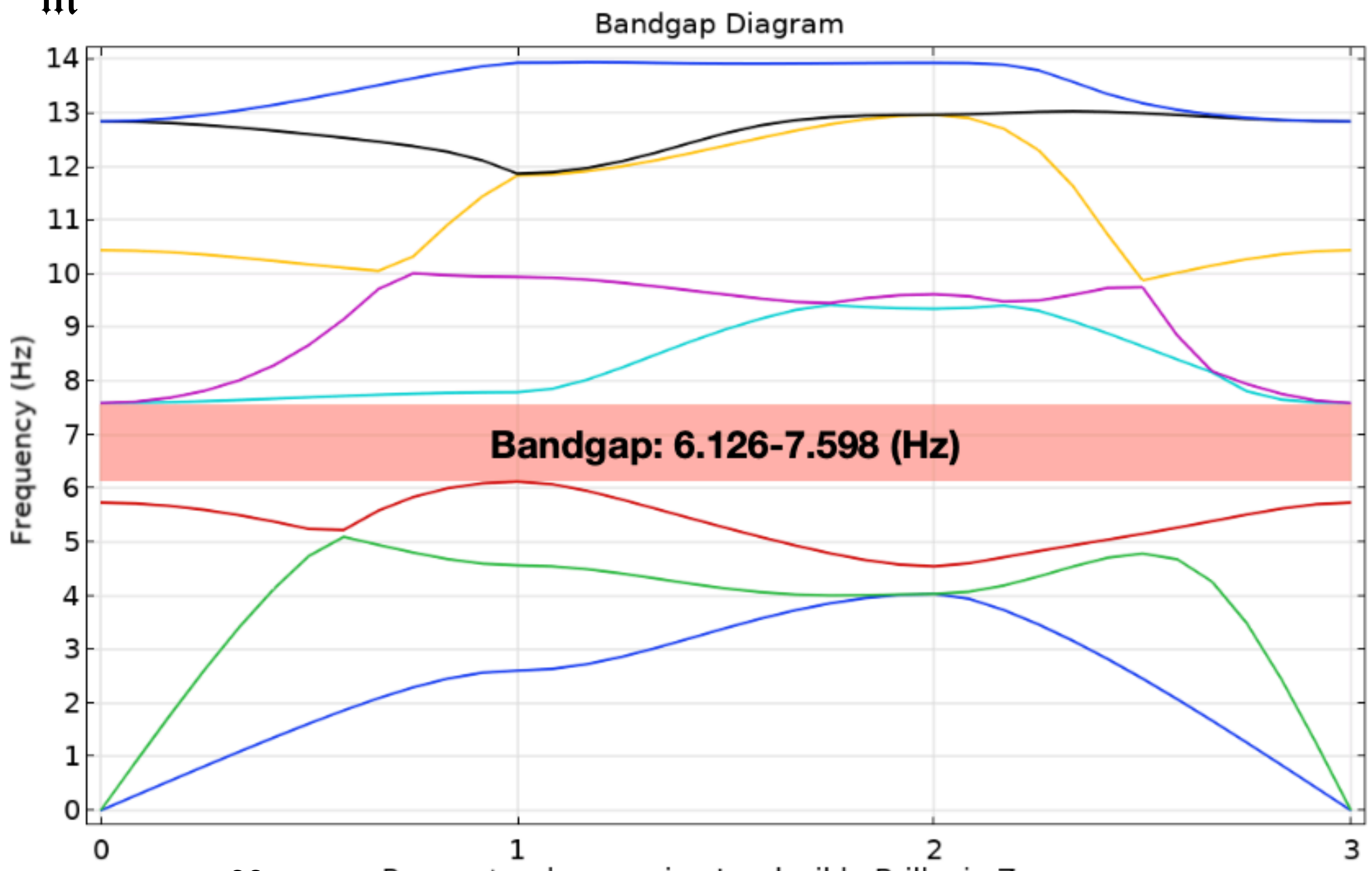

Eigen value problem on IBZ: 2D bandgap structure

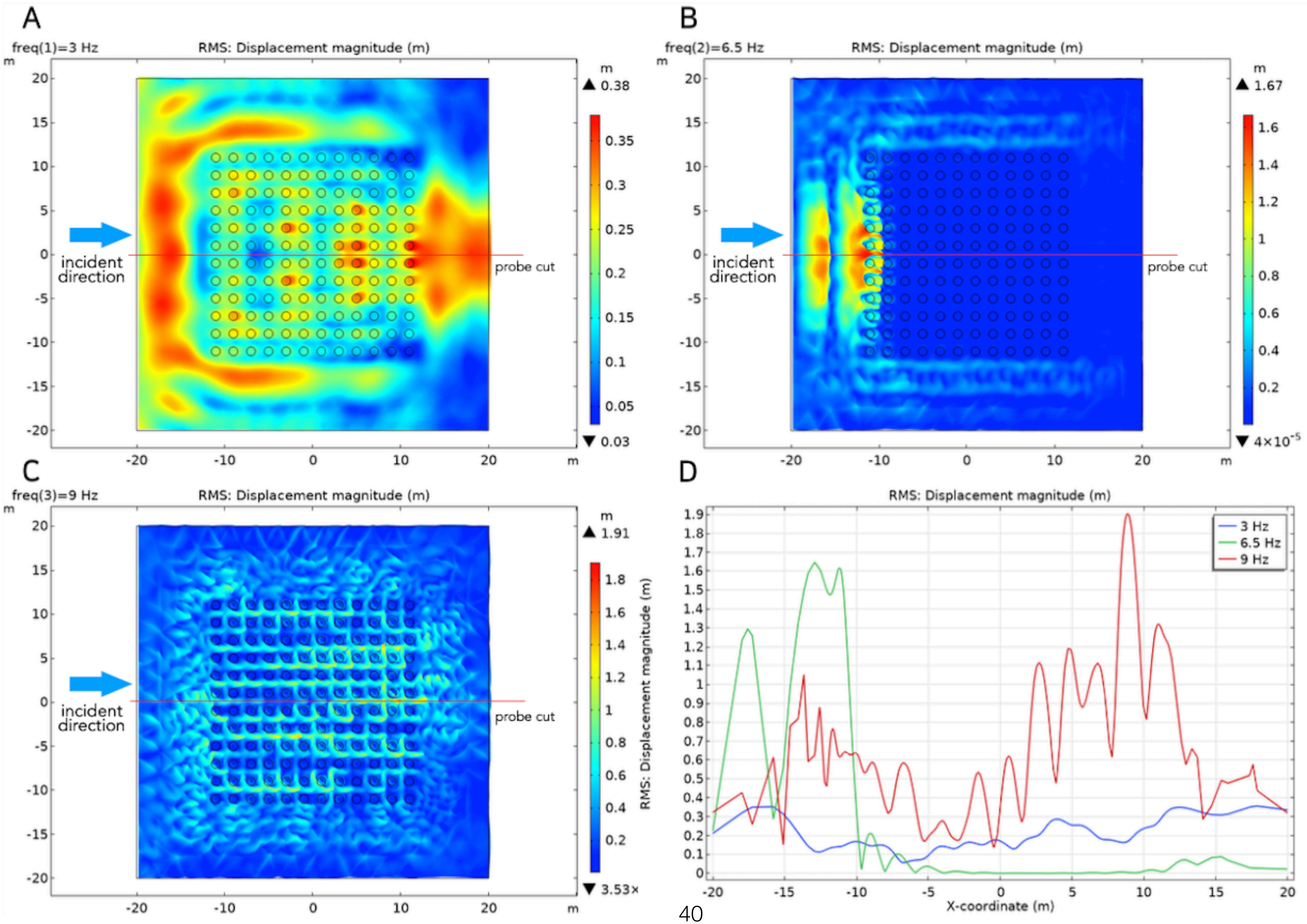

Eigen value problem on IBZ: 3D bandgap structure

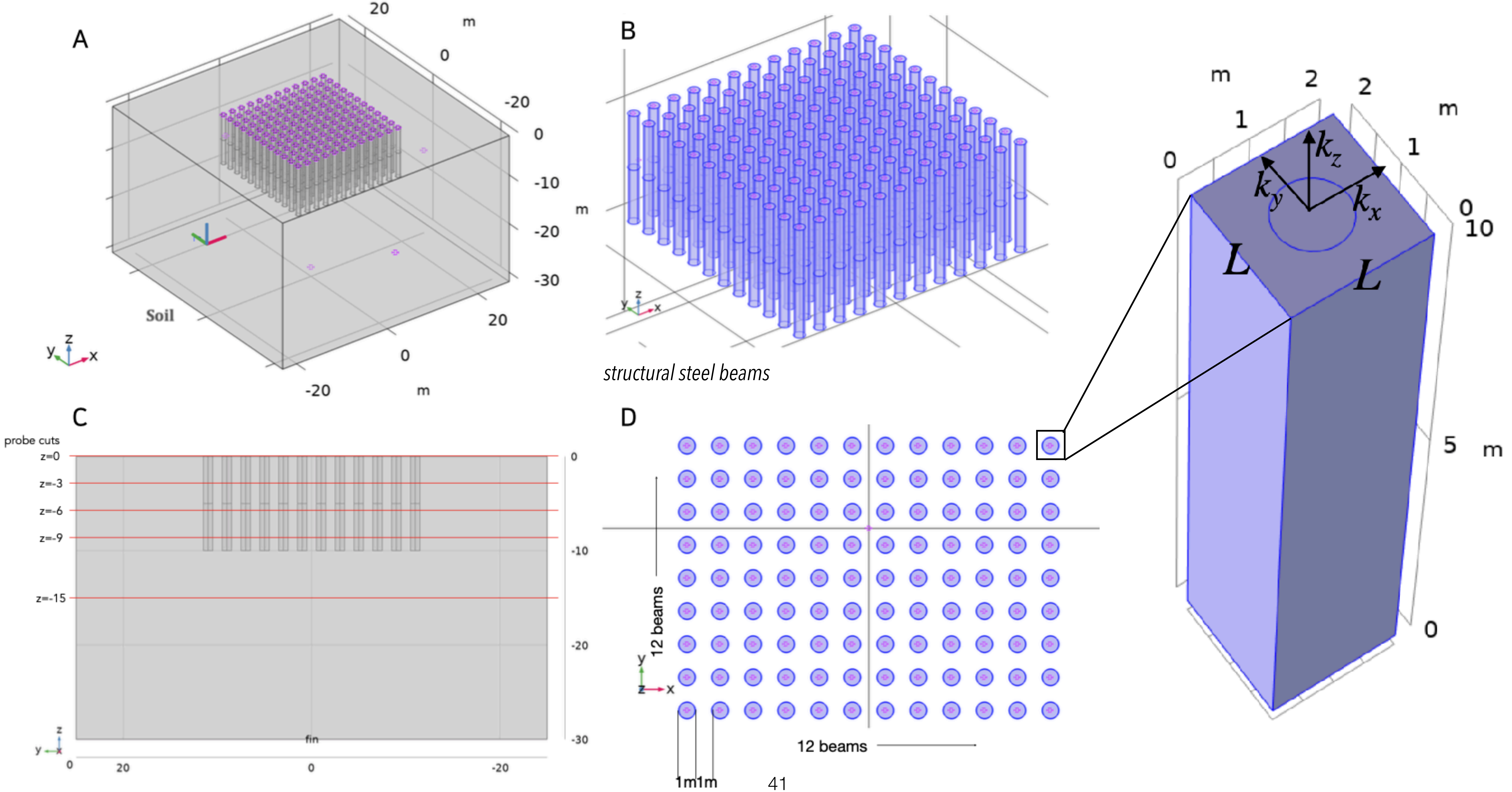

Eigen value problem on IBZ: 3D bandgap structure

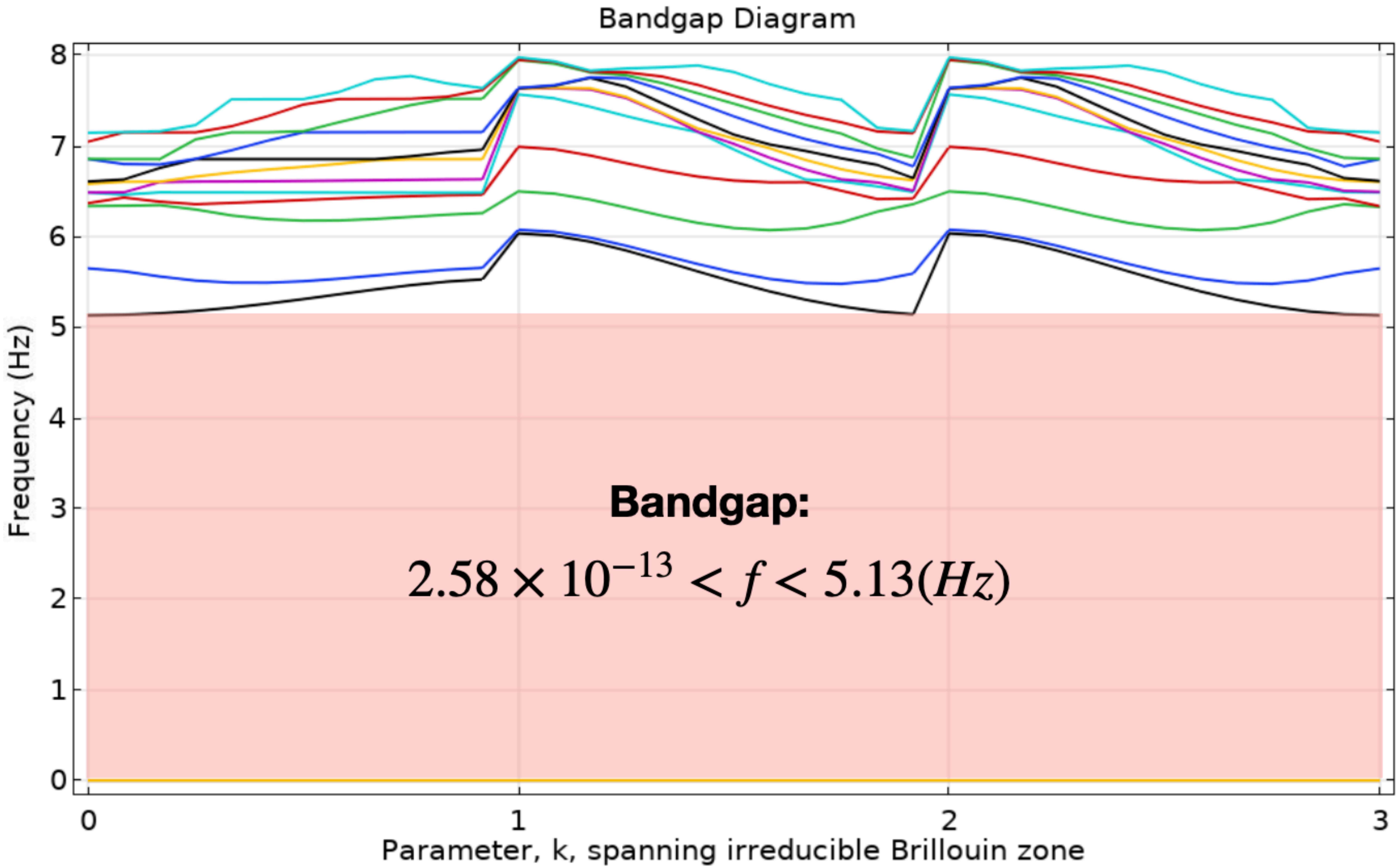

Eigen value problem on IBZ: 3D bandgap structure

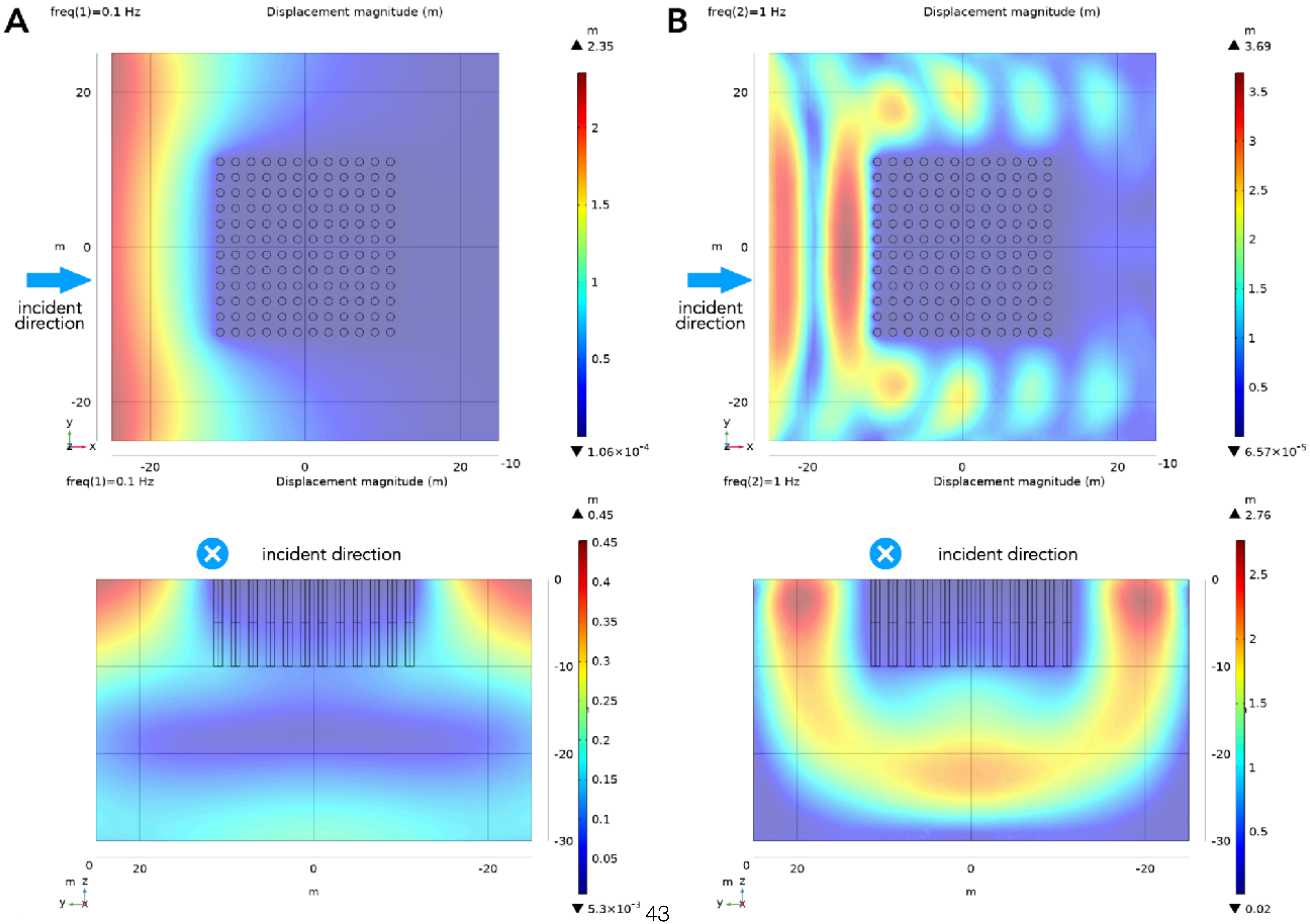

Eigen value problem on IBZ: 3D bandgap structure

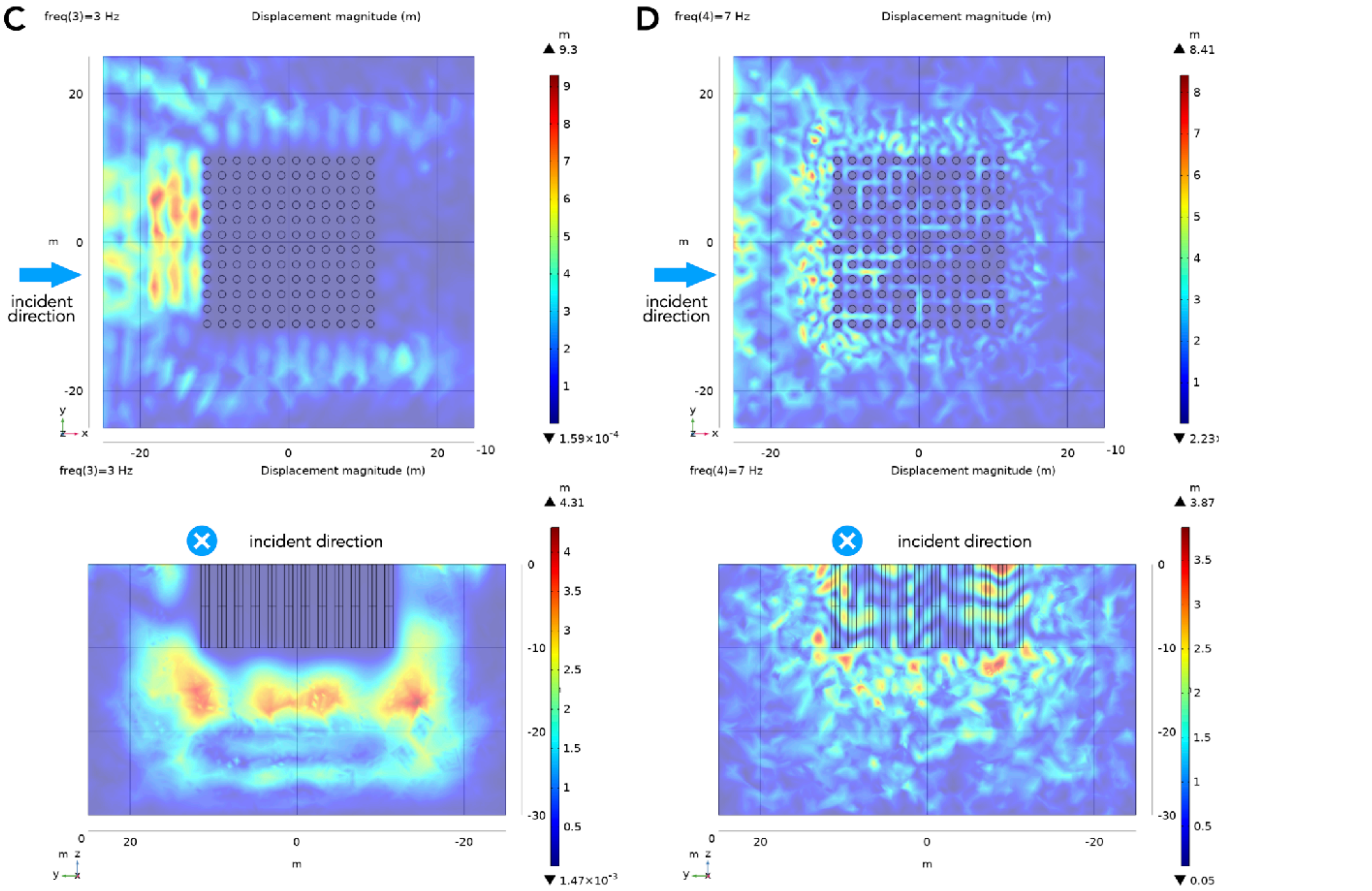

Eigen value problem on IBZ: 3D bandgap structure

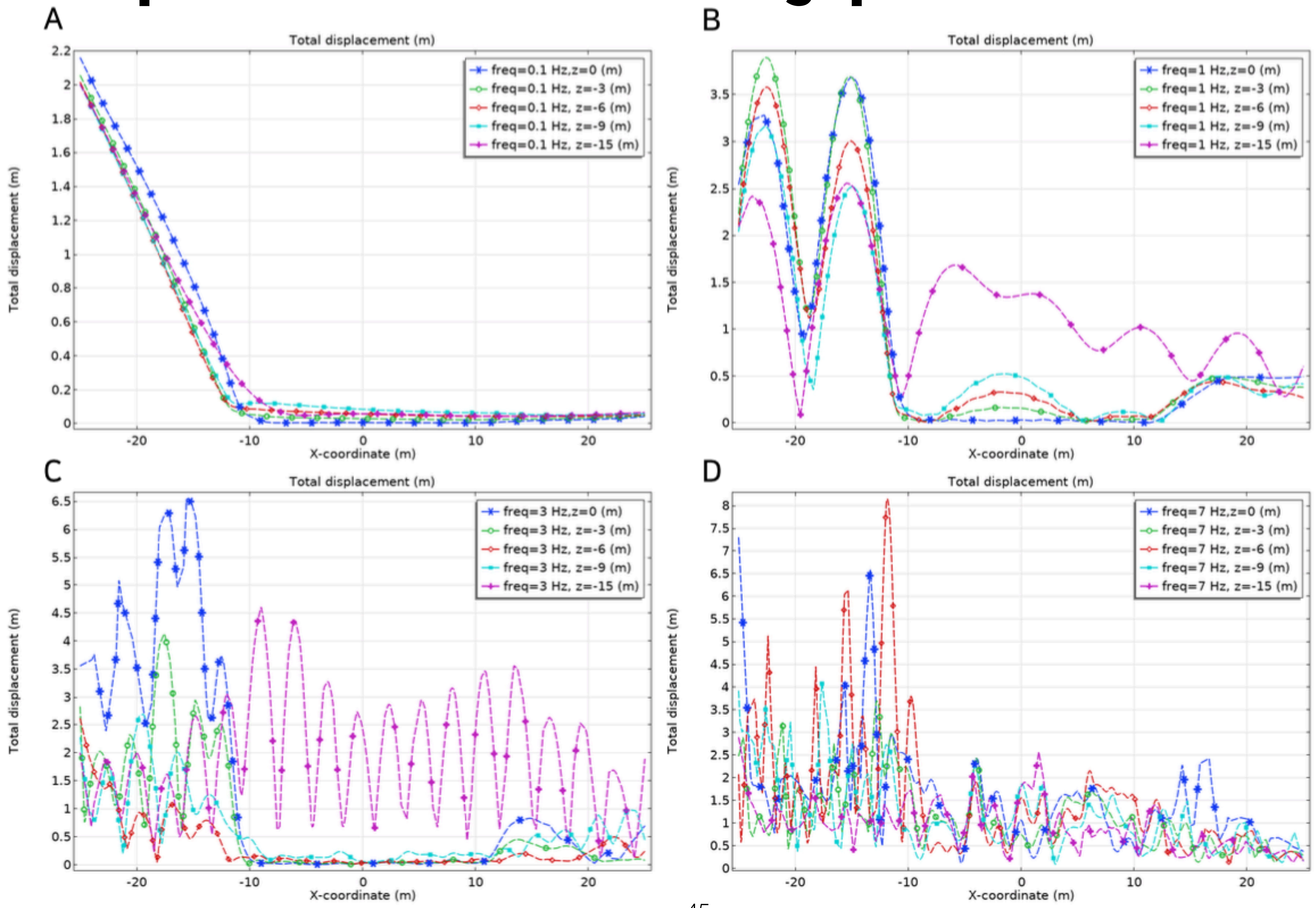

Eigen value problem on IBZ: Realistic Case of KAGRA Detector

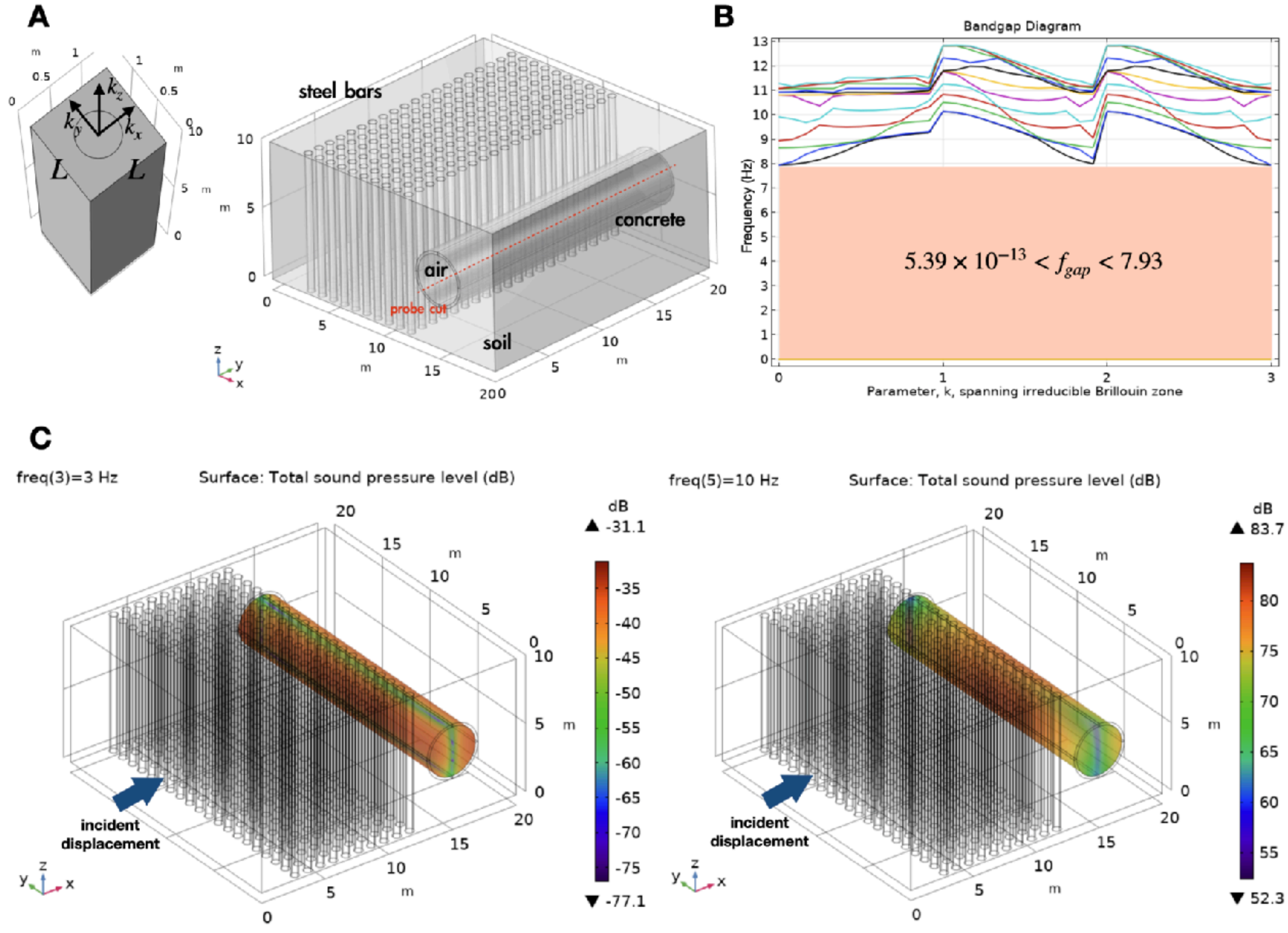

- **Solid Mechanics:**

$$\rho \frac{\partial^2 \mathbf{u}}{\partial t^2} = \mathbf{F}_v - \nabla_X \cdot \mathbf{P}^T$$

$\mathbf{P}$ is the 1st Piola-Kirchhoff stress tensor
$\mathbf{F}$ is the deformation gradient

- **Inhomogeneous Helmholtz eq:**

$$\frac{1}{\rho c^2}\frac{\partial^2 p}{\partial t^2} + \nabla \cdot \left(-\frac{1}{\rho}(\nabla p - \mathbf{s}_d)\right) = s_m,$$

- **Boundary condition on solid & air surface**

$$\mathbf{n} \cdot \left(-\frac{1}{\rho}(\nabla p - \mathbf{s}_d)\right) = -\mathbf{n} \cdot \ddot{\mathbf{u}}, \quad \mathbf{F}_A = p\mathbf{n}$$

Eigen value problem on IBZ: Realistic Case of KAGRA Detector

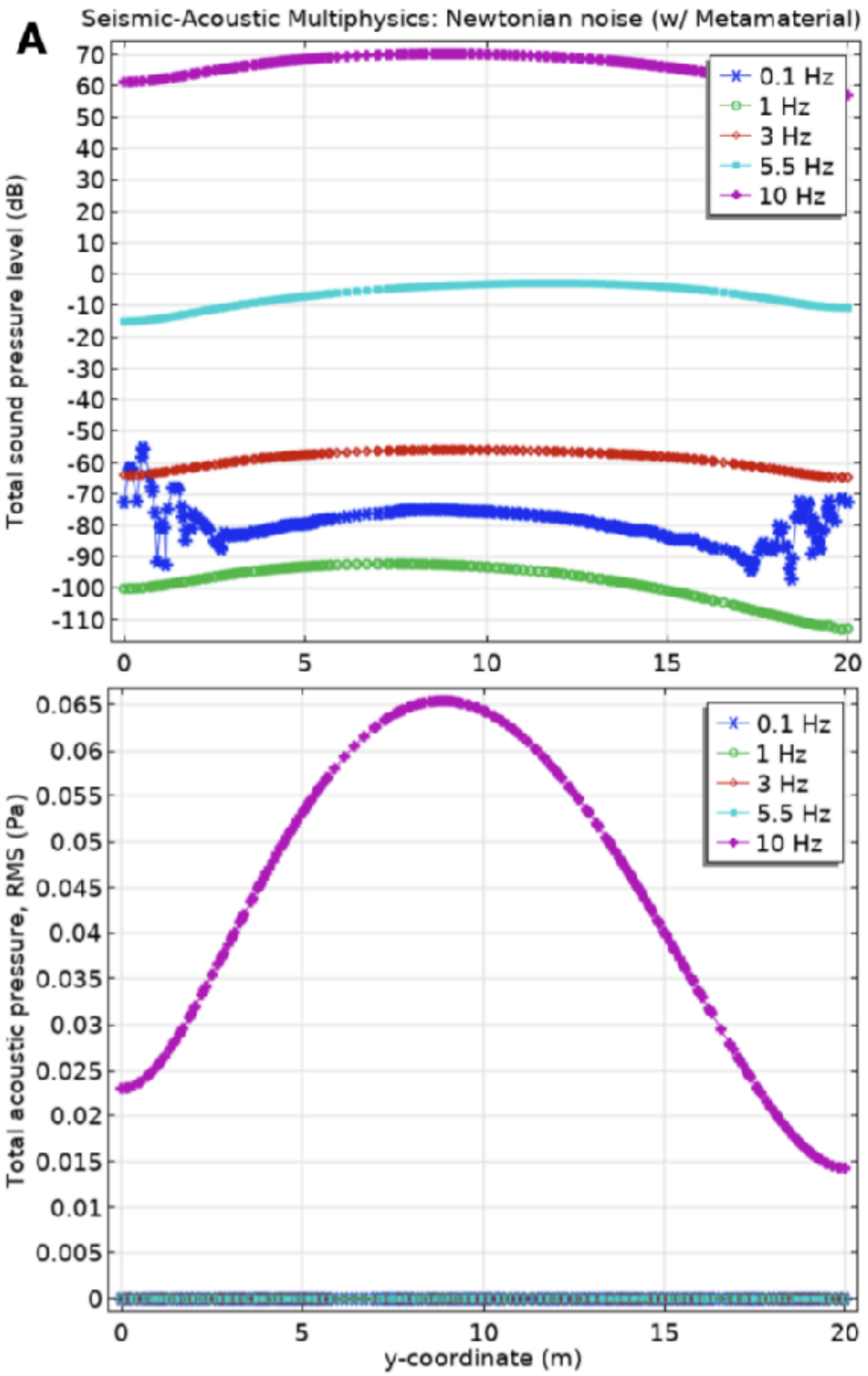

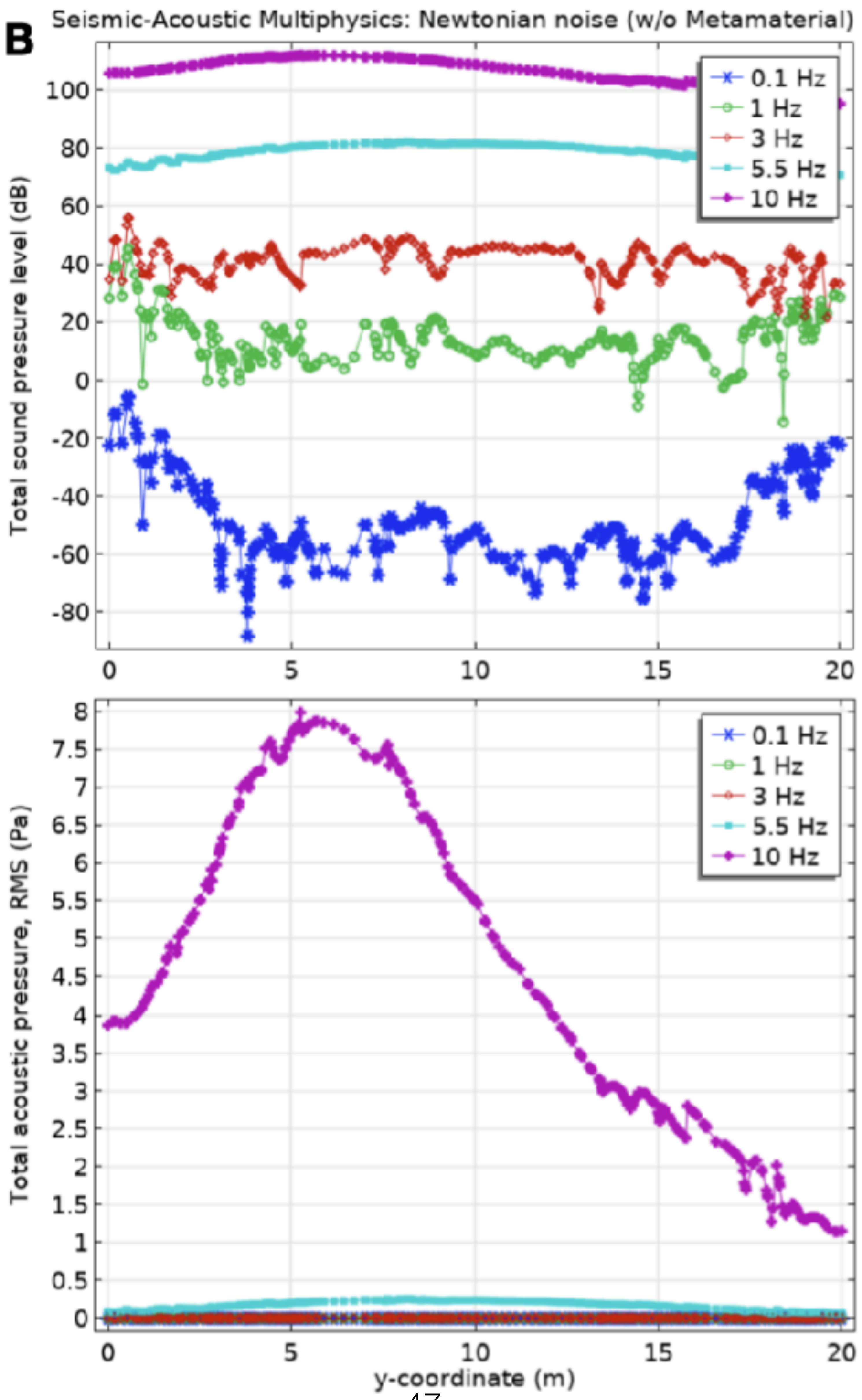

Microphone Ch.

Seismic Ch.

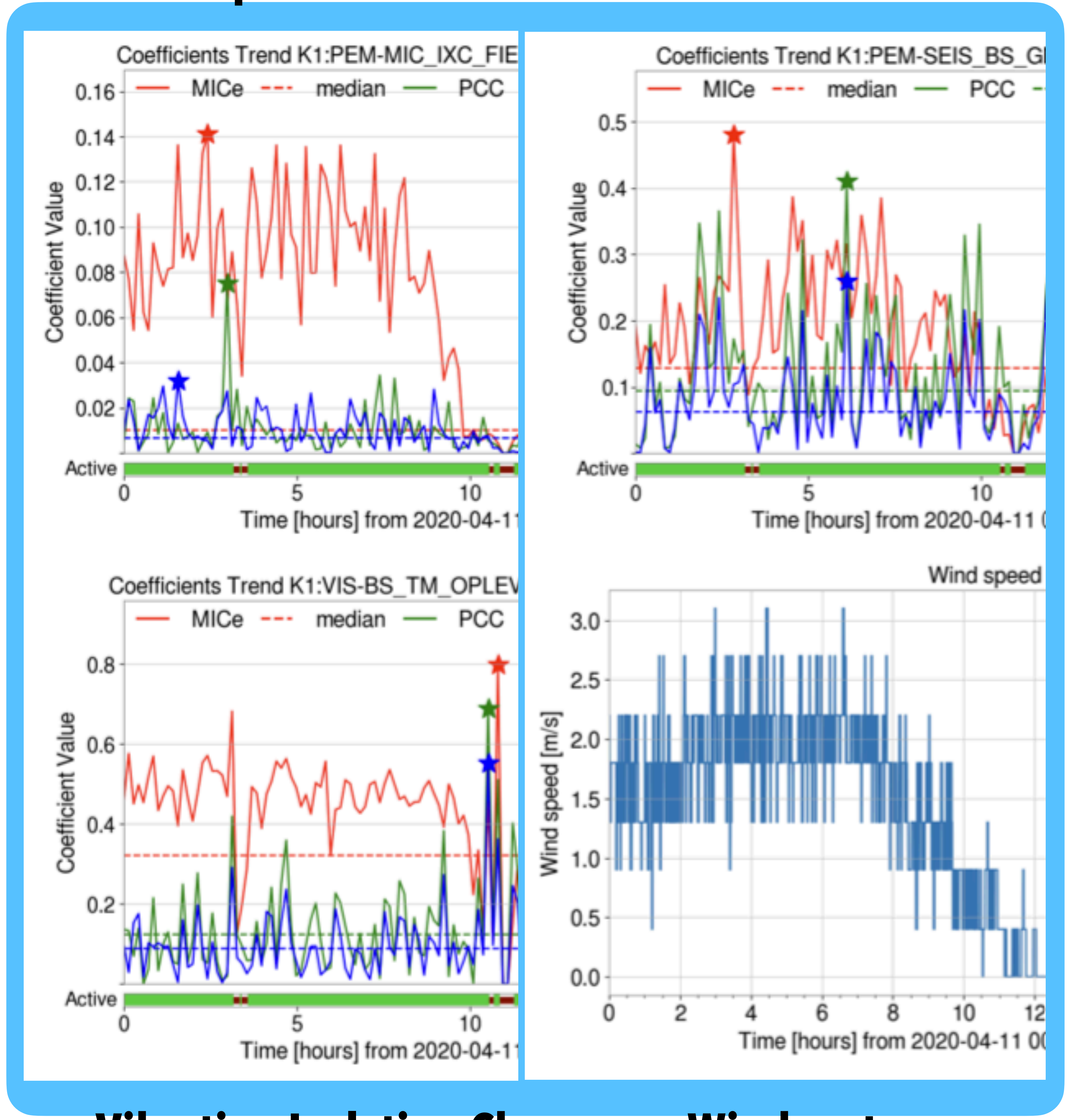

Vibration Isolation Ch.

Wind meter

Conclusions

- CAGMon Tool presents a reliable correlation index between two channels
- In particular, it provides a non-linear correlation measure by computing MIC
- The optimal parameter selection method of MIC was provided empirically by testing some datasets under various noise backgrounds (Jung et al., PTEP2022)
- We discovered some interesting correlations by applying this tool to GW Data: (Jung et al., PRD2022)
  1) Confirmed magnetic field transients from lightning strokes
  2) Found new periodic noises originating from air compressors
  3) Found glimpse of gravity gradient and acoustic noises from strong winds, in particular, dominant in the Y-arm tunnel
- This tool can be utilized for identifying and understanding the association and causal relationship between the GW channel and the environmental channels of GW detectors.
- The noise found in the KAGRA wind meter and PEM channels can be removed by using bandgap engineering, which can be verified by the multiphysics simulation at a certain condition. This method can be applied to the next-generation GW detector's noise mitigation. (JJOH, PTEP2023)

Conclusions

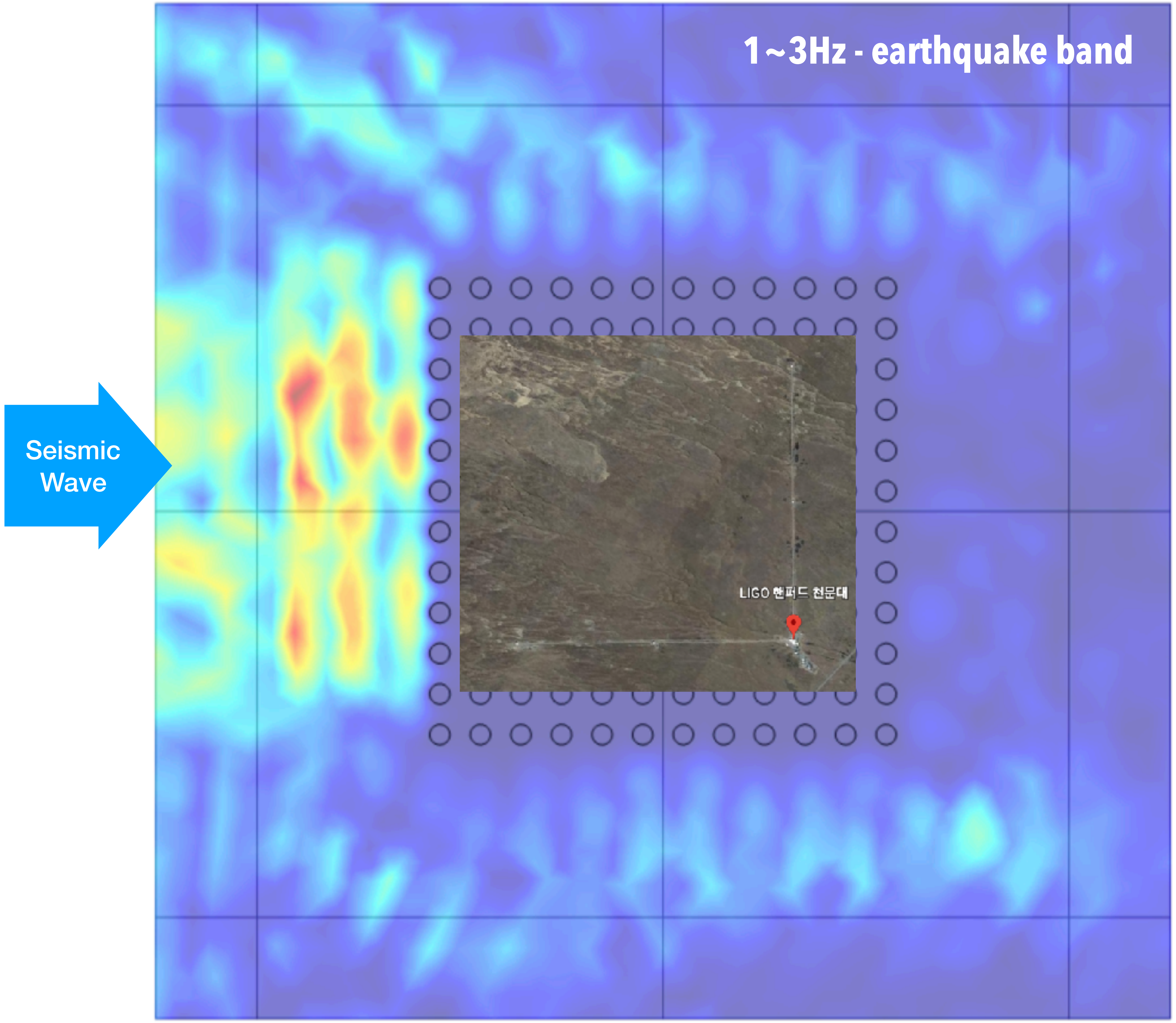

Prevent a sudden lockloss of the interferometer caused by

- nearby earthquakes
- anthropogenic activities (traffic etc)
- collective up-converting effect of gravity gradient noises

- this will enhancing the DataQuality by reducing low frequency noises
  - no lockloss by transient seismic vibrations (continuous observation)

Cosmic Explorer, Einstein Telescope etc

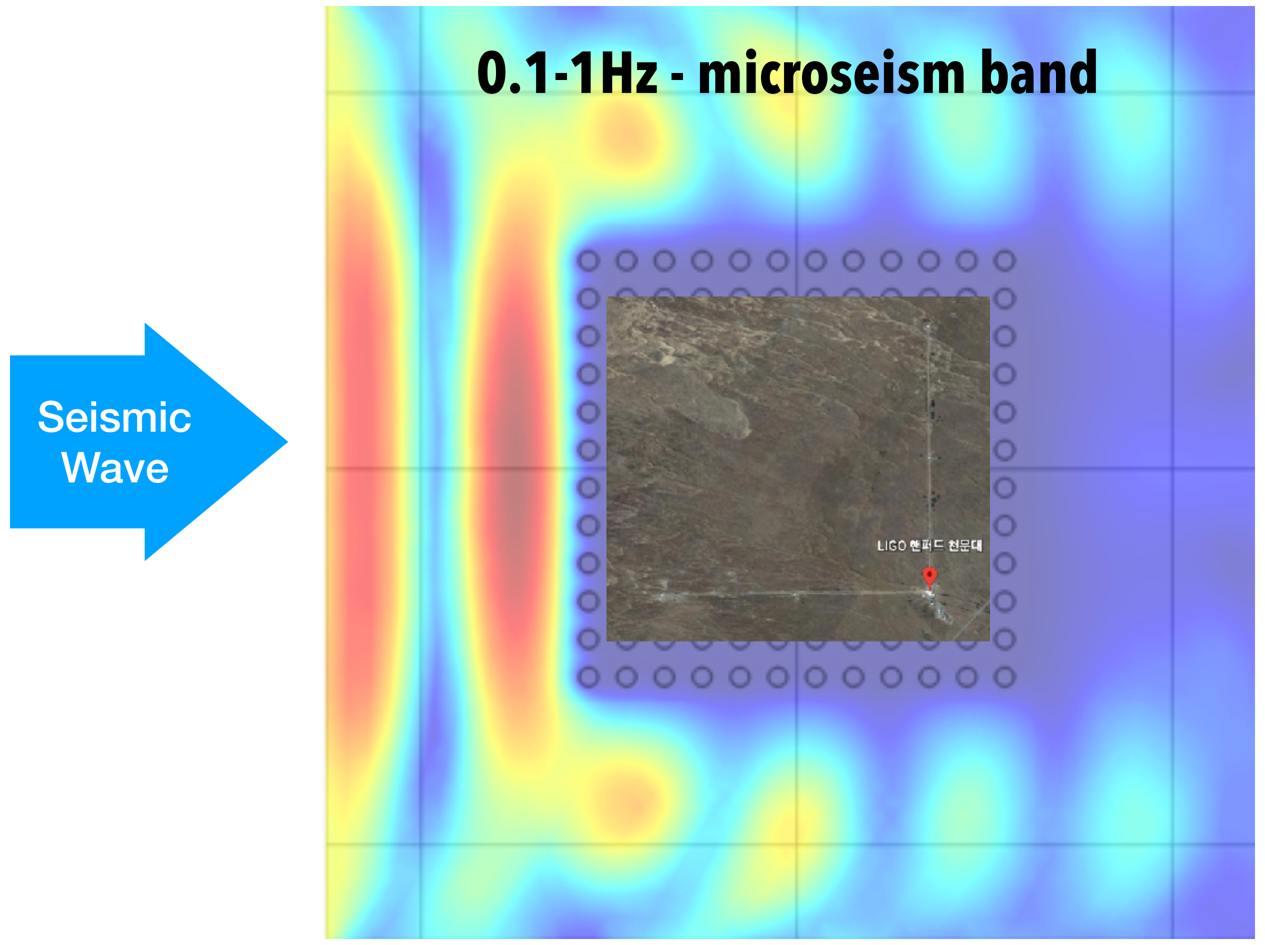


PHOTO ESSAY
NOISE

Thank you